The quantification of metabolic regulation

by

Jálene van Zyl

*Thesis presented in partial fulfilment of the requirements
for the degree of Master of Science (Biochemistry) in the
Faculty of Science at Stellenbosch University*

Department of Biochemistry
University of Stellenbosch
Private Bag X1, 7602 Matieland, South Africa

Supervisors:

Prof. J.-H.S. Hofmeyr (supervisor)   Prof. J.M. Rohwer (co-supervisor)

March 2013

i

Declaration

By submitting this thesis electronically, I declare that the entirety of the work
contained therein is my own, original work, that I am the sole author thereof
(save to the extent explicitly otherwise stated), that reproduction and pub-
lication thereof by Stellenbosch University will not infringe any third party
rights and that I have not previously in its entirety or in part submitted it for
obtaining any qualification.

Date: . . . .
March 2013

Acknowledgements

Contents

List of Figures

Summary

Metabolic systems are open systems continually subject to changes in the surrounding environment that cause fluctuations in the state variables and perturbations in the system parameters. However, metabolic systems have mechanisms to keep them dynamically and structurally stable in the face of these changes. In addition, metabolic systems also cope with large changes in the fluxes through the pathways, not letting metabolite concentrations vary wildly.

Quantitative measures have previously been proposed for "metabolic regulation", using the quantitative framework of Metabolic Control Analysis. However, the term "regulation" is so loosely used so that its content is mostly lost. These different measures of regulation have also not been applied to a model and comparably investigated prior to this study. Hence, this study analyses the usefulness of the different quantitative measures in answering different types of regulatory questions.

Thus, the aim of this study was to distinguish the above mentioned aspects of metabolic regulation and to find appropriate quantitative measures for each, namely dynamic stability, structurally stability, and homeostasis. Dynamic stability is the property of a steady state to return to its original state after a perturbation in a metabolite in the system, and can be analysed in terms of self and internal-response coefficients. Structural stability is concerned with the change in steady state after a perturbation of a parameter in the system, and can be analysed in terms of concentration-response coefficients. Furthermore, it is shown that control patterns are useful in understanding which system properties determine structural stability and to what degree. Homeostasis is defined as the change in the steady-state concentration of a metabolite relative to the change in the steady-state flux through the metabolite pool following a perturbation in a system parameter, and co-response coefficients are proposed as quantitative measures of homeostasis. More specifically, metabolite-flux co-response coefficients allow the definition of an index that quantifies to which

degree a metabolite is homeostatically regulated.

A computational model of a simple linear metabolic sequence subject to feedback inhibition with different sets of parameters provided a test-bed for the quantitative analysis of metabolic regulation. Log-log rate characteristics and parameter portraits of steady-state variables, as well as response and elasticity coefficients were used to analyse the steady-state behaviour and control properties of the system.

This study demonstrates the usefulness of generic models based on proper enzyme kinetics to further our understanding of metabolic behaviour, control and regulation and has laid the groundwork for future studies of metabolic regulation of more complex core models or of models of real systems.

Opsomming

Metaboliese sisteme is oop sisteme wat gedurig blootgestel word aan 'n fluktuerende omgewing. Hierdie fluktuasies lei tot veranderinge in beide interne veranderlikes en parameters van metaboliese sisteme. Metaboliese sisteme besit egter meganismes om dinamies en struktureel stabiel te bly. Verder verseker hierdie meganismes ook dat die konsentrasies van interne metaboliete relatief konstant bly ten spyte van groot veranderinge in fluksie deur die metaboliese pad waarvan hierdie metaboliete deel vorm.

Kwantitatiewe maatstawwe is voorheen voorgestel vir "metaboliese regulering", gebaseer op die raamwerk van Metaboliese Kontrole Analise. Die onkritiese gebruik van die term "regulering" ontneem egter hierdie konsep van sinvolle betekenis. Voor hierdie studie is die voorgestelde maatstawwe van regulering nog nie toegepas op 'n model ten einde hulle met mekaar te vergelyk nie. Die huidige studie ondersoek die toepaslikheid van die verskillende maatstawwe om verskillende tipe vrae oor regulering te beantwoord.

Die doelwit van hierdie studie was om aspekte van metaboliese regulering, naamlik dinamiese stabiliteit, strukturele stabiliteit en homeostase, te onderskei, asook om 'n gepaste maatstaf vir elk van die verskillende aspekte te vind. Dinamiese stabiliteit is 'n eienskap van 'n bestendige toestand om terug te keer na die oorspronklike toestand na perturbasie van die konsentrasie van 'n interne metaboliet. Hierdie aspek van regulering kan in terme van interne respons en self-respons koëffisiënte geanaliseer word. Strukturele stabiliteit van 'n bestendige toestand beskryf die mate van verandering van die bestendige toestand nadat 'n parameter van die sisteem geperturbeer is, en kan in terme van konsentrasie-responskoëffisiënte geanaliseer word. Verder wys hierdie studie dat kontrole patrone van nut is om vas te stel watter eienskappe van 'n sisteem die strukturele stabiliteit bepaal en tot watter mate. Homeostase word gedefiniëer as die verandering in die konsentrasie van 'n interne metaboliet relatief tot die verandering in die fluksie deur daardie metaboliese poel nadat 'n parameter van die sisteem verander het. Vir die analise van

hierdie aspek van regulering word ko-responskoëffisiënte as 'n maatstaf voorgestel. Meer spesifiek kan metaboliet-fluksie ko-responskoëffisiënte gebruik word om 'n indeks te definieer wat meet tot watter mate 'n metaboliet homeostaties gereguleer word.

'n Rekenaarmatige model van 'n eenvoudige lineêre metaboliese sekwens wat onderhewig is aan terugvoer inhibisie is gebruik om die verskillende aspekte van metaboliese regulering kwantitatief te analiseer met vier verskillende stelle parameters . Dubbel-logaritmiese snelheidskenmerke en parameter portrette van bestendige toestandsveranderlikes, asook van respons- en elastisiteit koëffisiënte is gebruik om die bestendige toestandsgedrag en kontrole eienskappe van die sisteem te analiseer.

Hierdie studie demonstreer die nut van generiese modelle wat op korrekte ensiemkinetika gebaseer is om ons verstaan van metaboliese gedrag, kontrole en regulering te verdiep. Verder dien hierdie studie as grondslag vir toekomstige studies van metaboliese regulering van meer ingewikkelde kernmodelle of modelle van werklike sisteme.

Chapter 1

Introduction

Metabolic regulation has been an intensely studied subject since the discovery of feedback by end-product inhibition in the 1950s [26, 41, 42]. Originally it was mostly an experimental subject and many of the concepts were formulated *ad hoc* without the benefit of a rigorous theoretical and quantitative framework; some of these concepts, such as the necessity for a so-called "rate-limiting step" in any pathway, and the so-called "cross-over theorem" later proved to be fallacious [5, 21]. Such frameworks became available in the late 1960s and early 1970s, notably Metabolic Control Analysis (MCA) [6, 21] and Biochemical Systems Theory (BST) [37–39]. However, it was only in the late 1980s and the 1990s in a series of papers by Hofmeyr, Cornish-Bowden and co-workers [9, 11, 12, 15, 19] that MCA was used to develop a new view of metabolic regulation that culminated in Supply-Demand Analysis [14, 17, 32].

The rise of computational systems biology and associated computational tools [2, 18, 20, 25, 35, 36] has boosted the study of metabolic regulation considerably by providing the wherewithal to develop mathematical models of metabolic systems that can be analysed within the context of MCA. This dissertation provides an example of such an analysis. The formulation of realistic metabolic models has been aided by the development of an enzyme kinetics for computational systems biology [4, 13, 30, 31].

The concept of "metabolic regulation" is a very broad one and the term is so loosely used that it has, to a large extent, lost its content. Instead of trying to define it rigorously, this study rather distinguishes aspects that are usually regarded as falling under the rubric of metabolic regulation and treats them and their quantification individually. The three aspects covered in this dissertation are *dynamical stability*, *structural stability*, and *homeostasis*. Another approach to quantifying regulation, that proposed by Sauro [34], is also

discussed. These different aspects of metabolic regulation can be considered to arise from the following questions:

- When the metabolites internal to a metabolic system fluctuate, which are the most important interactions that drive the system back to the steady state that existed before the fluctuation? This is a question of the dynamical stability of a steady state [23].

- When a system parameter is perturbed and the system settles into a new steady state, by how much do the metabolite concentrations change and what determines these changes? This is a question of the structural stability of the steady state [40].

- When metabolite concentration(s) are buffered in the face of parameter changes can the system be described as homeostatically regulated [11]? Is it enough the consider only the metabolite concentrations or must fluxes through the metabolite pools also be taken into account?

- When the activity of an enzyme catalysing a reaction in the system is perturbed, what determines how the steady-state flux through another reaction (or even the perturbed reaction) changes? This is the question Sauro [34] asked in his approach to metabolic regulation.

The aim of this study was therefore to tackle each of these "regulation" questions and find the appropriate quantitative measures for the different aspects of metabolic regulation. A computational model of a simple linear metabolic sequence subject to feedback inhibition with different sets of parameters provided a test-bed for the quantitative analysis of metabolic regulation. This core model is colloquially known as the "Stellenbosch organism" and has proved extremely useful in the studies by Hofmeyr and his collaborators mentioned earlier. Its steady-state behaviour is well understood.

Chapter 2 outlines the theoretical framework of MCA [6, 21] that underlies all of the analyses of the different aspects of regulation described above. The "Stellenbosch organism" is used to illustrate some of the concepts of MCA.

Chapter 3 introduces the computational model of the "Stellenbosch organism" that is used for all the numerical simulations (performed with PySCeS [27]) in this dissertation. Four different parameter sets illustrate different types of behaviour of the system. Log-log rate characteristics [9] and parameter portraits of steady-state variables and of control and elasticity coefficients are used to analyse the steady-state behaviour of the system.

2

Chapter 4 discusses the concepts of dynamic and structural stability and juxtaposes it with homeostasis. Dynamic stability is the property of a steady state to return to its original state after a perturbation in a metabolite in the system, and can be analysed in terms of *internal response coefficients*. Structural stability is concerned with the change in steady state after a perturbation of a parameter in the system, and can be analysed in terms of *concentration-response coefficients*. Homeostasis is defined as the change in the concentration of a metabolite relative to the change in the flux through the metabolite pool following a perturbation in a system parameter, and *co-response coefficients* are proposed as quantitative measures of homeostasis. All of these coefficients of MCA are introduced in Chapter 2.

Chapters 5, 6, and 7 in turn provide the theoretical background to the analysis of structural stability, homeostasis and dynamical stability and use the model system introduced in Chapter 3 to exemplify the different quantitative measures of these aspects of metabolic regulation. In particular, a new measure for homeostasis, the homeostatic index, is introduced in Chapter 6. In the discussion of structural stability in Chapter 5, control patterns as defined by Hofmeyr [8] are used to quantify the different interaction routes that contribute to the value of the concentration-control coefficients used to quantify structural stability. Chapter 7 links dynamic stability to the concepts of "regulatory strength" and "homeostatic strength" introduced by Kahn and Westerhoff [23].

Sauro [34] proposed so-called "partitioned regulatory coefficients" to quantify another aspect of the response of a steady state to a perturbation in the activity of one of the enzymes that catalyse a reaction in the metabolic system, namely how a flux through any step is affected through the metabolites that interact directly with the enzyme that catalyses that step. Chapter 8 explores this aspect of the metabolic response to a parameter perturbation.

Chapter 9 summarises, discusses and reflects on the foregoing chapters and makes some suggestion for future work. The PySCeS model description and the Python script used to generate the numerical results used in this study is provided in the Appendices.

Chapter 2

Metabolic control analysis

Metabolic systems are networks of coupled enzyme-catalysed chemical reactions and transport processes. System biologists generally use kinetic models to investigate quantitatively how the network structure of a metabolic system and the local properties of the individual enzyme-catalysed steps that constitute the system give rise to the observed dynamic behaviour of the metabolic system. Metabolic control analysis, the subject of this chapter, can be performed on any kinetic model in steady state in order to study the control properties of the system. The central questions asked by metabolic control analysis are how the steady-state variables change when the steady-state changes in response to a perturbation in one or more parameters, and how these changes can be explained in terms of the local kinetic properties of the individual steps in the system.

Metabolic control analysis in its most general form, i.e., one that caters for all types of metabolic structures, such as linear, branched, looped and cyclic structures with moiety conservation, is complex [10]. For the purposes of this study, which uses a simple linear pathway subject to end-product inhibition as example, a completely general treatment is unnecessary. This chapter discusses only that part of MCA that is relevant to this study.

2.1   The kinetic model of a metabolic system

A kinetic model contains both the stoichiometric data that describe the topology of the enzyme-catalysed reaction network and the rate equations that describe the kinetic properties of each of the reactions. The kinetic model for any metabolic system can be written as a set of nonlinear differential equations

(see e.g., [10, 28]):

$$\frac{d\mathbf{s}}{dt} = \mathbf{N}\mathbf{v}[\mathbf{s}, \mathbf{p}] \tag{2.1}$$

where, for a system of n coupled reactions that inter-convert m metabolites, $\mathbf{s}$ is an m-dimensional column vector of metabolite concentrations, $\mathbf{N}$ is an $m \times n$-dimensional matrix of stoichiometric coefficients (the stoichiometry matrix), $\mathbf{v}$ is an n-dimensional column vector of reaction rates, and $\mathbf{p}$ is a p-dimensional column vector of parameters. Vector $\mathbf{s}$ contains only variable metabolite concentrations; constant external metabolite concentrations are included in the parameter vector $\mathbf{p}$.

A expressed by eqn. 2.1, reaction rates $\mathbf{v}$ are functions of both metabolite concentrations $\mathbf{s}$ and parameters $\mathbf{p}$ such as kinetic constants and fixed external concentrations.

The structure or topology of the reaction network is described by the stoichiometric matrix $\mathbf{N}$, of which any element c_{ij} is the number of S_i molecules in the balanced chemical equation for reaction j. If S_i is a reactant, $c_{ij} < 0$; if a product, $c_{ij} > 0$; otherwise, $c_{ij} = 0$.

2.2 The steady state

A chemical reaction network can in principle exist in one of three states: if *closed* it tends to *chemical equilibrium* in which the concentration of all chemical species are constant at their equilibrium values and all net reaction rates are zero; if *open* it tends to a *steady state* in which the concentration of all chemical species are constant at non-equilibrium concentrations and reaction rates are non-zero (a point steady state), or oscillate (a limit cycle) or show deterministic chaos (a strange attractor); while both closed and open systems are in the process of approaching their final state they are in a *transient state* in which the concentrations of all chemical species vary and reaction rates are non-zero.

Metabolic reaction networks are open systems, hence the study of such systems is often confined to the behaviour of a system at steady-state conditions. To ensure that a kinetic metabolic model reaches steady state, the concentrations of external metabolites must be fixed. External metabolites are those that are either only produced or consumed, in other words, pathway entry and exit metabolites.

Steady state refers to system dynamics where the concentrations of internal variable metabolites stay constant over time although rates of production

5

and consumption are non-zero. The net rate or the sum of production and consumption rates at steady state through a system is referred to as system flux, J.

In the steady state the kinetic model $d\mathbf{s}/dt = \mathbf{0}$, and eqn. 2.1 simplifies to a system of non-linear equations of the form

$$\mathbf{N}\mathbf{v}[\mathbf{s}, \mathbf{p}] = \mathbf{0} \qquad (2.2)$$

The concentrations are now *steady-state* concentrations and the steady-state reaction rate vector

$$\mathbf{J} = \mathbf{v}[\mathbf{s}, \mathbf{p}] \qquad (2.3)$$

is now called a *steady-state flux vector*.

Systems of non-linear differential equations and systems of non-linear equations usually do not have analytical solutions and have to be solved numerically for a particular set of parameter values. In this study we used PySCeS, the Python Simulator for Cellular Systems (`pysces.sourceforge.net`) [27] to do these calculations. PySCeS is a Python (`www.python.org`) package built on top of the extensions NumPy (`www.numpy.org`), SciPy (`www.scipy.org`), and matplotlib (`matplotlib.org`).

2.3 System parameters and variables

The *parameters* of a metabolic system co-determine the state of the system at any time. System parameters include all chemical species that remain constant within the timeframe of the wet experiment on or numerical simulation of the system: initial substrates, final products and external effectors must be constant for the system to attain a steady state; enzyme and membrane translocator concentrations are usually constant unless the system includes their synthesis and degradation. Thermodynamic constants such as the equilibrium constant and kinetic constants such as rate constants, catalytic constants and half-saturation constants are also parameters. Where there is moiety conservation the sums of conserved moieties are parameters, as are pH, temperature and ionic strength (unless they vary).

System *variables* generally include the steady-state fluxes and the steady-state concentrations of variable metabolites or derivative functions such as ratios of metabolite concentrations or mole fractions, chemical and membrane potentials and Gibbs-energy changes.

System variables can be regarded as the entities that are controlled by the system parameters. The theory of Metabolic Control Analysis (MCA) originally developed by Kacser and Burns [21], Kacser *et al.* [22] and Heinrich and Rapoport [6] quantifies the degree to which a system variable is controlled by a system parameter, and hence is a type of sensitivity analysis. The sensitivities of fluxes and variable concentrations are quantified by the coefficients of MCA, namely response, elasticity and control coefficients, defined in the next section. Response and control coefficients are systemic, global entities, the values of which depend on the properties of all the reactions in the network. An elasticity coefficient, on the other hand, is a local enzyme property that can, in principle, be measured with the isolated enzyme using the techniques of enzyme kinetics.

2.4 Elasticity coefficients

An *elasticity coefficient* quantifies the sensitivity of an enzyme activity or rate with respect to a change in the concentration of a specie that directly modulates the reaction rate, e.g., a substrate, product, effector, or the enzyme itself.

The elasticity coefficient of a step i with respect to a metabolite S_j can be defined in three equivalent ways, either as the ratio of the fractional change in the rate v_i of step i to the fractional change in the concentration s_j (operationally, the percentage change in the rate v_i for a 1% change in s_j), or as a scaled derivative of v_i with respect to s_j, or as the derivative of $\ln v_i$ with respect to $\ln s_j$ (which shows that an elasticity coefficients is in essence the kinetic order of a reaction with respect to a substrate, product or modifier):

$$\varepsilon_{s_j}^{v_i} = \left(\frac{\partial v_i/v_i}{\partial s_j/s_j}\right)_{s_k, s_l, \ldots} = \frac{s_j}{v_i}\left(\frac{\partial v_i}{\partial s_j}\right)_{s_k, s_l, \ldots} = \left(\frac{\partial \ln v_i}{\partial \ln s_j}\right)_{s_k, s_l, \ldots} \quad (2.4)$$

Bracket subscripts s_k and s_l are the other state variables assumed to be constant during measurement of the elasticity.

An elasticity coefficient can also be defined for a parameter that directly affects the reaction rate, i.e., occurs in its rate equation:

$$\varepsilon_p^{v_i} = \left(\frac{\partial \ln v_i}{\partial \ln p}\right)_{s_j, s_k, s_l, \ldots} \quad (2.5)$$

A typical example of such an elasticity coefficient is that of the enzyme that catalyses the reaction. Generally, the activity of an enzyme is proportional to

the enzyme concentration, since enzyme concentration is a multiplier of the rate equation.

As stated in the previous section, elasticity coefficients are measured under isolated conditions where all variables and parameters other than the one of interest are kept constant. Hence, the elasticity of an enzyme is a local property.

2.5 Response coefficients

The *response coefficient* quantifies the sensitivity of any state variable y with respect to a change in a system parameter p, and is defined as:

$$R_p^y = \left(\frac{\partial y/y}{\partial p/p}\right)_{ss} = \frac{p}{y}\left(\frac{\partial y}{\partial p}\right)_{ss} = \left(\frac{\partial \ln y}{\partial \ln p}\right)_{ss} \tag{2.6}$$

As with the elasticity coefficient, there are three equivalent ways of defining a response coefficient. The bracket subscript ss denotes that the system is allowed to attain a steady state after the parameter perturbation.

If parameter p affects more than one step in the system, its overall response is the sum of a set of partial responses, one for each step affected. Therefore, the most general definition of any response coefficient is:

$$R_p^y = \sum_{i=1}^{n} {}^iR_p^y \tag{2.7}$$

for all n steps in the system. Each of the right-hand terms is called a *partial response coefficient*. Any response coefficient has as many non-zero right-hand terms as the number of individual enzymes directly affected by the parameter perturbation.

2.6 Control coefficients

For any system parameter p we can measure a response and an elasticity coefficient:

$$R_p^y = \frac{\partial \ln y}{\partial \ln p} \quad \text{and} \quad \varepsilon_p^{v_i} = \frac{\partial \ln v_i}{\partial \ln p} \tag{2.8}$$

The mathematical relation between the response and elasticity coefficients leads to the definition of the *control coefficient*:

$$\frac{R_p^y}{\varepsilon_p^{v_i}} = \frac{\left(\dfrac{\partial \ln y}{\partial \ln p}\right)}{\left(\dfrac{\partial \ln v_i}{\partial \ln p}\right)} = \frac{\partial \ln y}{\partial \ln v_i} = C_i^y \tag{2.9}$$

8

The v_i subscript of the control coefficient is usually abbreviated to i for the sake of notational simplicity.

Similar to the other coefficients of MCA a control coefficient can be expressed in three equivalent ways:

$$C_i^y = \left(\frac{\partial y/y}{\partial v_i/v_i} \right)_{ss} = \frac{v_i}{y} \left(\frac{\partial y}{\partial v_i} \right)_{ss} = \left(\frac{\partial \ln y}{\partial \ln v_i} \right)_{ss} \tag{2.10}$$

Operationally, a control coefficient is the percentage change in a state variable due to a 1% percent change in the activity of an enzyme, irrespective of how this change in enzyme activity is brought about.

2.7 The partitioned response property

Rearrangement of eqn. 2.9 gives the partitioned or combined response property of metabolic control analysis [24]:

$$R_p^y = C_i^y \varepsilon_p^{v_i} \tag{2.11}$$

The response of a steady-state variable to a parameter perturbation can therefore be understood as a combination of a local rate response to the perturbation (the elasticity coefficient) and the subsequent systemic response to the change in the rate of the affected reaction (the control coefficient).

It may be that p affects more than one reaction in the system, and in this case the response coefficient is the sum of the partial responses as given in eqn. 2.7. The generalised formulation of the partitioned response property is:

$$R_p^y = \sum_{i=1}^{n} C_i^y \varepsilon_p^{v_i} \tag{2.12}$$

where n is the number of enzymes in the system and p the parameter that is perturbed.

2.8 Summation theorems

The summation theorems show how control over any steady-state variable is shared among all the enzymes that constitute a metabolic system [6, 21]. They are completely general and independent of the structure of the network and of the properties of the enzymes.

The *flux-summation relationship* shows that if all the enzymes of a system that affects a particular metabolic flux are taken into account and the values

of their control coefficients are added, the sum is one. For any steady-state flux, J:

$$\sum_{i=1}^{n} C_i^J = 1 \tag{2.13}$$

where n is the number of enzyme-catalysed steps of a system that affects a particular flux. In other words, flux control can be distributed among all or many enzymes of a system. The summation relationship showed that the traditional paradigm of the necessity for one rate-limiting step in a pathway is a fallacy.

As an example, the summation and other theorems are shown for the metabolic system that is used in this study (Fig. 2.1).
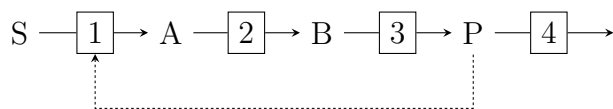
Figure 2.1: A linear pathway consisting of four enzyme-catalysed reactions with feedback inhibition of the committing enzyme 1 by pathway end-product P. S in an external metabolite to the system, and hence, a parameter.

The flux-summation relationship for the pathway in Fig. 2.1 is:

$$C_1^J + C_2^J + C_3^J + C_4^J = 1 \tag{2.14}$$

The *concentration-summation relationship* shows that the control coefficients of all enzymes of a system with respect to the steady-state concentration of an internal variable metabolite sum to zero [1]. For the steady-state concentration s_j of any internal variable metabolite S_j:

$$\sum_{i=1}^{n} C_i^{s_j} = 0 \tag{2.15}$$

where n is the number of enzyme-catalysed steps that constitute the system. The summation to zero implies that some concentration-coefficients must be positive and some negative, i.e., some reactions will increase the steady-state concentration of the metabolite, while others will decrease it in such a way that the net positive and negative effects are equal in magnitude.

The concentration-summation relationships for the linear pathway in Fig. 2.1 are:

$$C_1^a + C_2^a + C_3^a + C_4^a = 0 \tag{2.16}$$

$$C_1^b + C_2^b + C_3^b + C_4^b = 0 \tag{2.17}$$

$$C_1^p + C_2^p + C_3^p + C_4^p = 0 \tag{2.18}$$

10

2.9 Connectivity theorems

Whereas the summation theorems provide relationship between control coefficients, the connectivity theorems link control coefficients to elasticity coefficients. There are two types of connectivity theorems: the flux and concentration-connectivity relationships [6, 21]. In general, the connectivity relationship is the sum of all the *internal-response coefficients* that quantify change in a specific state variable through different enzymes of a system that are in direct contact with an internal variable metabolite that is perturbed. The flux-connectivity relationship for any steady-state flux, J, when the concentration of any internal variable metabolite S_j, s_j, is perturbed:

$$\sum_{i=1}^{n} C_i^J \varepsilon_{s_j}^{v_i} = 0 \tag{2.19}$$

where n is the number of enzymes in the system. Any connectivity relationship has as many non-zero right-hand terms as the number of individual enzymes of a system directly affected by a perturbation in the concentration of an internal variable metabolite.

The flux-connectivity relationships for the linear pathway in Fig. 2.1 are:

$$C_1^J \varepsilon_a^{v_1} + C_2^J \varepsilon_a^{v_2} = 0 \tag{2.20}$$

$$C_2^J \varepsilon_b^{v_2} + C_3^J \varepsilon_b^{v_3} = 0 \tag{2.21}$$

$$C_1^J \varepsilon_p^{v_1} + C_3^J \varepsilon_p^{v_3} + C_4^J \varepsilon_p^{v_4} = 0 \tag{2.22}$$

The concentration-connectivity relationship for the steady-state concentration of any internal variable metabolite S_k, s_k, when the concentration of any internal variable metabolite S_j, s_j, is perturbed:

$$\sum_{i=1}^{n} C_i^{s_k} \varepsilon_{s_j}^{v_i} = -\delta_{jk} \tag{2.23}$$

where δ_{jk} is the Kronecker delta, which is 0 when $j \neq k$ and 1 if $j = k$.

The concentration-connectivity relationships for the linear pathway in Fig. 2.1 are:

$$C_1^a \varepsilon_a^{v_1} + C_2^a \varepsilon_a^{v_2} = -1 \tag{2.24}$$

$$C_2^a \varepsilon_b^{v_2} + C_3^a \varepsilon_b^{v_3} = 0 \tag{2.25}$$

$$C_1^a \varepsilon_p^{v_1} + C_3^a \varepsilon_p^{v_3} + C_4^a \varepsilon_p^{v_4} = 0 \tag{2.26}$$

11

$$C_1^{\prime b}\varepsilon_a^{v_1} + C_2^{\prime b}\varepsilon_a^{v_2} = 0 \tag{2.27}$$

$$C_2^{\prime b}\varepsilon_b^{v_2} + C_3^{\prime b}\varepsilon_b^{v_3} = -1 \tag{2.28}$$

$$C_1^{\prime b}\varepsilon_p^{v_1} + C_3^{\prime b}\varepsilon_p^{v_3} + C_4^{\prime b}\varepsilon_p^{v_4} = 0 \tag{2.29}$$

$$C_1^{p}\varepsilon_a^{v_1} + C_2^{p}\varepsilon_a^{v_2} = 0 \tag{2.30}$$

$$C_2^{p}\varepsilon_b^{v_2} + C_3^{p}\varepsilon_b^{v_3} = 0 \tag{2.31}$$

$$C_1^{p}\varepsilon_p^{v_1} + C_3^{p}\varepsilon_p^{v_3} + C_4^{p}\varepsilon_p^{v_4} = -1 \tag{2.32}$$

The connectivity theorems show that the system relaxes back to its original steady state after a perturbation in the concentration of an internal variable metabolite. Hence, the steady-state values of state variables at any specific steady state are independent of variation in the concentrations of internal variable metabolites. The connectivity theorems describe how a system is dynamically stable (this will be discussed in Chapter 7).

Each term in the connectivity relationships expresses a partitioned response, similar to that encountered in the above discussion of response coefficients in Section 2.5. However, here the response is not towards a parameter, but towards an internal, variable metabolite. Each of these terms can therefore be regarded as an *internal-response coefficient*, and the connectivity theorems can be recast as:

$$\sum_{i=1}^{n} {}^{i}R_{s_j}^{J} = 0 \tag{2.33}$$

and

$$\sum_{i=1}^{n} {}^{i}R_{s_j}^{s_k} = -\delta_{jk} \tag{2.34}$$

The internal-response coefficient of a metabolite quantifies the contribution to the total response of an internal interaction route through an enzyme that is directly affected by a perturbation in that metabolite. The connectivity relationship for the system in Fig. 2.1 can therefore similarly be recast as:

$$ {}^{1}R_a^{J} + {}^{2}R_a^{J} = 0 \tag{2.35}$$

$$ {}^{2}R_b^{J} + {}^{3}R_b^{J} = 0 \tag{2.36}$$

$$ {}^{1}R_p^{J} + {}^{3}R_p^{J} + {}^{4}R_p^{J} = 0 \tag{2.37}$$

$$ {}^{1}R_a^{a} + {}^{2}R_a^{a} = -1 \tag{2.38}$$

$$ {}^{1}R_a^{b} + {}^{2}R_a^{b} = 0 \tag{2.39}$$

$$ {}^{1}R_a^{p} + {}^{2}R_a^{p} = 0 \tag{2.40}$$

$$^{2}R_{b}^{a} + {}^{3}R_{b}^{a} \;=\; 0 \qquad (2.41)$$

$$^{2}R_{b}^{b} + {}^{3}R_{b}^{b} \;=\; -1 \qquad (2.42)$$

$$^{2}R_{b}^{p} + {}^{3}R_{b}^{p} \;=\; 0 \qquad (2.43)$$

$$^{1}R_{p}^{a} + {}^{3}R_{p}^{a} + {}^{4}R_{p}^{a} \;=\; 0 \qquad (2.44)$$

$$^{1}R_{p}^{b} + {}^{3}R_{p}^{b} + {}^{4}R_{p}^{b} \;=\; 0 \qquad (2.45)$$

$$^{1}R_{p}^{p} + {}^{3}R_{p}^{p} + {}^{4}R_{p}^{p} \;=\; -1 \qquad (2.46)$$

Both the summation and connectivity theorems have been extended for systems of arbitrary complexity [3, 16].

2.10 The control-matrix equation

When combined, the summation and connectivity relationships allow the expression of control coefficients in terms of elasticity coefficients through a variety of matrix equations. Reder [28] initially derived a control-matrix equation, describing how the structural characterisations and properties of a system are only dependent on the structure of the network and not on the reaction kinetics:

$$\begin{bmatrix} \mathbf{C^{J}} \\ \mathbf{C^{s}} \end{bmatrix} \begin{bmatrix} \boldsymbol{\mathcal{K}} & -\boldsymbol{\varepsilon_{s}}\boldsymbol{\mathcal{L}} \end{bmatrix} = \begin{bmatrix} \boldsymbol{\mathcal{K}} & 0 \\ 0 & \boldsymbol{\mathcal{L}} \end{bmatrix} \qquad (2.47)$$

where $\mathbf{C^{J}}$ is a matrix of flux-control coefficients, $\mathbf{C^{s}}$ a matrix of concentration-control coefficients, and $\boldsymbol{\varepsilon_{s}}$ a matrix of scaled elasticity coefficients. $\boldsymbol{\mathcal{K}}$ is the scaled kernel matrix that relates all the dependent fluxes to the independent fluxes. $\boldsymbol{\mathcal{L}}$ is a scaled link matrix that relates the time-derivatives of dependent metabolites to those of the independent metabolites.

Hofmeyr and Cornish-Bowden [12] showed how, by considering only independent fluxes and concentrations, this equation reduces to a particularly elegant and useful form:

$$\begin{bmatrix} \mathbf{C^{J_{i}}} \\ \mathbf{C^{s_{i}}} \end{bmatrix} \begin{bmatrix} \boldsymbol{\mathcal{K}} & -\boldsymbol{\varepsilon_{s}}\boldsymbol{\mathcal{L}} \end{bmatrix} = \begin{bmatrix} \mathbf{I}_{n-r} & 0 \\ 0 & \mathbf{I}_{r} \end{bmatrix} \qquad (2.48)$$

More concisely,

$$\mathbf{C^{i}E} = \mathbf{I} \qquad (2.49)$$

where $\mathbf{C^{i}} = [\mathbf{C^{J_{i}}} \quad \mathbf{C^{s_{i}}}]^{T}$ is a matrix of independent flux and concentration-control coefficients, $\mathbf{E} = [\boldsymbol{\mathcal{K}} \quad -\boldsymbol{\varepsilon_{s}}\boldsymbol{\mathcal{L}}]$ is a matrix with all the structural and

13

local properties of the system, n is the number of reactions, and r is the number of independent metabolites. This control-matrix equation is applicable to systems of arbitrary complexity.

For a linear network of coupled reactions there is only one flux and no dependencies between the differential equation for the variable metabolites. This implies that $\mathcal{K}$ is a column vector of ones and that the link matrix $\mathcal{L} = \mathbf{I}$. For the linear pathway in Fig. 2.1 eqn. 2.49 translates to:

$$\begin{bmatrix} C_1^J & C_2^J & C_3^J & C_4^J \\ C_1^a & C_2^a & C_3^a & C_4^a \\ C_1^b & C_2^b & C_3^b & C_4^b \\ C_1^p & C_2^p & C_3^p & C_4^p \end{bmatrix} \begin{bmatrix} 1 & -\varepsilon_a^{v_1} & 0 & -\varepsilon_p^{v_1} \\ 1 & -\varepsilon_a^{v_2} & -\varepsilon_b^{v_2} & 0 \\ 1 & 0 & -\varepsilon_b^{v_3} & -\varepsilon_p^{v_3} \\ 1 & 0 & 0 & -\varepsilon_p^{v_4} \end{bmatrix} = \begin{bmatrix} 1 & 0 & 0 & 0 \\ 0 & 1 & 0 & 0 \\ 0 & 0 & 1 & 0 \\ 0 & 0 & 0 & 1 \end{bmatrix} \tag{2.50}$$

Control coefficients can be calculated by inverting the matrix $\mathbf{E}$:

$$\mathbf{C^i} = \mathbf{E}^{-1} \tag{2.51}$$

For the linear pathway in Fig. 2.1:

$$\begin{bmatrix} C_1^J & C_2^J & C_3^J & C_4^J \\ C_1^a & C_2^a & C_3^a & C_4^a \\ C_1^b & C_2^b & C_3^b & C_4^b \\ C_1^p & C_2^p & C_3^p & C_4^p \end{bmatrix} = \begin{bmatrix} 1 & -\varepsilon_a^{v_1} & 0 & -\varepsilon_p^{v_1} \\ 1 & -\varepsilon_a^{v_2} & -\varepsilon_b^{v_2} & 0 \\ 1 & 0 & -\varepsilon_b^{v_3} & -\varepsilon_p^{v_3} \\ 1 & 0 & 0 & -\varepsilon_p^{v_4} \end{bmatrix}^{-1} \tag{2.52}$$

Because both $\mathbf{C^i}$ and $\mathbf{E}$ are invertible the control-matrix eqn. 2.49 can also be written as [7, 10]:

$$\mathbf{EC^i} = \mathbf{I} \tag{2.53}$$

For the linear pathway in Fig. 2.1 eqn. 2.53 becomes

$$\begin{bmatrix} 1 & -\varepsilon_a^{v_1} & 0 & -\varepsilon_p^{v_1} \\ 1 & -\varepsilon_a^{v_2} & -\varepsilon_b^{v_2} & 0 \\ 1 & 0 & -\varepsilon_b^{v_3} & -\varepsilon_p^{v_3} \\ 1 & 0 & 0 & -\varepsilon_p^{v_4} \end{bmatrix} \begin{bmatrix} C_1^J & C_2^J & C_3^J & C_4^J \\ C_1^a & C_2^a & C_3^a & C_4^a \\ C_1^b & C_2^b & C_3^b & C_4^b \\ C_1^p & C_2^p & C_3^p & C_4^p \end{bmatrix} = \begin{bmatrix} 1 & 0 & 0 & 0 \\ 0 & 1 & 0 & 0 \\ 0 & 0 & 1 & 0 \\ 0 & 0 & 0 & 1 \end{bmatrix} \tag{2.54}$$

This form of the equation provides expressions for control coefficients in terms of concentration-control coefficients and elasticity coefficients. For example, C_4^J can be expressed in four ways:

$$C_4^J = \varepsilon_a^{v_1} C_4^a + \varepsilon_p^{v_1} C_4^p \tag{2.55}$$

$$C_4^J = \varepsilon_a^{v_2} C_4^a + \varepsilon_b^{v_2} C_4^b \tag{2.56}$$

$$C_4^J = \varepsilon_b^{v_3} C_4^b + \varepsilon_p^{v_3} C_4^p \tag{2.57}$$

$$C_4^J = 1 + \varepsilon_p^{v_4} C_4^p \tag{2.58}$$

Each of these equations described how a perturbation in the activity of reaction 4, $\delta \ln v_4$, affects the flux through a particular reaction through changes in the concentrations of those internal metabolites that interact directly with the enzyme, be they substrates, products, or effectors. For example, enzyme 1 interacts directly with A and P; the effects on the steady-state concentration of these metabolites are given by the concentration-control coefficients: $\delta \ln \bar{a} = C_4^a \cdot \delta \ln v_4$ and $\delta \ln \bar{p} = C_4^p \cdot \delta \ln v_4$. The individual effects of these concentration changes on the rate, v_1, of reaction 1 are $\delta \ln v_1 = \varepsilon_a^{v_1} \cdot \delta \ln \bar{a}$ and $\varepsilon_a^{v_1} \cdot \delta \ln \bar{a}$. Combining these equations yield

$$
\begin{aligned}
\delta \ln J &= \varepsilon_a^{v_1} \cdot \delta \ln \bar{a} + \varepsilon_p^{v_1} \cdot \delta \ln \bar{p} & (2.59)\\
&= \varepsilon_a^{v_1} C_4^a \cdot \delta \ln v_4 + \varepsilon_p^{v_1} C_4^p \cdot \delta \ln v_4 & (2.60)
\end{aligned}
$$

Dividing both sides with $\ln v_4$ yields eqn. 2.55.

These equations will be analysed in Chapter 8.

2.11 Control pattern analysis

Hofmeyr [8] developed the method of control-pattern analysis to derive algebraic relations between control and elasticity coefficients. Control-pattern analysis is a non-algebraic diagrammatic technique that generates mathematical expressions for flux and concentration-control coefficients in terms of elasticity expressions.

Control-pattern analysis has been implemented in the recently developed symbolic control analysis (SymCA) add-on to PySCeS [29]. SymCA computes an algebraic solution for eqn. 2.49 by inverting the symbolic representation of $\mathbf{E}$ for systems of arbitrary complexity.

Control coefficient expressions as obtained through SymCA are shown for the linear pathway in Fig. 2.1:

Flux-control coefficients a**-control coefficients**

$$
\begin{aligned}
C_1^J &= \varepsilon_a^2 \varepsilon_b^3 \varepsilon_p^4 / \Sigma \\
C_2^J &= -\varepsilon_a^1 \varepsilon_b^3 \varepsilon_p^4 / \Sigma \\
C_3^J &= \varepsilon_a^1 \varepsilon_b^2 \varepsilon_p^4 / \Sigma \\
C_4^J &= (-\varepsilon_a^1 \varepsilon_b^2 \varepsilon_p^3 - \varepsilon_a^2 \varepsilon_b^3 \varepsilon_p^1) / \Sigma
\end{aligned}
\qquad
\begin{aligned}
C_1^a &= (\varepsilon_b^3 \varepsilon_p^4 - \varepsilon_b^2 \varepsilon_p^4 + \varepsilon_b^2 \varepsilon_p^3) / \Sigma \\
C_2^a &= (-\varepsilon_b^3 \varepsilon_p^4 + \varepsilon_b^3 \varepsilon_p^1) / \Sigma \\
C_3^a &= (\varepsilon_b^2 \varepsilon_p^4 - \varepsilon_b^2 \varepsilon_p^1) / \Sigma \\
C_4^a &= (-\varepsilon_b^2 \varepsilon_p^3 - \varepsilon_b^3 \varepsilon_p^1 + \varepsilon_b^2 \varepsilon_p^1) / \Sigma
\end{aligned}
$$

15

b-control coefficients **p-control coefficients**

$$
\begin{aligned}
C_1^b &= (\varepsilon_a^2\varepsilon_p^4 - \varepsilon_a^2\varepsilon_p^3)/\Sigma \\
C_2^b &= (-\varepsilon_a^1\varepsilon_p^4 + \varepsilon_a^1\varepsilon_p^3)/\Sigma \\
C_3^b &= (-\varepsilon_a^2\varepsilon_p^4 + \varepsilon_a^1\varepsilon_p^4 + \varepsilon_a^2\varepsilon_p^1)/\Sigma \\
C_4^b &= (\varepsilon_a^2\varepsilon_p^3 - \varepsilon_a^1\varepsilon_p^3 - \varepsilon_a^2\varepsilon_p^1)/\Sigma
\end{aligned}
\qquad
\begin{aligned}
C_1^p &= \varepsilon_a^2\varepsilon_b^3/\Sigma \\
C_2^p &= -\varepsilon_a^1\varepsilon_b^3/\Sigma \\
C_p^p &= \varepsilon_a^1\varepsilon_b^2/\Sigma \\
C_4^p &= (-\varepsilon_a^2\varepsilon_b^3 + \varepsilon_a^1\varepsilon_b^3 - \varepsilon_a^1\varepsilon_b^2)/\Sigma
\end{aligned}
$$

where the denominator Σ is expressed as

$$
\Sigma = \varepsilon_a^2\varepsilon_b^3\varepsilon_p^4 - \varepsilon_a^1\varepsilon_b^3\varepsilon_p^4 + \varepsilon_a^1\varepsilon_b^2\varepsilon_p^4 - \varepsilon_a^1\varepsilon_b^2\varepsilon_p^3 - \varepsilon_a^2\varepsilon_b^3\varepsilon_p^1
$$

Each numerator term corresponds to a control pattern and represents a chain of local effects through which a perturbation in an enzyme activity propagates through a metabolic system to affect a particular steady-state variable. In such a way the complex systemic response to a perturbation in an enzyme activity can be dissected into quantifiable contributions through these chains of local effects, so providing a deep understanding of how a change in the activity of an enzyme is transmitted to the rest of the system.

2.12   Co-response and co-control coefficients

Of particular interest for this dissertation is the method of co-response analysis developed by Hofmeyr *et al.* [15] and Hofmeyr and Cornish-Bowden [12] as part of metabolic regulation analysis, formalising the ideas developed earlier [11]. Co-response coefficients can be used to relate simultaneous changes in any two state variables when a system parameter is perturbed. A co-response coefficient is the ratio of two response coefficients of metabolic control analysis. In general, the definition of a co-response coefficient for any state variables y_j, y_k and any parameter p is:

$$
\Omega_p^{y_j:y_k} = \frac{R_p^{y_j}}{R_p^{y_k}} = \frac{\sum_{i=1}^n C_i^{y_j}\varepsilon_p^{v_i}}{\sum_{i=1}^n C_i^{y_k}\varepsilon_p^{v_i}} \tag{2.61}
$$

where v_i is the activity of an enzyme that is directly affected by the parameter perturbation and n is the number of steps in the reaction network (only those enzymes directly affected by p can have non-zero elasticity coefficients).

If the parameter p that is perturbed affects the rate of only one step (e.g., an enzyme concentration), its co-responses depend only on the relevant control coefficients of that step, and the coefficients are called co-control coefficients

with symbol $O_p^{y_j:y_k}$. As an example, consider the co-response in y_j, y_k to a perturbation in enzyme concentration e_i:

$$O_{e_i}^{y_j:y_k} = \frac{R_{e_i}^{y_j}}{R_{e_i}^{y_k}} = \frac{C_i^{y_j}\,\varepsilon_{e_i}^{y_j}}{C_i^{y_k}\,\varepsilon_{e_i}^{y_k}} = \frac{C_i^{y_j}}{C_i^{y_k}} \qquad (2.62)$$

In order to derive an equation for co-control coefficients similar to the control matrix eqn. 2.49, Hofmeyr *et al.* [15] defined the diagonal matrices $\mathbf{D^x}$ and $(\mathbf{D^x})^{-1}$ of control coefficients, the product of which gives the identity matrix $\mathbf{I}$:

$$(\mathbf{D^x})^{-1}\mathbf{D^x} = \mathbf{I} \qquad (2.63)$$

where x is the steady-state variable with respect to which the control coefficients are defined.

For the linear pathway in Fig. 2.1 eqn. 2.63 translates to:

$$\begin{bmatrix} 1/C_1^x & 0 & 0 & 0 \\ 0 & 1/C_2^x & 0 & 0 \\ 0 & 0 & 1/C_3^x & 0 \\ 0 & 0 & 0 & 1/C_4^x \end{bmatrix} \begin{bmatrix} C_1^x & 0 & 0 & 0 \\ 0 & C_2^x & 0 & 0 \\ 0 & 0 & C_3^x & 0 \\ 0 & 0 & 0 & C_4^x \end{bmatrix} = \begin{bmatrix} 1 & 0 & 0 & 0 \\ 0 & 1 & 0 & 0 \\ 0 & 0 & 1 & 0 \\ 0 & 0 & 0 & 1 \end{bmatrix} \qquad (2.64)$$

These matrices are interposed between the $\mathbf{C}$ and $\mathbf{E}$-matrices of the control-matrix eqn. 2.49 to give

$$\mathbf{C}(\mathbf{D^x})^{-1}\mathbf{D^x}\mathbf{E} = \mathbf{I} \qquad (2.65)$$

Using the definitions $\mathbf{C}(\mathbf{D^x})^{-1} = \mathbf{O}$ and $\mathbf{D^x}\mathbf{E} = \mathbf{R}$, eqn. 2.65 becomes

$$\mathbf{OR} = \mathbf{I} \qquad (2.66)$$

where $\mathbf{O}$ is a matrix that contains co-control coefficients, i.e., ratios of control coefficients that relate simultaneous changes in two state variables when the activity of a specific enzyme is perturbed. Which variables are in question depends on the control coefficients in $\mathbf{D^x}$. $\mathbf{R}$ is a matrix that contains *control coefficients* as well as *internal-response coefficients*.

For the linear system in Fig. 2.1 eqn. 2.66 translates to:

$$\begin{bmatrix} O_1^{J:p} & O_2^{J:p} & O_3^{J:p} & O_4^{J:p} \\ O_1^{a:p} & O_2^{a:p} & O_3^{a:p} & O_4^{a:p} \\ O_1^{b:p} & O_2^{b:p} & O_3^{b:p} & O_4^{b:p} \\ O_1^{p:p} & O_2^{p:p} & O_3^{p:p} & O_4^{p:p} \end{bmatrix} \begin{bmatrix} C_1^p & -^1R_a^p & 0 & -^1R_p^p \\ C_2^p & -^2R_a^p & -^2R_b^p & 0 \\ C_3^p & 0 & -^3R_b^p & -^3R_p^p \\ C_4^p & 0 & 0 & -^4R_p^p \end{bmatrix} = \begin{bmatrix} 1 & 0 & 0 & 0 \\ 0 & 1 & 0 & 0 \\ 0 & 0 & 1 & 0 \\ 0 & 0 & 0 & 1 \end{bmatrix}$$
$$(2.67)$$

An important advantage of co-control analysis is that it is not necessary to know the exact amount of change in the concentration of an enzyme that is

perturbed for the results to be useful in the analysis of metabolic regulation, provided that all enzyme components of a system can be perturbed. This eliminates the need to isolate individual enzymes to determine their individual kinetic properties and to calculate control coefficients. This advantage does not imply that studies of enzyme mechanism and properties are not useful. It depends on the goal of experimentation and the questions asked.

The next chapter introduces the computational model of the metabolic system that is used as an example in this dissertation.

Chapter 3

The metabolic system

Throughout this study of the quantification of metabolic regulation we use, for illustrative purposes, the simple system in Fig. 3.1.
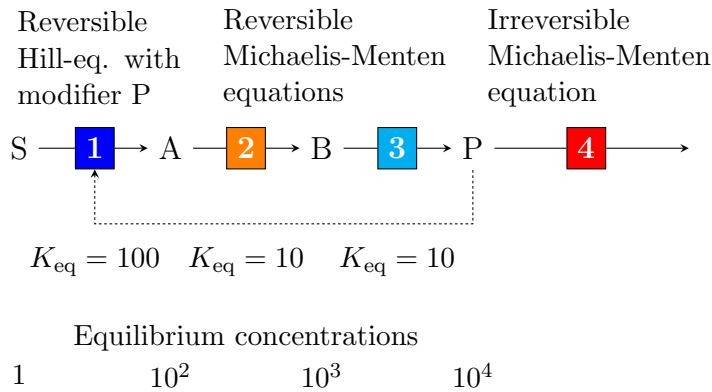
Figure 3.1: A metabolic pathway consisting of four enzyme-catalysed reactions with end-product inhibition of the committing enzyme, E_1, by pathway product P. The rate equations are discussed in the text. The colours of the steps are used in graphs to facilitate discussion.

This system has been studied in detail and its steady-state behaviour and regulation are well understood. The system consists of a biosynthetic pathway comprising three enzymes that produce a product P from a pathway substrate S. The first enzyme, E_1, in the biosynthetic sequence is allosterically inhibited by P. Product P links the biosynthetic pathway, i.e., its *supply* pathway, to a reaction that consumes P and therefore constitutes the *demand* for P. The full supply-demand pathway is colloquially known as the "Stellenbosch organism" because it has been used by Hofmeyr and collaborators in the development of the framework of supply-demand analysis [9, 11, 14, 15]. Although this

19

is a generic metabolic model that does not correspond to a particular real metabolic system, the rate equations and parameter values are chosen to be as realistic as possible. If one wants to keep a metabolic example of such a pathway in mind then this system could represent the synthesis of an amino acid P that is consumed by the process of protein synthesis.

The rate equations

The rate equations and parameter values used to construct a kinetic model for the pathway in Fig. 3.1 are provided in Appendix 10.1 in the form of a PySCeS-input file.

The committing enzyme to the biosynthetic pathway is modelled with the reversible Hill-equation for a uni-uni reaction developed by Hofmeyr and Cornish-Bowden [13]:

$$v_1 = \frac{\dfrac{k_1}{s_{0.5}} e_1 \left(s - \dfrac{a}{K_{\text{eq1}}} \right) \left(\dfrac{s}{s_{0.5}} + \dfrac{a}{a_{0.5}} \right)^{h-1}}{\left(\dfrac{s}{s_{0.5}} + \dfrac{a}{a_{0.5}} \right)^h + \dfrac{1 + \left(\dfrac{p}{p_{0.5}} \right)^h}{1 + \alpha \left(\dfrac{p}{p_{0.5}} \right)^h}} \tag{3.1}$$

where s is the substrate concentration, a the product concentration, p the allosteric modifier concentration; $s_{0.5}$, $a_{0.5}$, and $p_{0.5}$ are the half-saturating concentrations in the absence of other ligands; h is the Hill coefficient that describes the degree of cooperativity of binding of S, A and P; α is the interaction factor (inhibitory when $0 < \alpha < 1$; activating when $\alpha > 1$; no effect when $\alpha = 1$); k_1 and K_{eq1} are the catalytic and equilibrium constants respectively, and e_1 is the total concentration of the enzyme.

Enzymes 2 and 3 were modelled using the reversible Michaelis-Menten equation:

$$v_2 = \frac{\dfrac{k_2}{K_{2A}} e_2 \left(a - \dfrac{b}{K_{\text{eq2}}} \right)}{\left(1 + \dfrac{a}{K_{2A}} + \dfrac{b}{K_{2B}} \right)} \quad \text{and} \quad v_3 = \frac{\dfrac{k_3}{K_{3B}} e_3 \left(b - \dfrac{p}{K_{\text{eq3}}} \right)}{\left(1 + \dfrac{b}{K_{3B}} + \dfrac{p}{K_{3P}} \right)} \tag{3.2}$$

where K_{2A}, K_{2B}, K_{3B}, and K_{3P} denote Michaelis constants, k_2 and k_3 catalytic constants, K_{eq2} and K_{eq3} equilibrium constants, and e_2 and e_3 enzyme concentrations.

20

Because E_4 is a sink reaction it is modelled with an irreversible Michaelis-Menten equation:

$$v_4 = \frac{k_4 e_4 p}{K_{4P} + p} \tag{3.3}$$

This is quite realistic since products, such as polypeptides or polynucleotides, of the processes that consume metabolic end-products, such as amino acids or nucleotides, generally do not inhibit the processes that produce them.

Four sets of parameters values were chosen to demonstrate different types of behaviour of the model system. In the rest of this dissertation these four different parameter sets will be denoted parameter set 1, parameter set 2, parameter set 3, and parameter set 4. Certain parameters were the same in all four sets (note that, since this a generic model, no units are assigned to parameters and variables; they are assumed to be consistent):

- For enzyme 1:

    - $k_1 = 1$ and $e_1 = 200$, i.e., the limiting forward rate $V_{f1} = 200$.

    - $s = 1$ and $s_{0.5} = 1$. This implies that E_1 is always half-saturated, so that its maximum flux-carrying capacity is 100. Because in all parameter sets the V_f-values of E_2 and E_3 are 1000, except in parameter set 3 where they are 100, E_1 determines the maximum flux-carrying capacity of the biosynthetic supply.

    - $K_{eq1} = 100$.

    - $a_{0.5} = 10^5$. The combination of a large equilibrium constant of 100 and extremely weak binding of product A to enzyme 1 ensures that, for the whole range of steady states under consideration, enzyme 1 is always far from equilibrium and never subject to direct product inhibition, although at near-equilibrium concentration it is of course inhibited by A through mass-action. This means that E_1 controls the flux local to the supply pathway (unless, as is the case in parameter set 3 described below, enzymes 2 and 3 have effective limiting rates comparable or lower than V_{f1}).

    - $p_{0.5} = 1$. This determines the p-region in which the allosteric effector P can inhibit the rate of E_1.

    - $\alpha = 0.001$. This determines the limit below which v_1 cannot be further inhibited by P.

- For enzymes 2 and 3:

- $k_2 = k_3 = 1$.

- $K_{2A} = K_{2B} = K_{3B} = K_{3P} = 1$.

- $K_{eq2} = K_{eq3} = 10$. As shown in Fig. 3.1, when s is fixed at a concentration of 1, the equilibrium constants of the three biosynthetic enzymes determine the equilibrium concentrations that a, b, and p would reach in the absence of a demand reaction for P.

- For enzyme 4:

  - $k_4 = 1$.

The parameters that were varied in the four parameter sets were the Hill coefficient of enzyme 1, h, the concentrations of enzymes 2 and 3, and the Michaelis constant of enzyme 4 for its substrate P.

1. Parameter set 1: $h = 4$, $e_2 = e_3 = 1000$, $K_{4P} = 0.01$. This set of parameters defines the reference system, which, as explained in Section 3.1, has excellent regulatory properties. The small Michaelis constant of E_4 for P ensures that the enzymes is easily saturated by P.

2. Parameter set 2: $h = 1$, $e_2 = e_3 = 1000$, $K_{4P} = 0.01$. The degree of cooperativity of the binding of P to E_1 is decreased by changing h from 4 to 1.

3. Parameter set 3: $h = 4$, $e_2 = e_3 = 100$, $K_{4P} = 0.01$. Here the three biosynthetic enzymes effectively have the same limiting rates of 100 (although $V_{f1} = 200$ it is half saturated with S).

4. Parameter set 4: $h = 4$, $e_2 = e_3 = 1000$, $K_{4P} = 100.0$. P binds weakly to E_4, which affects the elasticity of E_4 for P and, thereby, the degree of flux-control exerted by E_4 (discussed in Section 3.1).

3.1 Supply-demand rate characteristic analysis

The metabolic system in Fig. 3.1 can be divided into two conversion blocks, with E_1, E_2, and E_3 acting as the supply of P and E_4 as the demand for P. The flux, J, and p-control coefficients of the supply are simply the sum of the individual control coefficients:

$$C_{\text{supply}}^J = C_1^J + C_2^J + C_3^J \quad \text{and} \quad C_{\text{supply}}^p = C_1^p + C_2^p + C_3^p \qquad (3.4)$$

22

while the control coefficients for the demand are:

$$C_{\text{demand}}^{J} = C_{4}^{J} \quad \text{and} \quad C_{\text{demand}}^{p} = C_{4}^{p} \tag{3.5}$$

As discussed in Chapter 2 flux-control and concentration-control coefficients obey the following summation relationships:

$$C_{\text{supply}}^{J} + C_{\text{demand}}^{J} = 1 \tag{3.6}$$

$$C_{\text{supply}}^{p} + C_{\text{demand}}^{p} = 0 \tag{3.7}$$

While flux-control is distributed over the supply and the demand, p-control is not because C_{supply}^{p} is always equal to $-C_{\text{demand}}^{p}$. Therefore only the magnitude of the variation in p is of interest.

The sensitivity of the flux local to the supply block, or to rate in the case of the single demand reaction, is quantified by the relevant elasticity coefficient:

$$\varepsilon_{p}^{v_{\text{supply}}} = \frac{d \ln v_{\text{supply}}}{d \ln p}, \quad \varepsilon_{p}^{v_{\text{demand}}} = \frac{d \ln v_{\text{demand}}}{d \ln p} \tag{3.8}$$

Note that $\varepsilon_{p}^{v_{\text{demand}}}$ is typically positive because P is a substrate of the demand; an increase in substrate concentration typically increases the reaction rate. The product elasticity coefficient $\varepsilon_{p}^{v_{\text{supply}}}$ is typically negative because P is a product of the supply that inhibits the supply rate through product inhibition and mass action.

The connectivity theorems relate control coefficients to elasticity coefficients as follows:

$$C_{\text{supply}}^{J}\varepsilon_{p}^{v_{\text{supply}}} + C_{\text{demand}}^{J}\varepsilon_{p}^{v_{\text{demand}}} = 0 \tag{3.9}$$

$$C_{\text{supply}}^{p}\varepsilon_{p}^{v_{\text{supply}}} + C_{\text{demand}}^{p}\varepsilon_{p}^{v_{\text{demand}}} = -1 \tag{3.10}$$

Together, the summation and connectivity theorems allow the expression of control coefficients in terms of elasticities of supply and demand [11]. The flux-control coefficients are

$$C_{\text{supply}}^{J} = \frac{\varepsilon_{p}^{v_{\text{demand}}}}{\varepsilon_{p}^{v_{\text{demand}}} - \varepsilon_{p}^{v_{\text{supply}}}} \tag{3.11}$$

and

$$C_{\text{demand}}^{J} = \frac{-\varepsilon_{p}^{v_{\text{supply}}}}{\varepsilon_{p}^{v_{\text{demand}}} - \varepsilon_{p}^{v_{\text{supply}}}} \tag{3.12}$$

and the concentration-control coefficients:

$$C_{\text{supply}}^{p} = -C_{\text{demand}}^{p} = \frac{1}{\varepsilon_{p}^{v_{\text{demand}}} - \varepsilon_{p}^{v_{\text{supply}}}} \tag{3.13}$$

From eqns. 3.12 and 3.13 it follows that the ratio of elasticities determines the distribution of flux-control between supply and demand [14]. If $|\varepsilon_p^{v_\text{supply}}/\varepsilon_p^{v_\text{demand}}| > 1$ the demand has more control over the flux than the supply; if $|\varepsilon_p^{v_\text{supply}}/\varepsilon_p^{v_\text{demand}}| < 1$ the demand has less control over the flux than the supply. On the other hand it is the sum of the absolute values of the elasticities that determines the magnitude of the variation in p and, therefore, the degree to which it is buffered: the larger $|\varepsilon_p^{v_\text{demand}} - \varepsilon_p^{v_\text{supply}}|$, the smaller the absolute values of both C_supply^p and C_demand^p, and the better the buffering of p.

The behaviour of a supply-demand system around a steady state can be visualised with combined *rate characteristics*. A rate characteristic is a graph that shows how the rate through a reaction (or the flux local to a reaction block) varies with the concentration of a chemical species that affects that reaction (such as a substrate, a product, or an effector). If the rate characteristic is plotted in double logarithmic space the slope of the tangent to the rate characteristic at a particular species concentration is equal to the elasticity coefficient that obtains at that concentration [9].

If the rate characteristics for the supply and demand blocks are plotted on the same graph they intersect at a point that represents the steady state, which is characterised by the flux, J, and concentration $\bar{p}$.[1] Rate characteristics therefore also illustrate the result from control analysis that the response in the steady state to small perturbations in the activities of supply or demand depends completely on the slopes of the tangents to the rate characteristics at the steady-state point, i.e., their elasticity coefficients [14].

The log-log rate characteristics of supply and demand for the four parameter sets are shown in Fig. 3.2. They were calculated with PySCeS by fixing the concentration of P (making it a parameter) and varying it over a large concentration range that extends up to the equilibrium concentration of P at 10^4.

Parameter set 1—Fig. 3.2-1

The black supply rate characteristic is compared to the red demand rate characteristics for four different demand activities. The four steady states are numbered and describe different situations:

1. Steady state 1: $|\varepsilon_p^{v_\text{supply}}/\varepsilon_p^{v_\text{demand}}| \ll 1$, so that supply controls the flux. The steady-state concentration of P is lower than its E_4-Michaelis con-

---

[1]Steady-state concentrations of metabolites a, b, and p will be denoted by $\bar{a}$, $\bar{b}$, and $\bar{p}$.
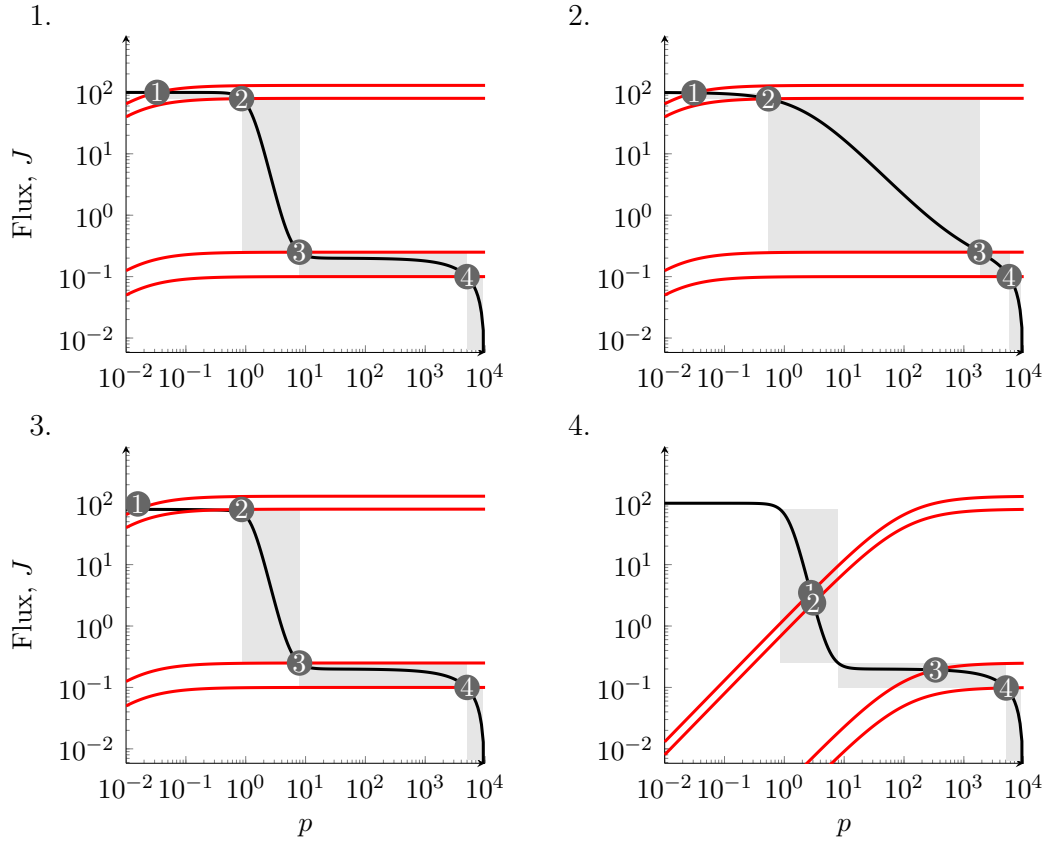
Figure 3.2: Combined rate characteristics around regulatory metabolite P for the supply and for four different V_f-values of the demand (130, 80, 0.25, 0.1). The numbering of the four graphs corresponds to parameter sets 1 to 4.

stant so that E_4 is not saturated with P, as it is at the other steady states.

2. Steady state 2: $|\varepsilon_p^{v_{\text{supply}}}/\varepsilon_p^{v_{\text{demand}}}| \gg 1$, so that demand controls the flux. This is the top limit (determined by V_{f1}) of the region in which the supply flux responds sensitively to p orders of magnitude away from equilibrium.

3. Steady state 3: $|\varepsilon_p^{v_{\text{supply}}}/\varepsilon_p^{v_{\text{demand}}}| \gg 1$, so that demand controls the flux. This is the bottom limit (determined by α) of the region in which the supply flux responds sensitively to p orders of magnitude away from equilibrium.

4. Steady state 4: $|\varepsilon_p^{v_{\text{supply}}}/\varepsilon_p^{v_{\text{demand}}}| \gg 1$, so that demand controls the flux, but here at a near-equilibrium concentration of P (determined by $K_{\text{eq1}} \cdot K_{\text{eq2}} \cdot K_{\text{eq3}} = 10^4$).

There are two distinct P-concentration regions in which p is buffered with respect to changes in the flux caused by changes in the demand activity, namely the region between steady states 2 and 3—the region of *kinetic regulation*—and the region above steady state 4;—the region of *thermodynamic regulation*. Where in the concentration range the region of kinetic regulation occurs depends on $p_{0.5} = 1$, while the steepness of supply flux response to p (degree of cooperativity) is determined by the Hill coefficient of E_1. The range of possible supply-flux response to p depends on the difference between V_{f1} (the plateau between steady states 1 and 2) and α (the plateau between steady states 3 and 4).

Parameter set 2—Fig. 3.2-2

The decrease in the Hill coefficient from $h = 4$ to $h = 1$ (non-cooperative binding by P) decreases the supply slope between steady states 2 and 3 so that in the kinetic regulation region p now varies over a concentration range of approximately 2000 instead of 10.

Parameter set 3—Fig. 3.2-3

Superficially, this graph appears to be identical to Fig. 3.2-1, although close inspection reveals that the steady states at 1 and 2 are slightly lower. In this parameter set the concentrations of enzymes 2 and 3 are 10-fold lower than in parameter sets 1, 2 and 4 so that the three biosynthetic enzymes have the same flux-carrying capacity. The effect of this on flux control by the three supply enzymes is discussed at the end of this chapter.

Parameter set 4—Fig. 3.2-4

The supply the identical to that in Fig. 3.2-1. Here the demand binds its substrates very weakly (K_{4P} is now 100 instead of 0.01). At steady states 1, 2 and 3 the elasticities of supply and demand have similar magnitudes, which results in sharing of flux control between supply and demand. In steady state 4 demand regains flux control.

3.2 Parameter portraits for E_4 (a demand scan)

Whereas rate characteristics provide insight into the response of metabolic subsystems to a metabolite that links them, a parameter portrait shows how steady-state variables and other derived entities such as the coefficients of MCA vary over a range of values of one of the system parameters. In Fig. 3.2 the steady states corresponding to four different demand-values were shown. In this section the demand for P is now continuously scanned by changing the concentration of E_4. The E_4-parameter portraits of concentrations and fluxes in Fig. 3.3-A are plotted in double logarithmic space; the slopes of these curves are equal to the response coefficients of E_4 that are plotted in Fig. 3.3-B. Since the elasticity coefficient of v_4 with respect to its enzyme concentration e_4 is 1, *these response coefficients are equal to their respective control coefficients.*

First, the general features of the parameter plots are discussed. For parameter sets 1, 2 and 3 the flux J is fully controlled by E_4, i.e., $R_4^J = 1$, in that part of the E_4-range that corresponds to the demands that yield steady states 2 and 4 in Fig. 3.2-1–3. In this range two distinct regions are discernible in which the steady-state concentrations of the internal metabolite are buffered: at low e_4 they are buffered near equilibrium (below steady state 4 in Fig. 3.2), while in the adjacent region they are buffered at concentrations orders of magnitude away from equilibrium. At $e_4 > 10^2$ flux control shifts abruptly to the supply (the region around steady state 1 in Fig. 3.2). These three regions will be denoted the NE-region (near equilibrium region), the FFE-region (far from equilibrium region), and the SC-region (region where supply controls the flux). In the NE-region the high metabolite concentrations would interfere with optimal cellular function as the solvent capacity of the cell is limited. In the SC-region, on the other hand, the supply is incapable of matching the high demand and cannot fulfil its function of supplying P fast enough. The FFE-region is therefore the region in which supply can fulfil its physiological function of supplying P while keeping $\bar{p}$ far from equilibrium.

An observation that will be important for the discussion of homeostasis in Chapters 4 and 6 is that in the NE and FFE-regions the metabolite concentrations are kept within a narrow range despite a proportional change in flux J with E_4. Exceptions include the FFE-region of parameter set 2 where all metabolite concentrations vary over a much larger range of approximately 2000 instead of 10, and the higher e_4 range in the FFE-region of parameter

27
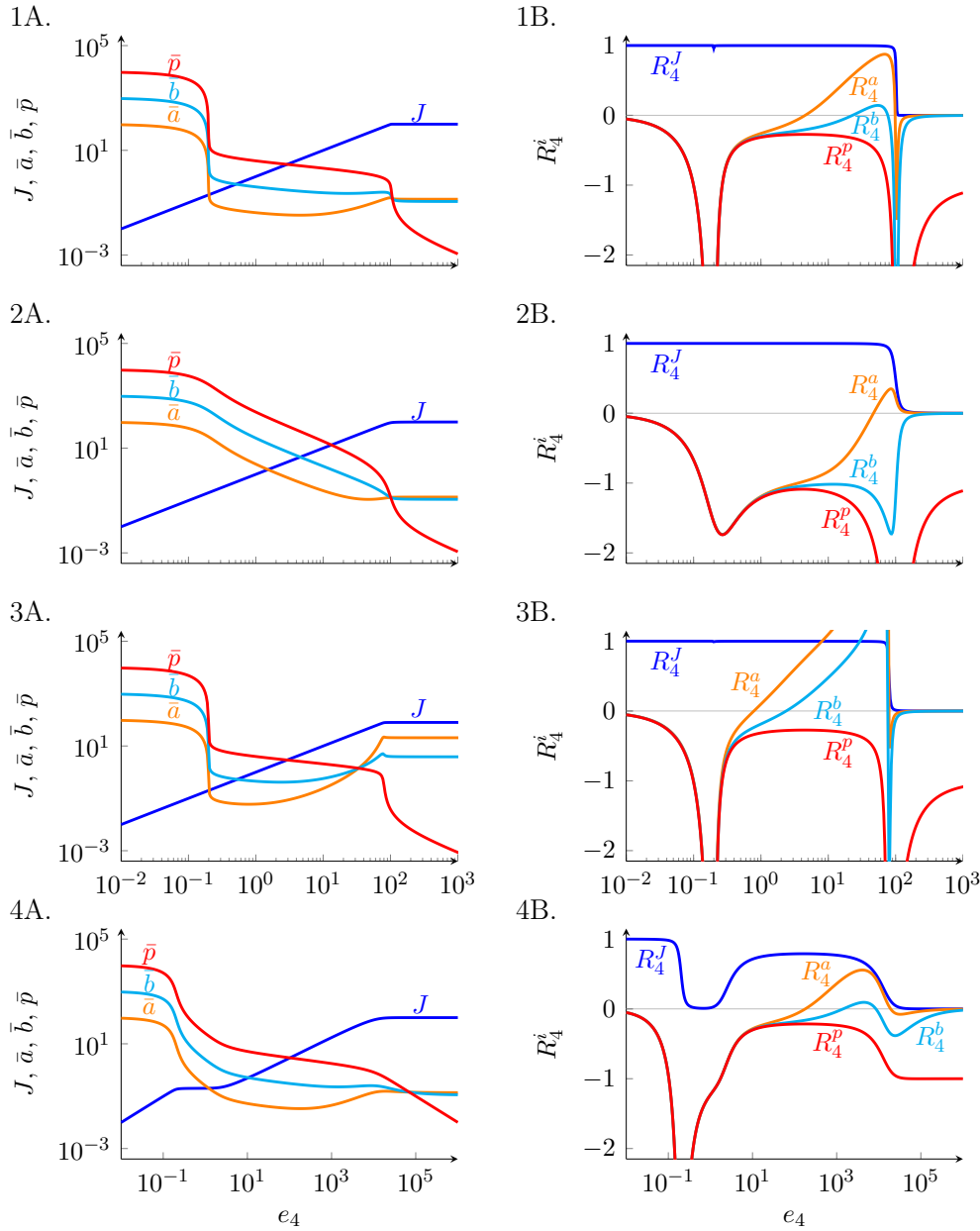
Figure 3.3: E_4-parameter portraits of the flux and steady-state concentrations (A) and corresponding E_4-response coefficient plots (B) for parameter sets 1 to 4. Colours are used here only to distinguish the lines and not to refer to the steps of the system.

sets 3 where a and b no longer track p and obtain much greater steady-state values. In the SC-region only $\bar{p}$ changes while $\bar{a}$ and $\bar{b}$ remain constant. Unlike the thermodynamic buffering in the NE-region and the kinetic buffering in the FFE-region, here the constancy in $\bar{a}$ and $\bar{b}$ is due to the fact that the flux does not change with a change in e_4 and not to any regulatory mechanism. That

$\bar{p}$ is required to decrease with an increase in e_4 is obvious if the rate equation
for E_4 is re-arranged as follows:

$$\bar{p} = \frac{J \cdot K_{4P}}{k_4 e_4 - J} \tag{3.14}$$

with v_4 now equal to the constant flux, J.

The differences between parameter sets 1, 2 and 3 mostly affect the concentration profiles. While with parameter set 1 the transition between the NE and FFE-regions is very steep and separates two regions of excellent concentration buffering, this transition is more gradual with parameter set 2 and the buffering of all metabolites is much less effective, as can also be seen by comparing the concentration-control coefficients of these two parameter sets. In the FFE-region with parameter set 3 the lower activities of E_2 and E_3 cannot keep $\bar{a}$ and $\bar{b}$ at near-equilibrium concentrations relative to $\bar{p}$ at the higher e_4 end of the region, so that $\bar{a}$ and $\bar{b}$ stabilise at much higher concentrations than that for the other three parameter sets and, as R_4^a and R_4^b in Fig. 3.3-3B show, become much more sensitive to changes in e_4 as compared to parameter set 1.

Parameter set 4 presents a scenario that differs from the other sets in that here the demand is 10^4 times less sensitive to its substrate P. The first consequence is that e_4-values of up to 10^6 are needed to present a response profile similar to that of the other parameter sets. As is clear from the flux-response coefficients and concentration-response coefficients, the main difference is that the demand has full flux control only in the NE-region. During the transition to the FFE-region the demand loses flux control completely, and regains it partially in the FFE-region. Why the demand loses flux-control during the transition from NE to FFE can be understood by examining the slopes of the rate characteristics for this parameter set at steady state 3 in Fig. 3.2-4: during the transition the demand elasticity exceeds the supply elasticity, which approaches zero, shifting flux control to the supply. The other marked difference is that the transition from the FFE to the SC-region at the end of which $\bar{a}$ and $\bar{b}$ become constant and R_4^a and R_4^b become zero is not as abrupt as with the other parameter sets.

The concentration-response coefficients—how they change with e_4 and how these changes can be understood in terms of chains of local effects that reverberate through the system—are the subject of Chapter 5, which discusses the relationship of these coefficients with structural stability, a concept introduced in the next chapter.
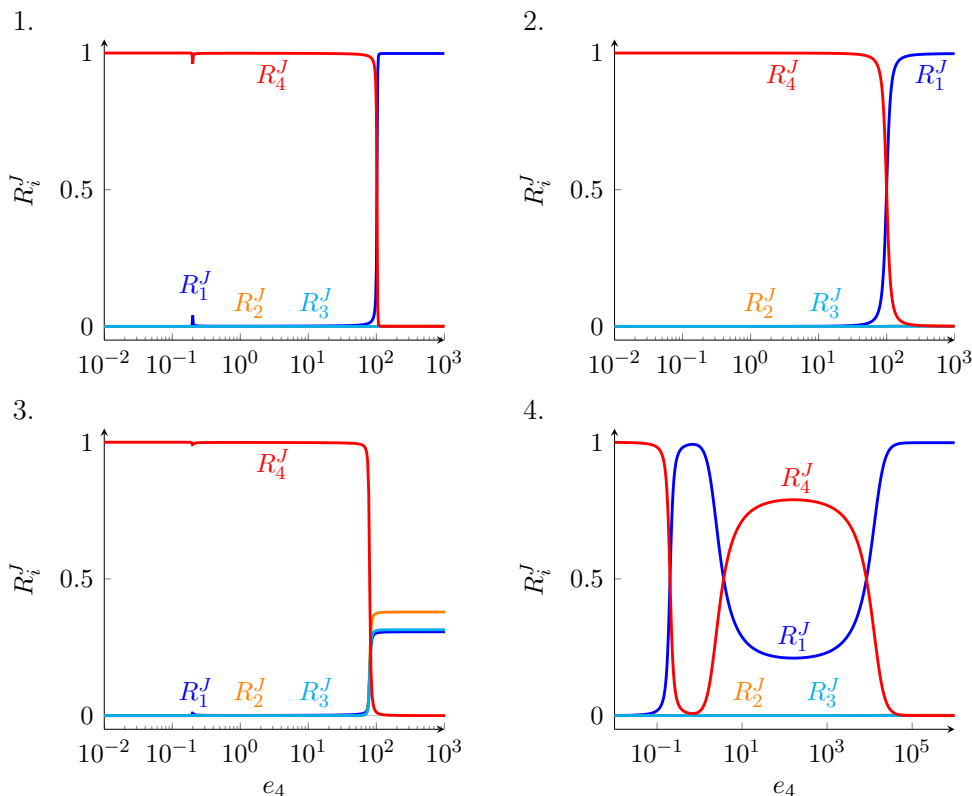
Figure 3.4: E_4-parameter portrait of flux-response coefficients for parameter sets 1 to 4.

We now consider in more detail the *control of flux* by the supply and demand enzymes for the four parameter sets. Whereas Fig. 3.3 showed only how R_4^J responded to e_4, Fig. 3.4 also shows the response in the flux-control coefficients of the three supply enzymes.

First, it is clear that in all parameter sets except in parameter set 3 the control of flux is shared between E_1 and E_4 only. In parameter sets 1 and 2 E_1 gains full control in the SC-region, while having no control in the other two regions. Why parameter set 4 differs from parameter set 1 and 2 has been discussed above.

Parameter set 3 differs markedly from the others in the SC-region: the control of flux is now nearly evenly shared between the three supply enzymes, instead of fully residing in E_1. As mentioned earlier in this chapter, in parameter set 3 the concentration of enzymes 2 and 3 are 10-fold lower than in parameter sets 1, 2, and 4 so that the three biosynthetic enzymes have the same flux-carrying capacity. This and the associated increase in the $\bar{a}$ and $\bar{b}$ in the SC-region (at least two orders of magnitude higher that in the other cases)

results in sharing of flux control between E_1, E_2 and E_3 in the SC-region. We shall return to this in Chapter 6.

In later chapters we shall also need to know how *the concentration-control coefficients of* E_1, E_2, *and* E_3 vary with e_4, so we also provide these parameter portraits in Figs. 3.5–3.7, but without discussion.

To conclude this chapter the *elasticity coefficient profiles* for the four parameter sets in Fig. 3.8 are discussed because we shall need this information in subsequent chapters.

For all four parameter sets the substrate and product elasticities of enzymes 2 and 3 veer off to $\pm\infty$ in the NE and FFE-regions. The product elasticity $\varepsilon_a^{v_1}$ is zero in the FFE and SC-regions due to extremely weak binding of A to E_1. Only in the NE-region where $\bar{a}$ increases sharply does $\varepsilon_a^{v_1}$ fall away to $-\infty$. Because of the lower e_2 and e_3 in parameter set 3 the concentrations of A and B do not track that of P in the FFE-region, but actually increase (see Fig. 3.3-3A), so that the elasticity coefficients start increasing at much lower values of the scan parameter e_4. The other effect of the increased $\bar{a}$ and $\bar{b}$ in the SC-region is that $\varepsilon_a^{v_2}$ and $\varepsilon_b^{v_3}$ are less than 1 because of partial saturation of these enzymes with their substrates.

In the NE and FFE-regions E_4 is saturated with its substrate P and $\varepsilon_p^{v_4} = 0$. In the SC-region $\bar{p}$ decreases sharply and $\varepsilon_p^{v_4}$ increases to its maximum value of 1.

The feedback elasticity $\varepsilon_p^{v_1}$ is zero in the NE and SC-regions and only reaches its maximum value of -4 (or -1 in the case of parameter set 2 where the Hill coefficient is 1 instead of 4) in the FFE-region where it regulates the rate of E_1.

The next chapter introduces three important concepts for the treatment of metabolic regulation, namely structural and dynamic stability of steady states and homeostasis.

Figure 3.5: E_4-parameter portrait of concentration-control coefficients for A for parameter sets 1 to 4.

Figure 3.6: E_4-parameter portrait of concentration-control coefficients for B for parameter sets 1 to 4.

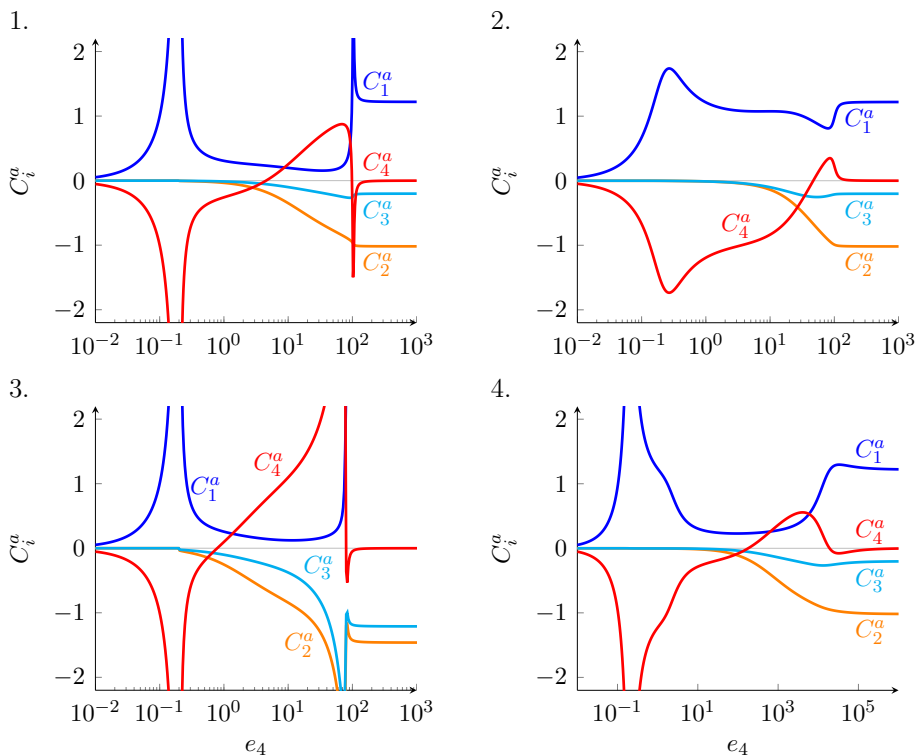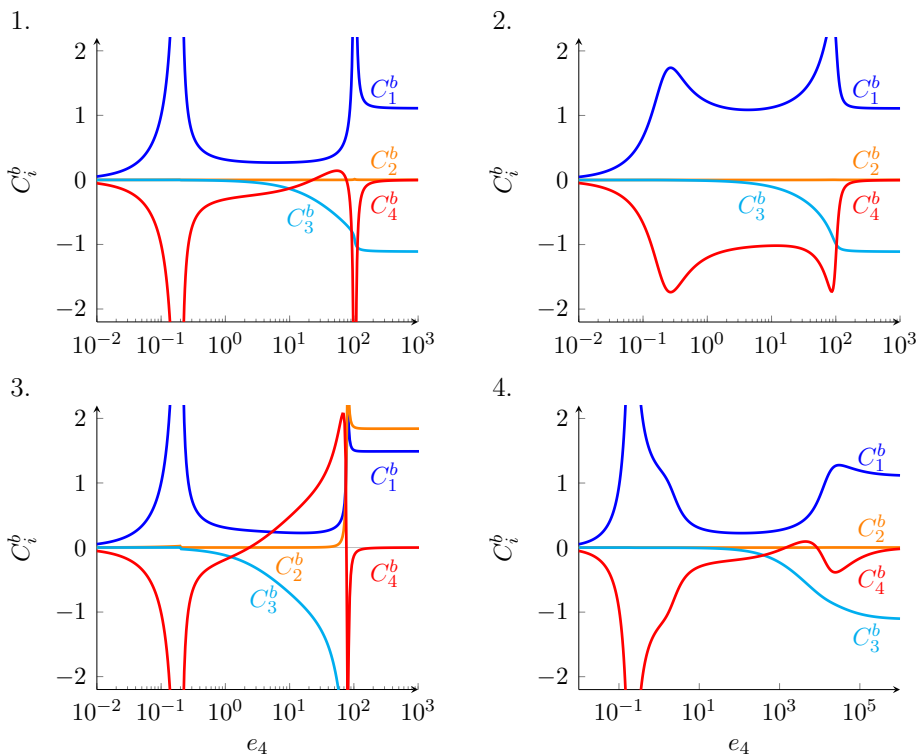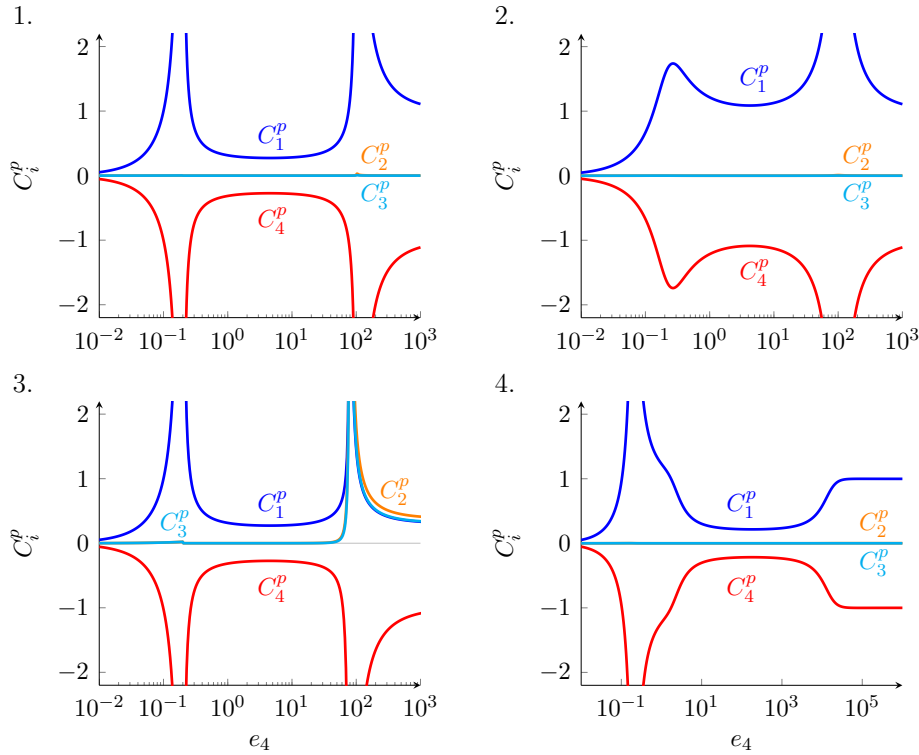Figure 3.7: E$_4$-parameter portrait of concentration-control coefficients for P for parameter sets 1 to 4.
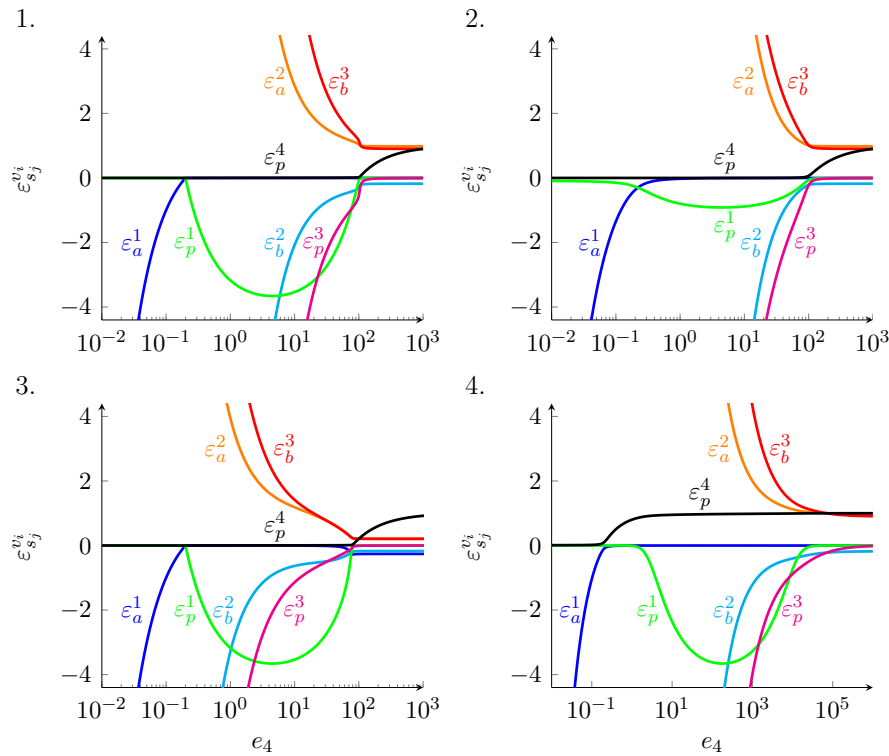
Figure 3.8: E$_4$-parameter portrait of elasticity coefficients for parameter sets 1 to 4.

33

Chapter 4

Interlude: The meaning of "metabolic homeostasis"

In general, an analysis of metabolic regulation is concerned with the responses of a steady state to perturbations. Whereas metabolic control analysis provides a way of quantifying these responses, metabolic regulation analysis seeks to understand which properties of the system determine these responses, and often, how these responses serve a particular metabolic function [9].

Consider a metabolic system in steady state. One can envisage two ways in which the system can be perturbed: either by a change in the activity of a particular step through a parameter such as enzyme concentration, or by a perturbation (or fluctuation) of a variable metabolite concentration. How does the system respond? In the case of a parameter change one wants to know to what degree the new steady state differs from the original one, i.e., how *structurally stable*[1] the system is. In the case of a variable metabolite change one wants to explain what drives the system back to the original steady state, i.e., what determines the *dynamic stability* of the system (the concepts of dynamic and structural stability are compared in Fig. 4.1). These questions are important for any inquiry into metabolic regulation, because both structural and dynamic stability have been linked to that of homeostasis [23, 33], causing much confusion in discussions of metabolic regulation.

In the first of a series of papers on metabolic regulation and supply-demand

---

[1]In dynamical systems theory a system is structurally stable if small changes in its parameters do not change the geometric type and stability of its steady states, be they fixed points or limit cycles [40], i.e. a system becomes structurally *unstable* at bifurcation points. The steady states of the system in this study are all structurally stable—for an understanding of metabolic regulation the *degree* of structurally stability is of importance, i.e., by how much the steady-state variables change relative to the parameter perturbation.
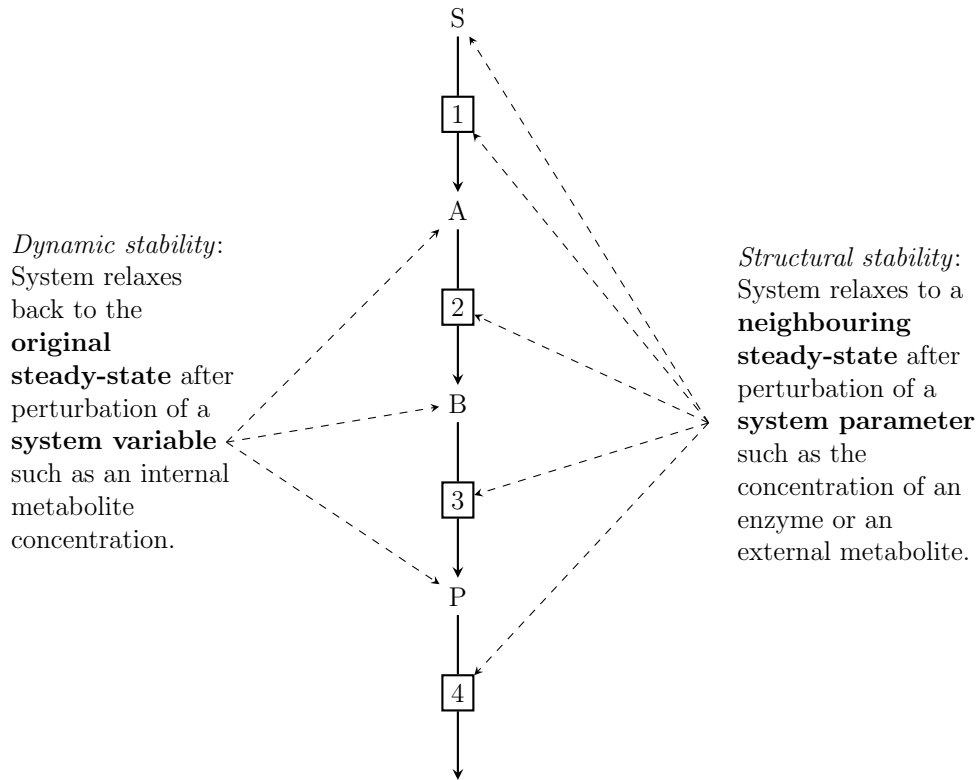
Figure 4.1: The difference between the concepts of dynamic and structural stability.

analysis, Hofmeyr and Cornish-Bowden [11] considered the relationship between metabolic regulation and homeostasis on the one hand, and regulation of technological systems such as a thermostatted water bath on the other:

> "In the technological systems that biochemists are fond of using as analogies for metabolic systems, the concept of regulation is intimately linked with the function for which such systems have been designed; it usually entails constancy of some property of the regulated system, such as the temperature in a thermostatically controlled water bath, in the face of external changes (this feature is equivalent to homeostasis in biological systems). Regulation is therefore evaluated in terms of the performance of the system, not in terms of the existence of specific mechanisms. Likewise, in metabolic systems, our interpretation of regulation of a steady state should be linked to our perception of the function of a specific pathway and, therefore, to certain measurable performance characteristics. With regard to choosing a suitable performance

35

characteristic there is a marked difference between treatments of technological and metabolic regulation. Rates seldom enter the discussion of technological systems, e.g., the rate at which heat flows from the heating element through the water and out through the container walls of a thermostatted water bath; the focus is usually on the constancy of some property such as temperature. However, for the biochemist the primary result of metabolic regulation is sensitive adjustment of the rates of processes, i.e., the adaptation of metabolic fluxes to changing external conditions. Various designs which achieve this goal efficiently have evolved; all of these designs automatically feature some degree of homeostasis of certain key metabolite concentrations. Nevertheless, despite the difference in emphasis, we think there is a reasonably exact parallel: In a water bath we do want to allow for variation in the flux of heat, but we do not want the "concentration" of heat (i.e., the temperature) to vary; *an effectively regulated metabolic system must likewise allow the flux of matter to vary with the least possible variation in metabolic concentrations. We judge the success of the design by how much the first can vary without variation in the second* (my italics).

The above considerations suggest which entities are appropriate for a quantitative analysis of metabolic regulation:

- *Response coefficients* quantify the sensitivity of the steady-state variables with respect to parameter perturbations and are therefore the appropriate measures of *structural stability*.

- The change in a metabolite concentration relative to the change in the flux through that metabolite pools is quantified by a *co-response coefficient*, and is therefore an appropriate measure of *homeostasis*.

- The connectivity relationships of MCA describe the stability of a steady state with respect to fluctuations in the internal metabolites. *Internal-response coefficients* are therefore the appropriate measures of *dynamic stability*.

The next three chapters explore these three aspects of metabolic regulation using the metabolic system in Fig. 3.1 with its four parameter sets as model system.

36

Chapter 5

Structural stability and response coefficients

As noted in the previous chapter the change in the steady-state concentrations of internal metabolites caused by a change in a system parameter is quantified by the set of concentration-response coefficients with respect to that parameter.

Consider again a perturbation $\delta \ln e_4$ in the concentration of enzyme E_4 of the system in Fig. 3.1. The E_4 perturbation causes a change in the rate

$$\delta \ln v_4 = \varepsilon_{e_4}^{v_4} \cdot \delta \ln e_4 \tag{5.1}$$

This increase in rate decreases the concentration of P, which initiates a chain of local effects through the rest of the system that culminates in a new steady state in which the concentrations of A, B, and P have changed by $\delta \ln a$, $\delta \ln b$, and $\delta \ln p$ respectively. The magnitude of these changes depend on the respective concentration-control coefficients:

$$\delta \ln a \;=\; C_4^a \cdot \delta \ln v_4 = C_4^a \varepsilon_{e_4}^{v_4} \cdot \delta \ln e_4 \tag{5.2}$$

$$\delta \ln b \;=\; C_4^b \cdot \delta \ln v_4 = C_4^b \varepsilon_{e_4}^{v_4} \cdot \delta \ln e_4 \tag{5.3}$$

$$\delta \ln p \;=\; C_4^p \cdot \delta \ln v_4 = C_4^p \varepsilon_{e_4}^{v_4} \cdot \delta \ln e_4 \tag{5.4}$$

The partitioned-response equations follow:

$$R_4^a \;=\; \frac{\delta \ln a}{\delta \ln e_4} = C_4^a \varepsilon_{e_4}^{v_4} \tag{5.5}$$

$$R_4^b \;=\; \frac{\delta \ln b}{\delta \ln e_4} = C_4^b \varepsilon_{e_4}^{v_4} \tag{5.6}$$

$$R_4^p \;=\; \frac{\delta \ln p}{\delta \ln e_4} = C_4^p \varepsilon_{e_4}^{v_4} \tag{5.7}$$

which, because of the proportionality of rate to enzyme concentration, which implies that $\varepsilon_{e_4}^{v_4} = 1$, reduce to:

$$
\begin{align}
R_4^a &= C_4^a \tag{5.8} \\
R_4^b &= C_4^b \tag{5.9} \\
R_4^p &= C_4^p \tag{5.10}
\end{align}
$$

How these concentration-response coefficients of E_4 change when e_4 is scanned has already been shown in the parameter portraits in Fig. 3.3 for the four parameter sets. However, the question is not just how they change, but especially how the interactions in the system contribute to these changes. It is here where the control patterns discussed in Section 2.11 come into play.

5.1 Control-pattern analysis of response coefficients

Any control coefficient can be expressed as a function of elasticity coefficients. In section 2.11 these expressions were given for the system in Fig. 3.1. The three concentration-control coefficients for E_4 are:

$$
\begin{align}
C_4^a &= (-\varepsilon_b^2\varepsilon_p^3 - \varepsilon_b^3\varepsilon_p^1 + \varepsilon_b^2\varepsilon_p^1)/\Sigma \tag{5.11} \\
C_4^b &= (\varepsilon_a^2\varepsilon_p^3 - \varepsilon_a^1\varepsilon_p^3 - \varepsilon_a^2\varepsilon_p^1)/\Sigma \tag{5.12} \\
C_4^p &= (-\varepsilon_a^2\varepsilon_b^3 + \varepsilon_a^1\varepsilon_b^3 - \varepsilon_a^1\varepsilon_b^2)/\Sigma \tag{5.13}
\end{align}
$$

where

$$\Sigma = \varepsilon_a^2\varepsilon_b^3\varepsilon_p^4 - \varepsilon_a^1\varepsilon_b^3\varepsilon_p^4 + \varepsilon_a^1\varepsilon_b^2\varepsilon_p^4 - \varepsilon_a^1\varepsilon_b^2\varepsilon_p^3 - \varepsilon_a^2\varepsilon_b^3\varepsilon_p^1$$

Each numerator term, a product of elasticity coefficients with its associated sign, is called a control pattern, which, when scaled by the denominator, can be assigned a numerical value. The scaled control patterns then sum to the control coefficient. A control pattern represents a chain of local effects from the perturbed step to the metabolite with respect to which the control coefficient is defined. Consider, for example, the three control patterns in C_4^a and remember that substrate elasticities are positive, product elasticities are negative, and the feedback elasticity ε_p^1 is negative:

- $-\varepsilon_b^2\varepsilon_p^3$: The immediate effect of an increase in v_4 is a decrease in p. The sequence of events that follow can be chased through the elasticities in

38

the pattern—the chain of local effects is by mass action up the reaction sequence, $\uparrow v_4 \downarrow p \uparrow v_3 \downarrow b \uparrow v_2 \downarrow a$. This pattern therefore decreases a and agrees with sign of the pattern $-(-)(-)$.

- $-\varepsilon_b^3\varepsilon_p^1$ and $+\varepsilon_b^2\varepsilon_p^1$: in both of these control patterns the chain of local effects is via the feedback loop $\uparrow v_4 \downarrow p \uparrow v_1 \uparrow a$. This part of the pattern is represented by $-\varepsilon_p^1$ which is positive $-(-)$. B does not participate in the chain of local effects from E_4 to A, but must nevertheless be represented in the control pattern: either by ε_b^3, a positive elasticity, or by $-\varepsilon_b^2$, which is also positive $-(-1)$). Both these patterns are therefore positive. What happens here is that the effect on a via this chain of local effects is modified by what happens in that part of the system that does not form part of the chain of local effects, i.e., $-\varepsilon_p^1(\varepsilon_b^3 - \varepsilon_b^2)$. The term in brackets is the denominator of expressions for control coefficients in the isolated subsystem from A to P that falls outside the chain of local effects (this aspect of the analysis of concentration-control patterns is fully discussed by Hofmeyr [8]).

In the case of C_4^b there are also two chains of local effects: up the chain from P, $\uparrow v_4 \downarrow p \uparrow v_3 \downarrow b$ (which is the ε_b^3 part of the two negative patterns $\varepsilon_a^2\varepsilon_p^3$ and $-\varepsilon_a^1\varepsilon_p^3$) and the positive pattern via the feedback loop $\uparrow v_4 \downarrow p \uparrow v_1 \uparrow a \uparrow v_2 \uparrow b$.

In the case of C_4^p there is only one direct local effect, namely $\uparrow v_4 \downarrow p$ and that can only be represented by -1. What happens in the rest of the system from S to P falls outside this local effect and must be represented by the denominator of control coefficients local to the isolated supply subsystem, which is $(\varepsilon_a^2\varepsilon_b^3 - \varepsilon_a^1\varepsilon_b^3 + \varepsilon_a^1\varepsilon_b^2)$, all positive patterns, which are multiplied with -1 to give the negative control patterns for C_4^p.

Therefore, whereas C_4^p is always negative, C_4^a and C_4^b can be positive or negative, depending on the relative contribution of their control patterns.

Let us now consider the quantitative behaviour of R_4^a, R_4^b, R_4^p and their respective control patterns for our system with the four parameter sets. Figs. 5.1–5.3 show the response coefficients in the A-panel and the corresponding control patterns in the B-panel (note again that, although we continue to use the term response coefficients for E_4 they are in our system equivalent to control coefficients of E_4).

To reiterate, concentration-response coefficients quantify the sensitivities of the state variables to changes in a parameter. The greater the magnitude of these sensitivities, the less structurally stable the system is. A concentration-

response coefficient of zero indicates perfect structural stability with respect to the metabolite in question. However, it is possible that while the steady state is structurally stable with respect to one or more metabolites it is less stable with respect to others.

In general, in the discussion that follows, we shall regard a metabolite to be structurally stable with respect to a particular perturbation when it has a concentration-response coefficient between -1 and 1.

The one common feature of the response coefficient profiles for all three metabolites and all four parameter sets is that the system is much less structurally stable at the transitions between the regions than in the regions themselves, although the degree of instability differs markedly. Very near equilibrium and in the FFE-region P is structurally the most stable of the three metabolites. In the FFE-region C_4^a and C_4^b can change sign and vary more than C_4^p, especially with parameter set 3 where the weaker activity of E_2 and E_3 fail to keep $\bar{a}$ and $\bar{b}$ in sync with $\bar{p}$ causing very large values of C_4^a and C_4^b.

What is of even more interest here is to analyse the contributions of the control patterns to the control coefficients, because that provides insight into which chains of local effects determine the structural stability of a particular metabolite with respect to, in this case, a perturbation in e_4. For A and B the mass-action control pattern $-\varepsilon_b^2\varepsilon_p^3$ up the chain dominates the control coefficient in the NE-region and at least in the lower part of the FFE-region. In the SC-region all the control patterns are zero. Only in the upper part of the FFE-region do the other control patterns via the feedback loop contribute substantially to the control coefficients. For C_4^a, it actually makes more sense to add the two $\varepsilon_p^{v_1}$-containing patterns together since they represent the same chain of local effects from E_4 to A; the same holds for the two $\varepsilon_p^{v_3}$-containing patterns of C_4^b. In the case of C_4^b only one of these feedback control patterns operate since the other one contains $\varepsilon_a^{v_1}$ which is zero in the NE and FFE-regions.

In the NE and FFE-regions of Fig. 5.3 C_4^p is completely determined by one of the control patterns $(-\varepsilon_a^2\varepsilon_b^3)$ in the upstream pathway. Note again that the chain of local effects in this case is a direct one from E_4 to P with a value of -1. The three patterns are terms in the control coefficient denominator of the subsystem outside the chain of local effects, i.e., from P up the chain to S. Two of these patterns contain the elasticity coefficient $\varepsilon_a^{v_1}$, which is zero in the FFE and SC-regions. Furthermore, even though $\varepsilon_a^{v_1}$ becomes large in the NE-region causing $-\varepsilon_a^1\varepsilon_b^2$ and $\varepsilon_a^1\varepsilon_b^3$ to increase dramatically, the combined effect of two
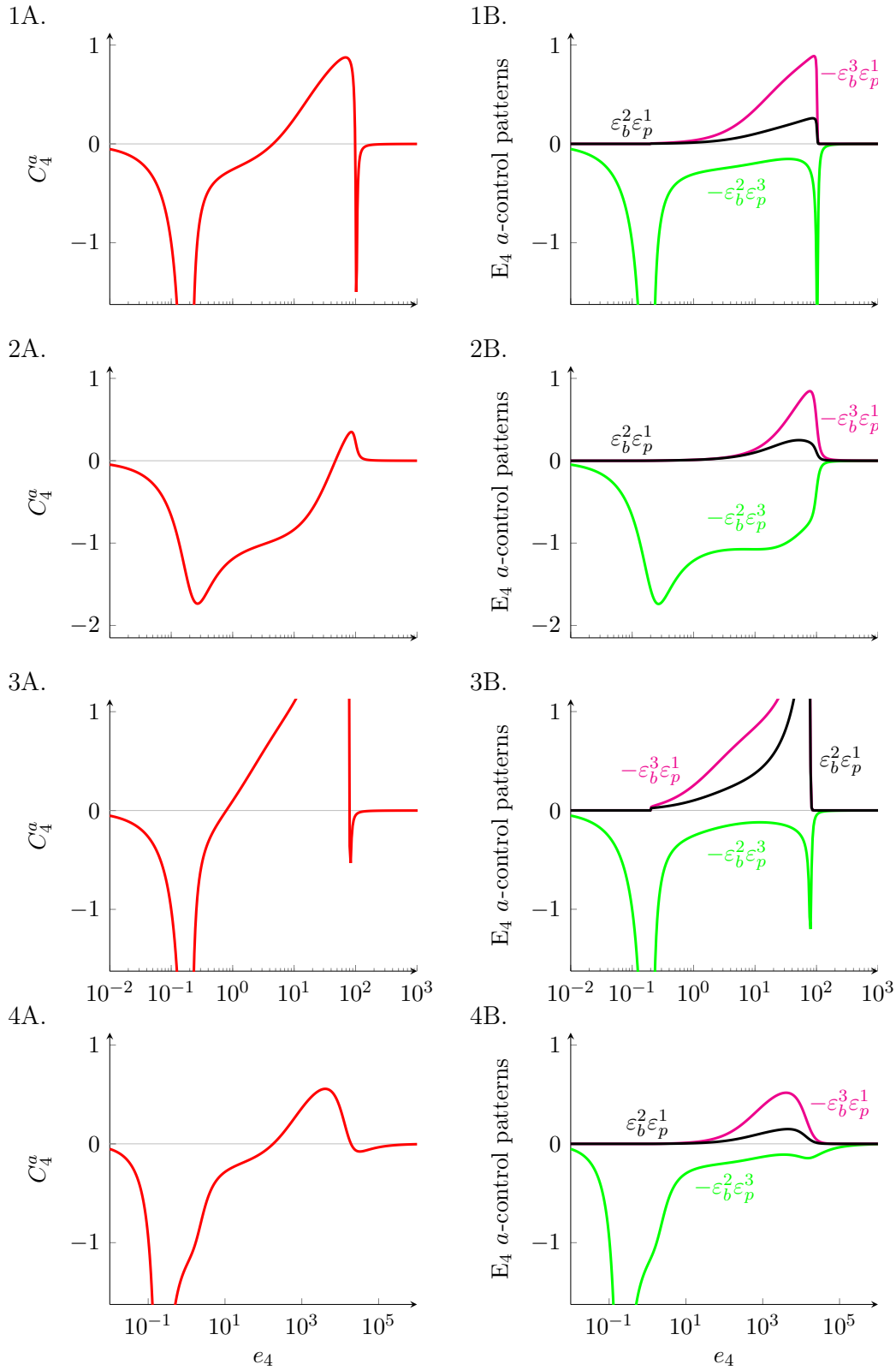
Figure 5.1: E_4-parameter portrait of C_4^a (A) and its control patterns (B) for parameter sets 1 to 4.
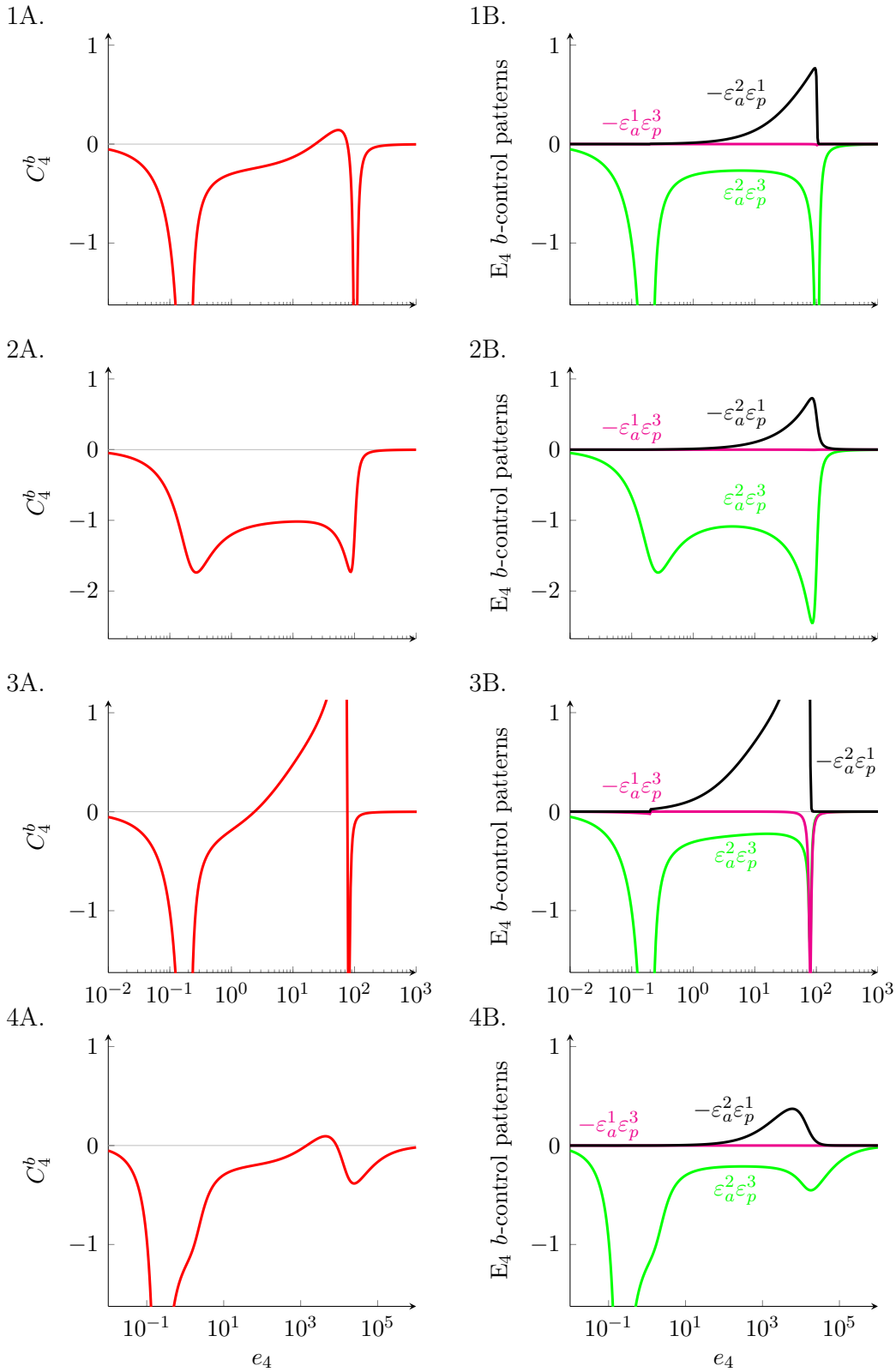
Figure 5.2: E_4-parameter portrait of C_4^b (A) and its control patterns (B) for parameter sets 1 to 4.
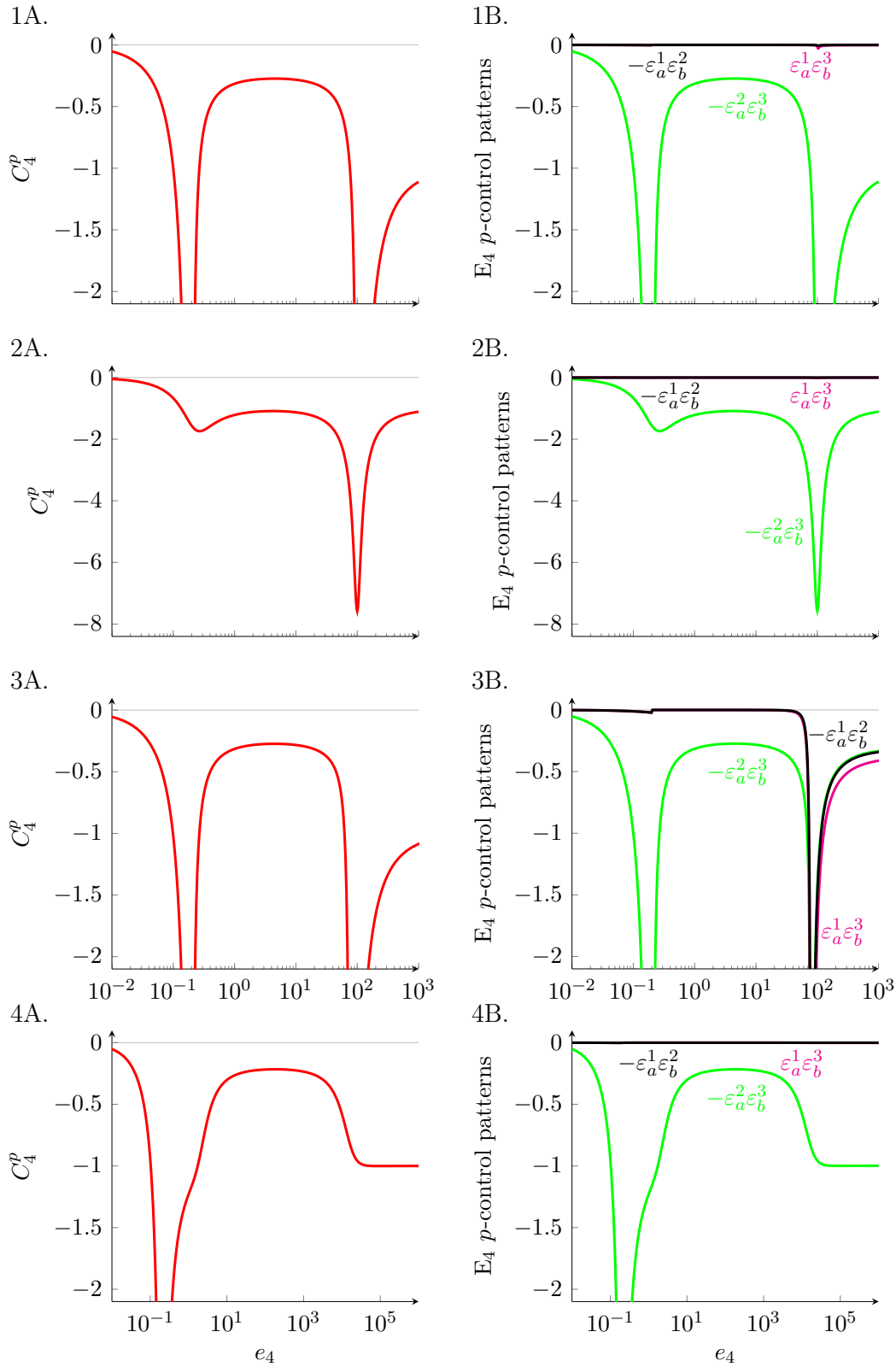
Figure 5.3: E_4-parameter portrait of C_4^p (A) and its control patterns (B) for parameter sets 1 to 4.

even larger elasticities in the $-\varepsilon_a^2\varepsilon_b^3$ pattern makes their contribution to the control coefficient negligible. In the next pages the concentration-response coefficients and their control patterns of E$_1$ (Figs. 5.4–5.6), E$_2$ (Figs. 5.7–5.9), and E$_3$ (Figs. 5.10–5.12) are given. C_1^p, C_2^p, and C_3^p in Fig. 5.6, Fig. 5.9, and Fig. 5.12 respectively have only one control pattern which is of course identical to the response coefficient.

The a-concentration-response coefficient profile of E$_1$ in Fig. 5.4-A is a mirror around the horizontal of that of E$_4$ in Fig. 5.1-A. A is structurally stable with respect to changes in e_1 in the NE and FFE-regions, except for the highly unstable transition between regions. The profiles of C_1^a, C_1^b, and C_1^p in Figs. 5.4–5.6 are qualitatively the same, only differing around the FFE to SC transition. In the NE and FFE-regions the determining control pattern is the one via the the chain ($\varepsilon_b^2\varepsilon_p^3$, $-\varepsilon_a^2\varepsilon_p^3$, and $\varepsilon_a^2\varepsilon_b^3$ for C_1^a, C_1^b, and C_1^p respectively). In the SC region the control patterns that contain ε_p^4 determine the concentration response.

The trend in the concentration-response coefficients profiles of E$_2$ and E$_3$ is that, for metabolites that lie upstream from the enzyme, the coefficients are zero in the NE-region and start increasing in the FFE-region towards a constant value in the SC-region. In the FFE-region the feedback control pattern containing ε_p^1 is determining while in the SC-region the mass-action pattern up the chain is determining. For the metabolites that lie downstream the response coefficients are either very small (C_2^b in Fig. 5.8) or zero (C_2^p in Fig. 5.9 and C_3^p in in Fig. 5.12).

An important general conclusion to be made from all these results is that what makes a control pattern determining is usually not due to the values of the elasticity coefficients that make up the pattern, but because the other patterns are zero because they contain a zero elasticity coefficient. In our system these elasticity coefficients are $\varepsilon_a^{v_1}$, $\varepsilon_p^{v_1}$, and $\varepsilon_p^{v_4}$.

With regard to the overall structural stability of the system the generalisation can be made that near equilibrium all metabolites are stable to perturbations of any reaction in the system. This should be obvious, since any system in equilibrium is structurally perfectly stable to perturbations in any reaction. In the FFE-region the metabolites are also structurally stable, but much less so with parameter set 2 where the Hill-coefficient and therefore the sensitivity of feedback to changes in P is less than with the other parameter sets where the Hill coefficient is 4.
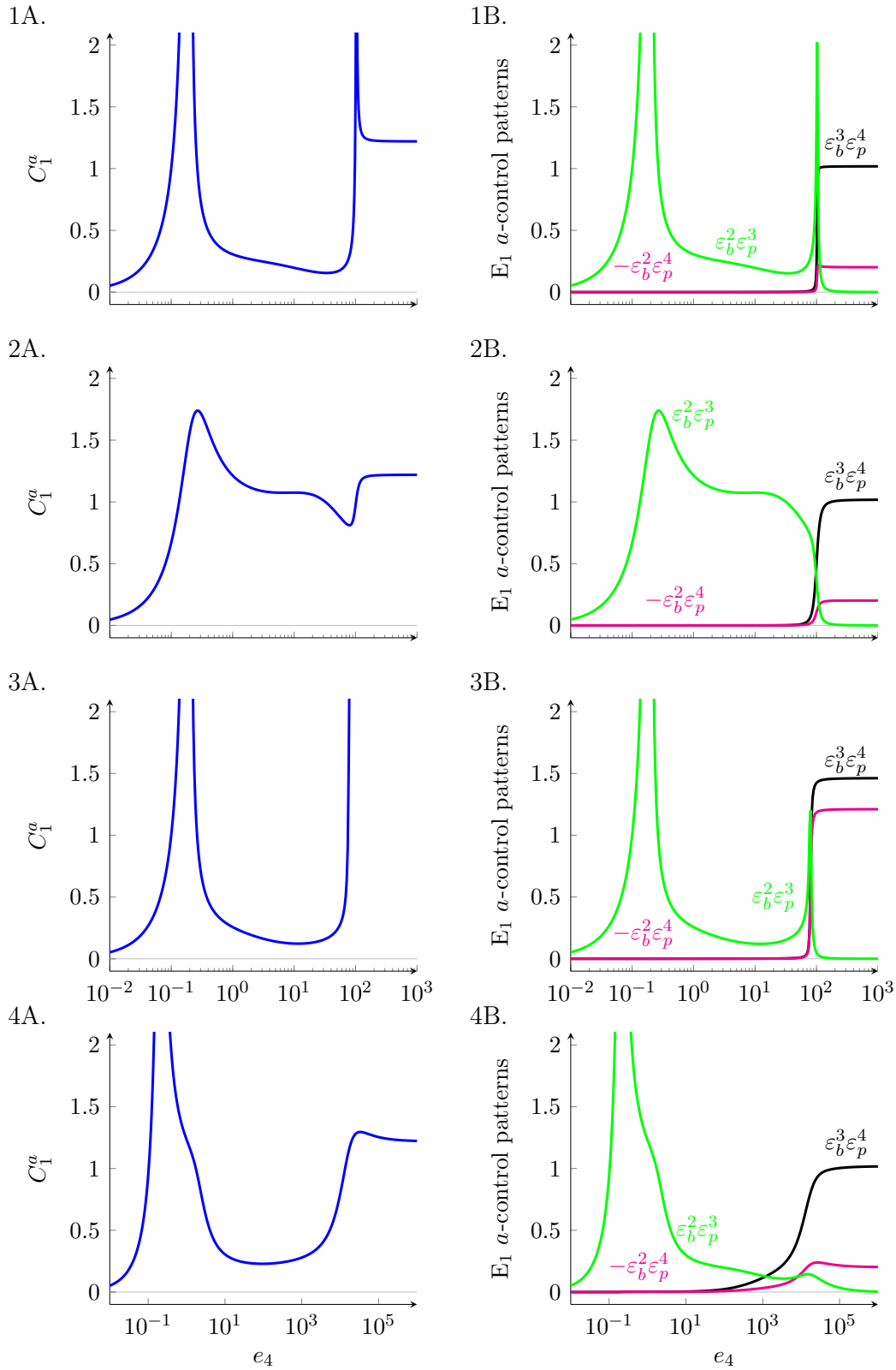
Figure 5.4: E_4-parameter portrait of C_1^a (A) and its control patterns (B) for parameter sets 1 to 4.
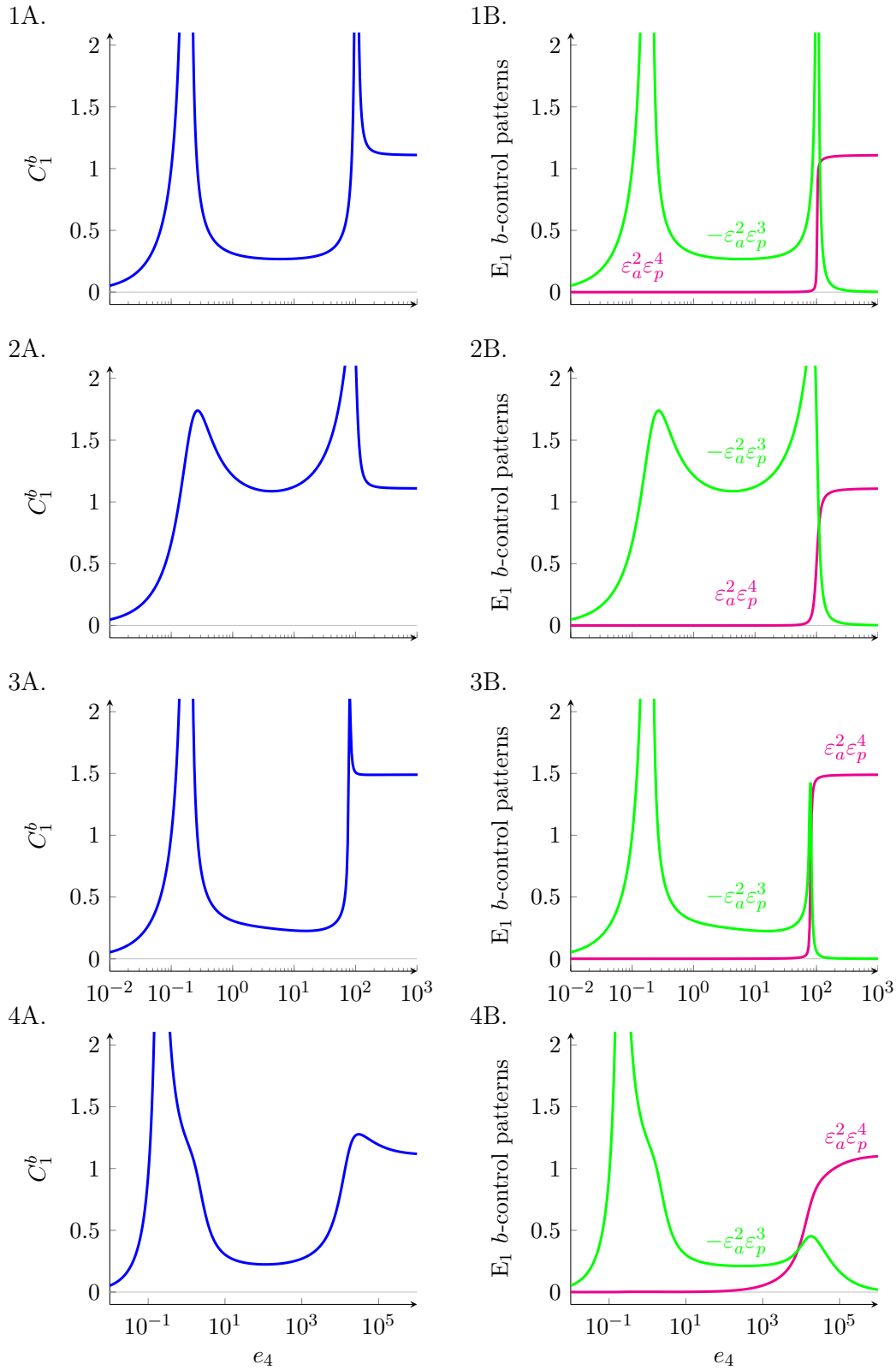
Figure 5.5: E_4-parameter portrait of C_1^b (A) and its control patterns (B) for parameter sets 1 to 4.
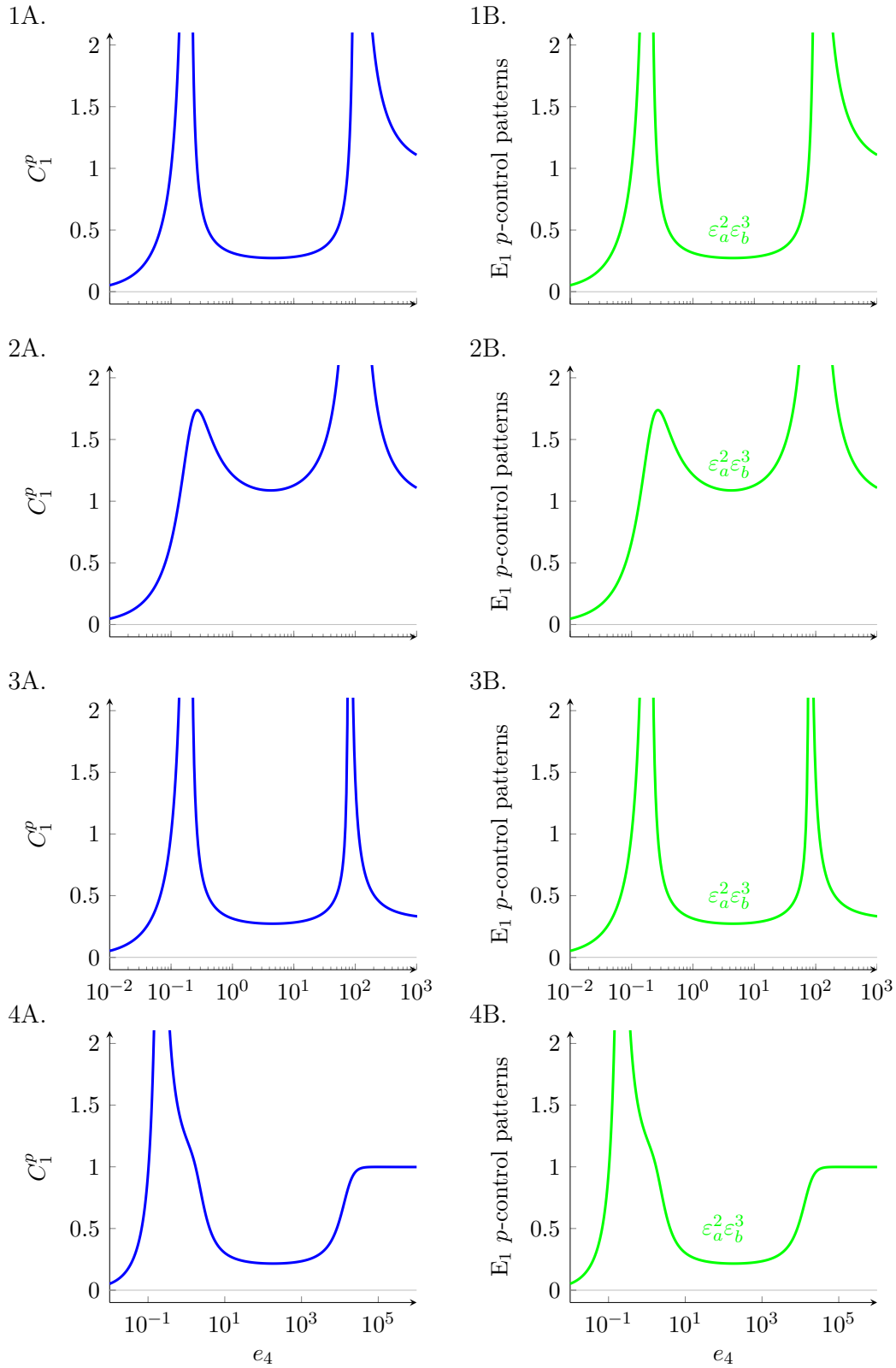
Figure 5.6: E_4-parameter portrait of C_1^p (A) and its control patterns (B) for parameter sets 1 to 4.
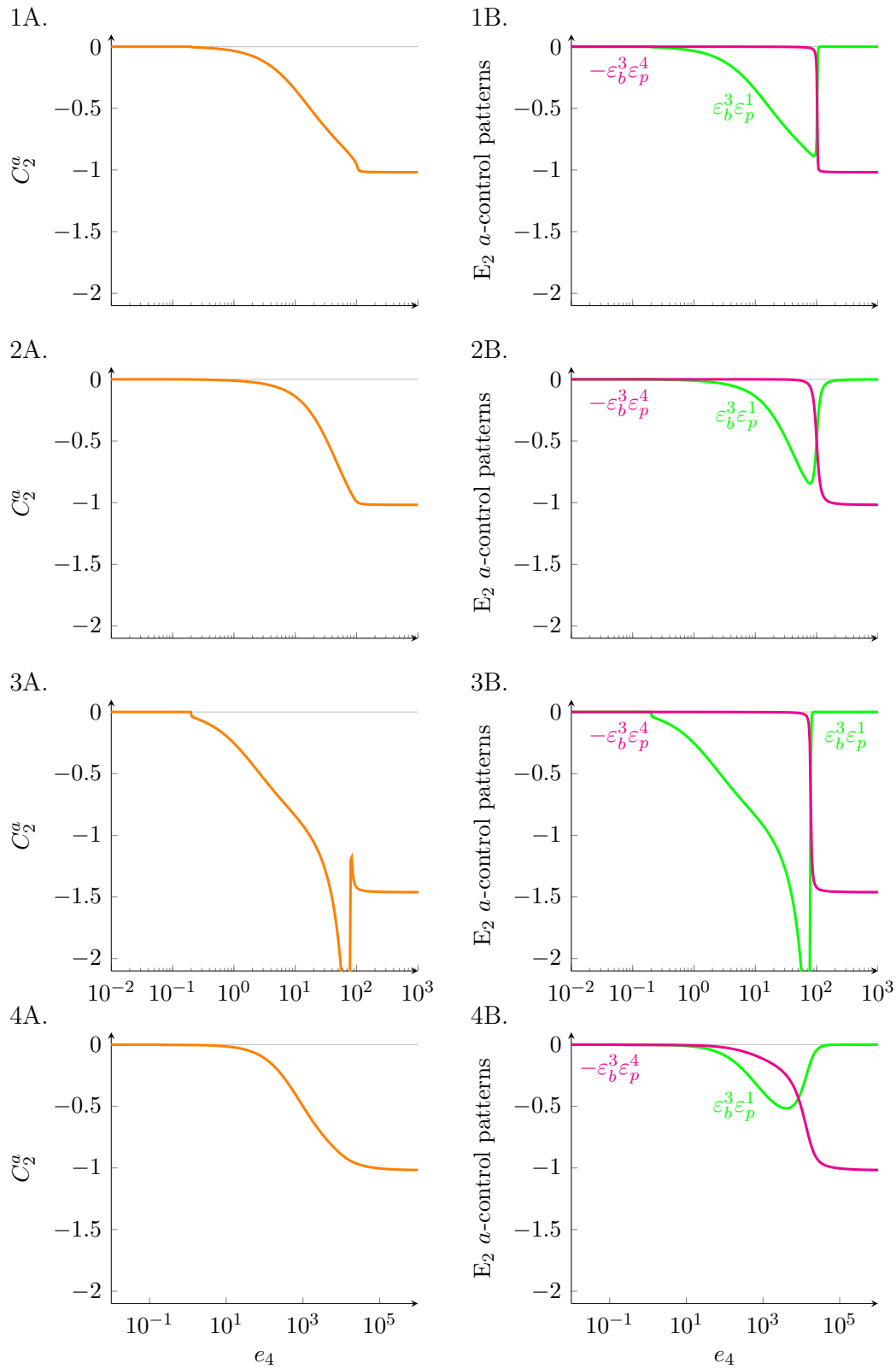
Figure 5.7: E_4-parameter portrait of C_2^a (A) and its control patterns (B) for parameter sets 1 to 4.
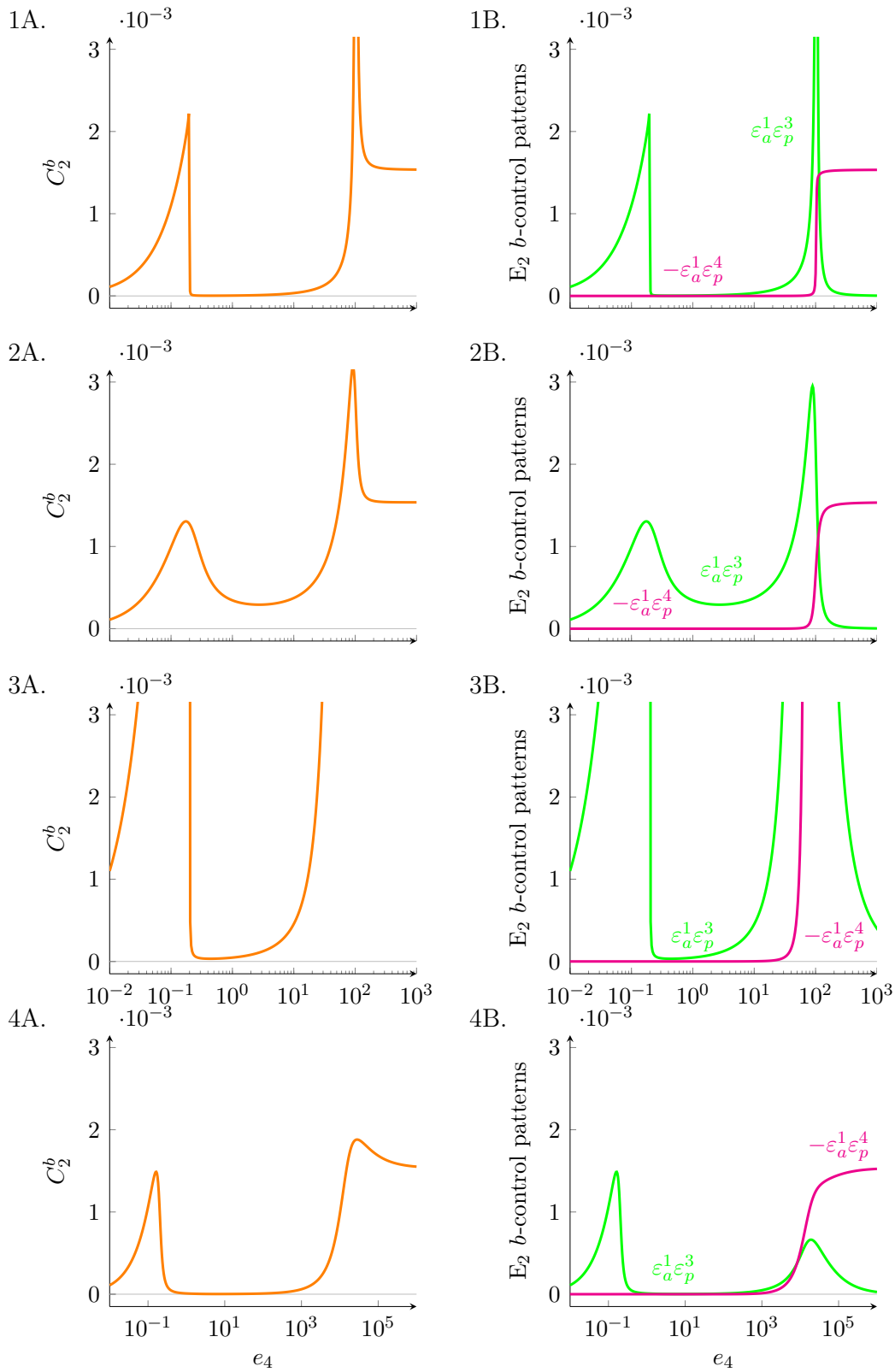
Figure 5.8: E_4-parameter portrait of C_2^b (A) and its control patterns (B) for parameter sets 1 to 4.
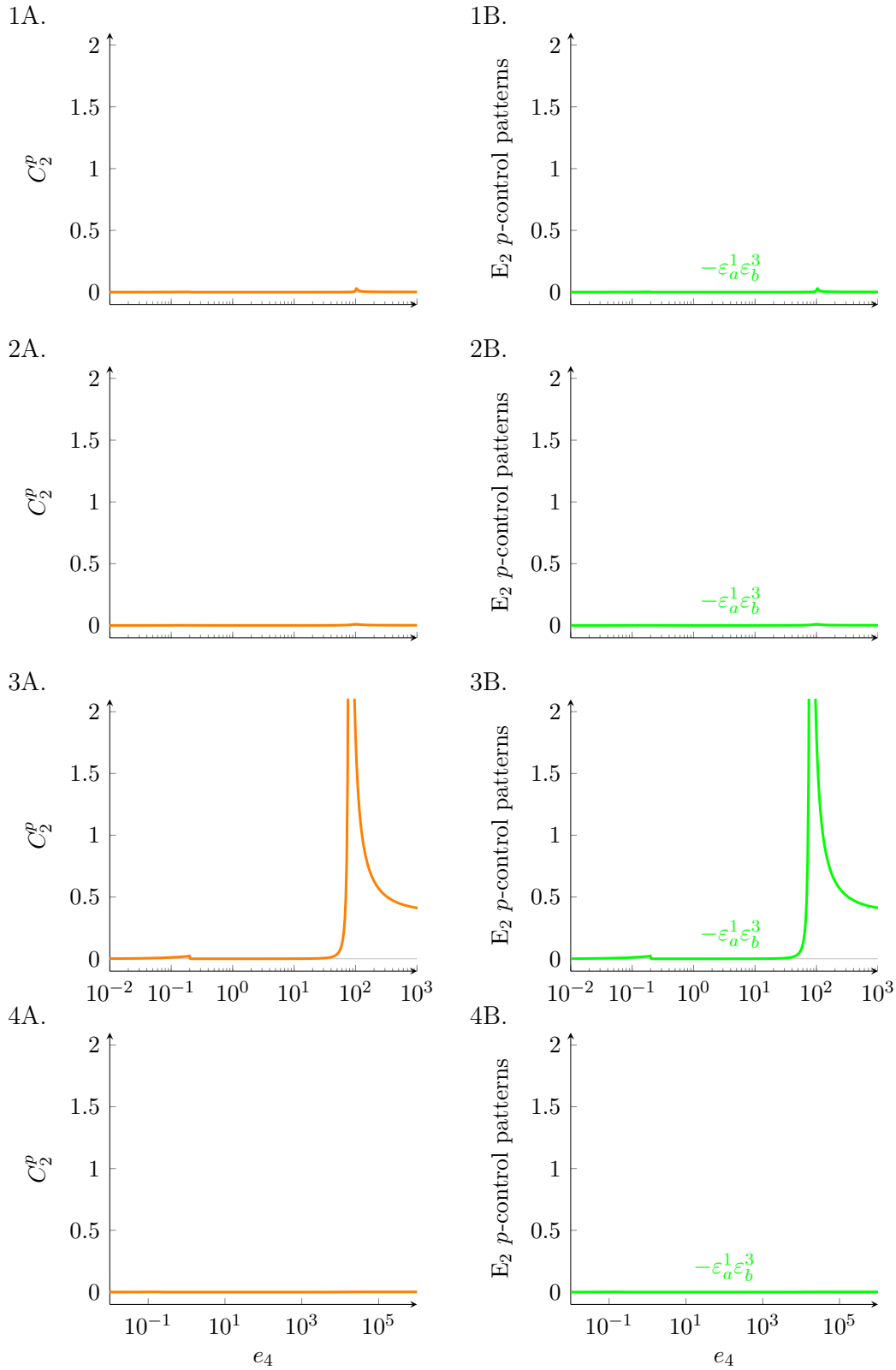
Figure 5.9: E_4-parameter portrait of C_2^p (A) and its control patterns (B) for parameter sets 1 to 4.
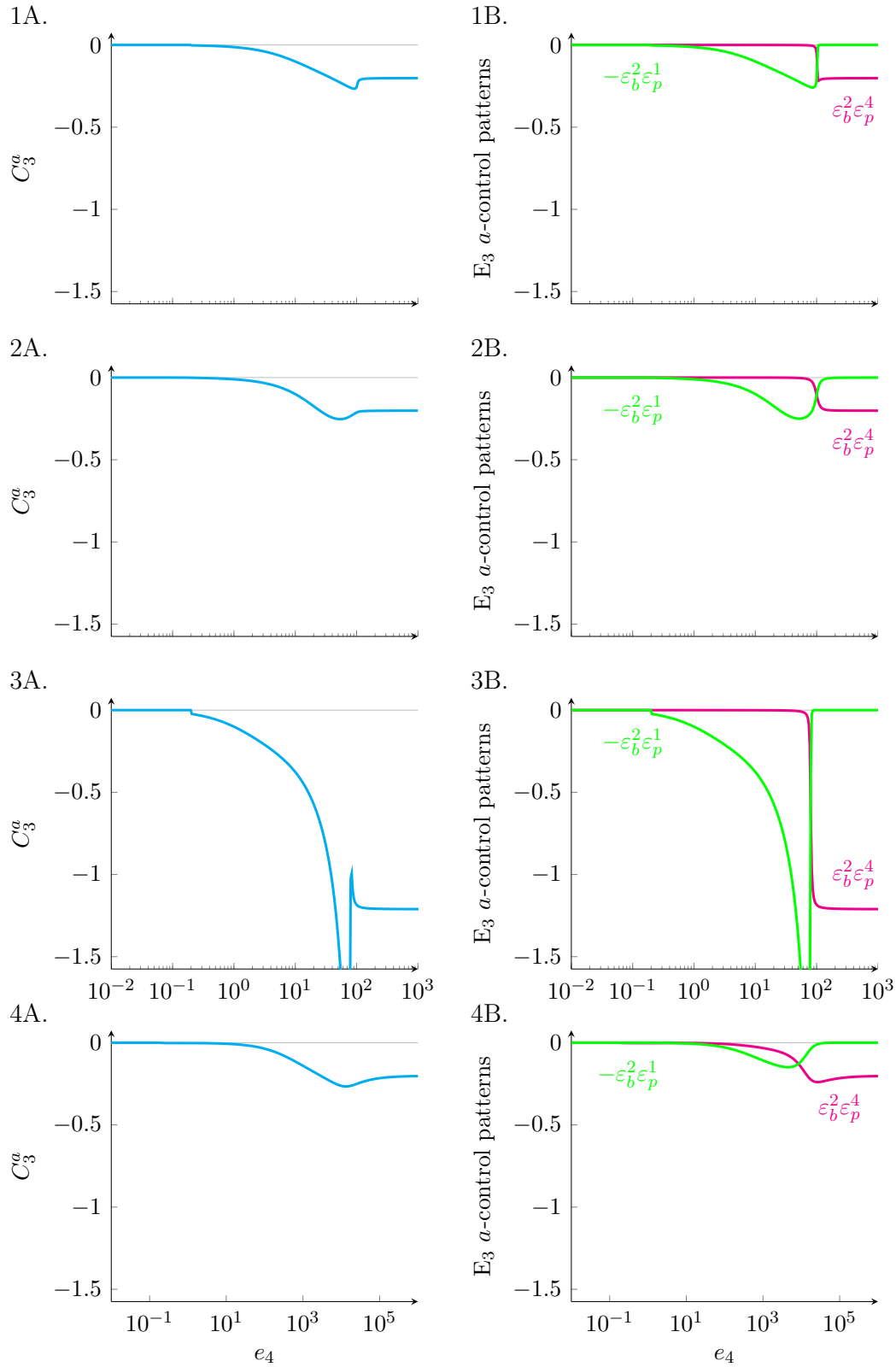
Figure 5.10: E_4-parameter portrait of C_3^a (A) and its control patterns (B) for parameter sets 1 to 4.
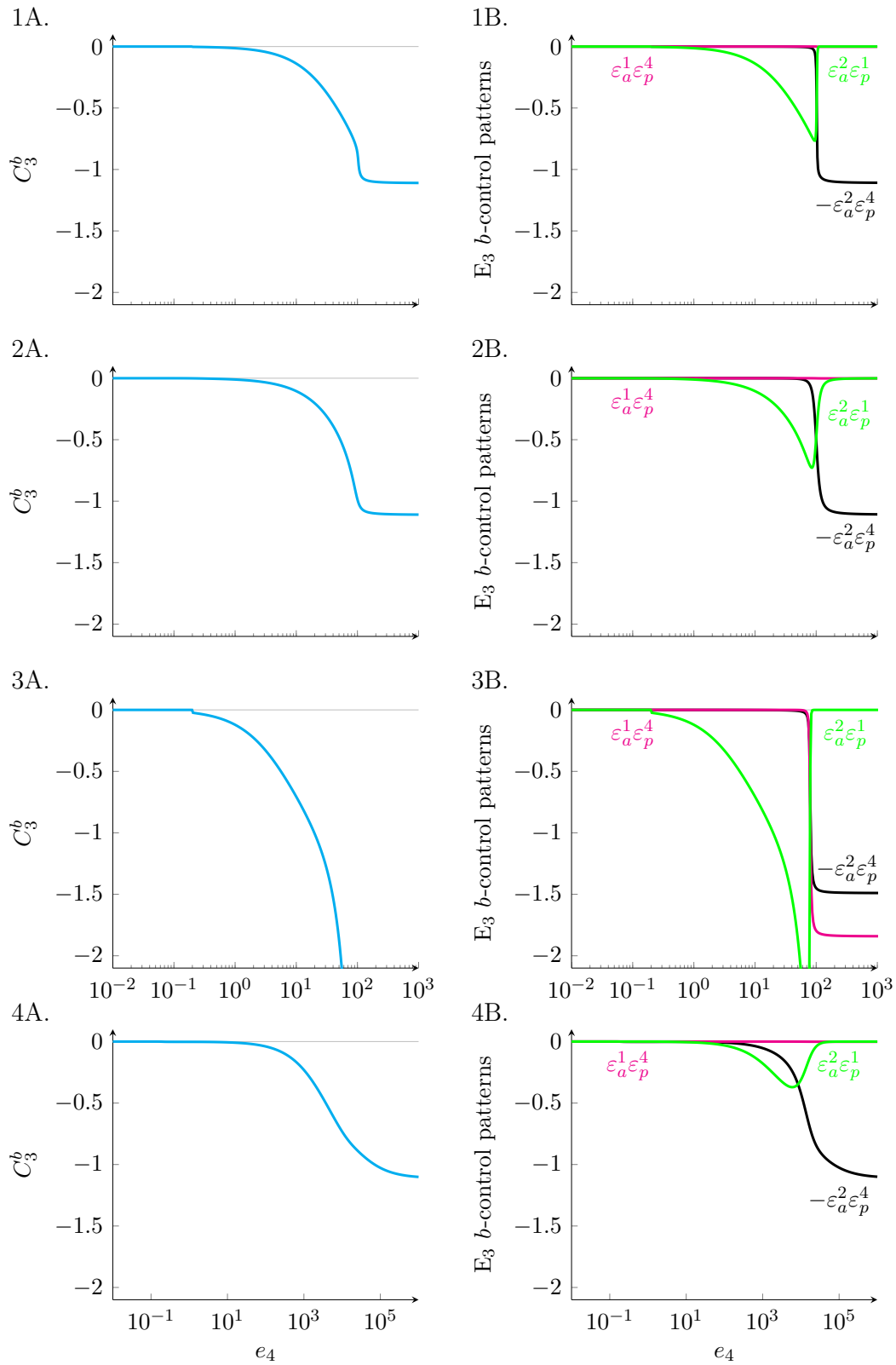
Figure 5.11: E_4-parameter portrait of C_3^b (A) and its control patterns (B) for parameter sets 1 to 4.
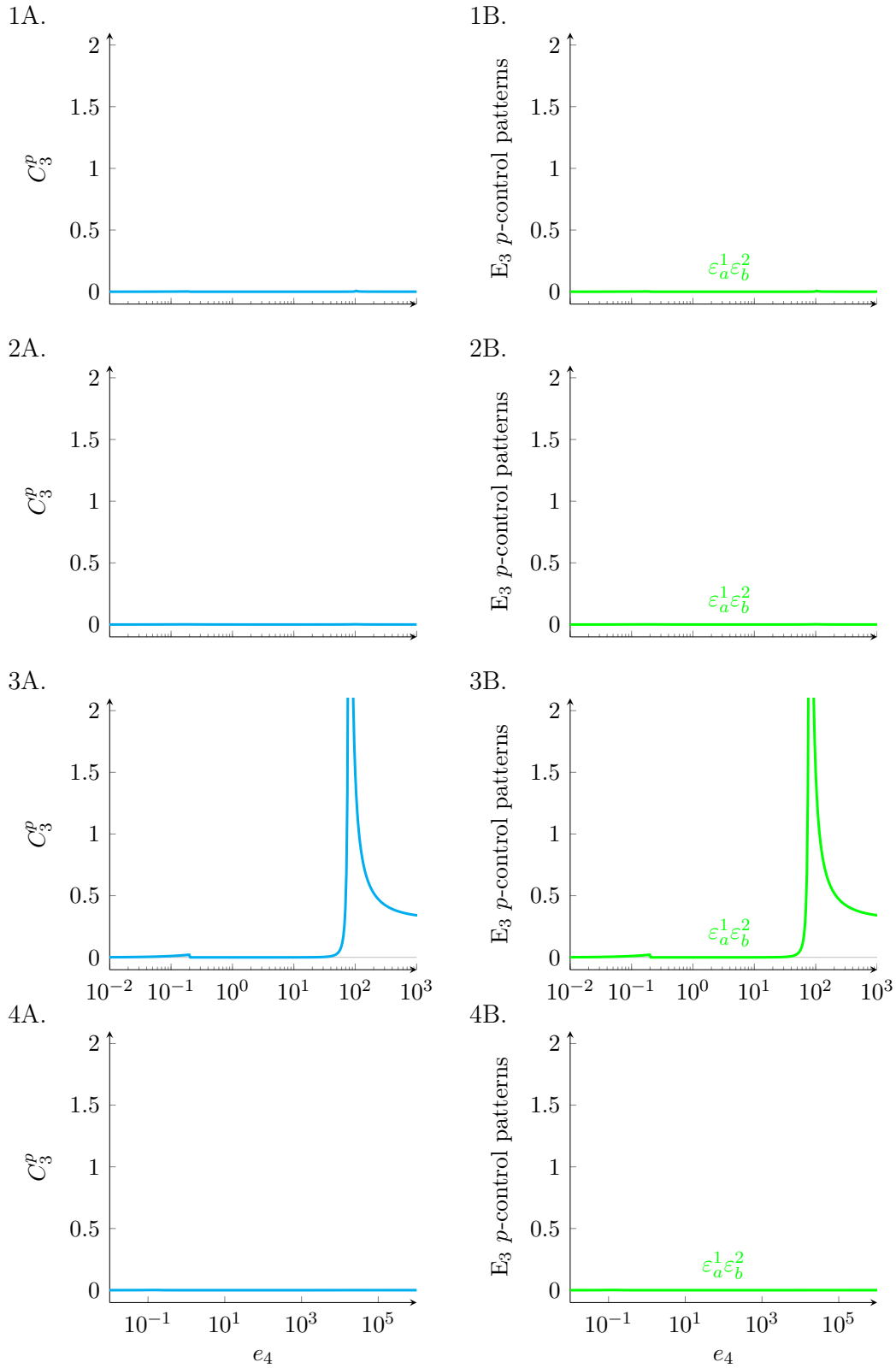
Figure 5.12: E_4-parameter portrait of C_3^p (A) and its control patterns (B) for parameter sets 1 to 4.

Chapter 6

Homeostasis and co-response coefficients

The analysis of the model system up to now has provided us with two views of structural stability. First, the parameter portrait in Fig. 3.3 showed how the steady-state concentrations of the internal metabolites $\bar{a}$, $\bar{b}$, and $\bar{p}$ change with e_4, which allowed us to partition the response into three distinct regions where concentrations were buffered to some degree; this provided a qualitative view of structural stability. Second, concentration-response coefficients profiles in Figs. 5.1–5.12 allowed us to quantify the sensitivity of $\bar{a}$, $\bar{b}$, and $\bar{p}$ towards changes in e_4 in any steady state and thereby gave us a quantitative measure for structural stability of the steady state with respect to a particular internal metabolite; the lower the value, the more structurally stable the system with regard to that metabolite. However, as argued in Chapter 4, just knowing that a concentration-response coefficient is small does not necessarily imply that that concentration is homeostatically *regulated*. For that one needs to relate the concentration change to the concomitant flux change through the metabolite pool. The lower the ratio of the relative change in concentration to the relative change in flux the better the degree of homeostasis in that metabolite. Note that the use of relative rather that absolute changes makes the measure independent of units and allows comparison between systems.

6.1   The homeostatic index

With respect to a quantitative measure for homeostasis in terms of relative concentration and flux changes it is clear that co-response coefficients are the
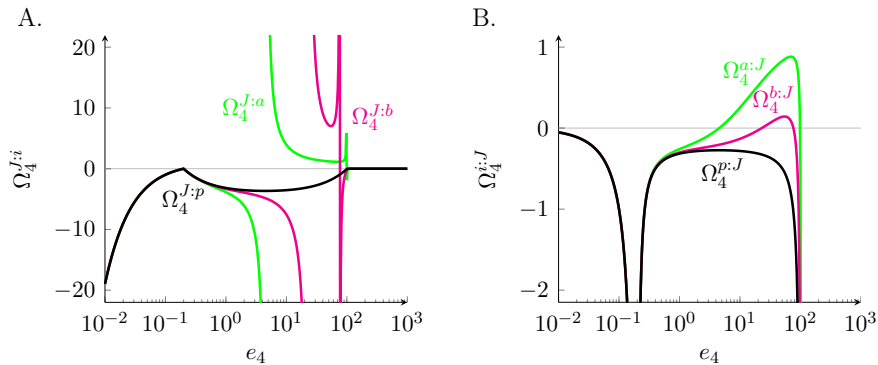
Figure 6.1: Comparison between flux-to-concentration (A) and concentration-to-flux (B) co-response coefficients of E_4 for parameter set 1.

appropriate entities. The question is, however, whether one should use the flux-to-concentration or the concentration-to-flux co-response coefficients. Fig. 6.1 compares these two types of co-response profiles for $\bar{a}$, $\bar{b}$ and $\bar{p}$ with respect to e_4. Note that because parameter e_4 affects only one reaction its co-response coefficients actually reduce to co-control coefficients (see Section 2.12), but we shall continue to refer to them as co-response coefficients. Whereas an increase in the value of a flux-to-concentration co-response coefficients indicates an increase in homeostasis (with an infinitely large value corresponding to "perfect" homeostasis), the opposite holds for concentration-to-flux co-response coefficients: a decrease indicates an increase in homeostasis ("perfect" homeostasis obtaining at a value of zero).

Consider $\Omega_4^{J:p}$ and $\Omega_4^{p:J}$ in Fig. 6.1A and B respectively. One could argue that there is little to choose between the two pictures—they of course represent the same information: both clearly show the regions in which there is homeostatic regulation of $\bar{p}$ (in the NE and FFE-regions where $|\Omega_4^{J:p}| > 1$ and $|\Omega_4^{p:J}| < 1$) and those where there is not (in the transition between the NE and FFE-regions and in the SC-region where $\Omega_4^{J:p} \to 0$ and $\Omega_4^{p:J} \to -\infty$). $\Omega_4^{J:a}$ and $\Omega_4^{J:b}$, however, point to a problem with the picture in A: both these co-response coefficients change signs twice in the FFE-region and their values go through discontinuities where they approach $-\infty$ and ∞. The $\Omega_4^{a:J}$ and $\Omega_4^{b:J}$ profiles just go smoothly through zero at these points and therefore provide a much simpler and satisfying view.

There is, however, a more compelling reason to prefer concentration-to-flux co-response coefficients as a measure of the degree of homeostatic regulation. To explain this we first need to decide on a reference point for homeostatic

regulation. Consider the supply-demand system described in Section 3.1. From eqns. 3.11–3.13 we can derive expressions for the two types of co-response coefficients. For the supply

$$\Omega^{J:p}_{\text{supply}} = \frac{C^J_{\text{supply}}}{C^p_{\text{supply}}} = \varepsilon^{v_{\text{demand}}}_p \quad \text{and} \quad \Omega^{p:J}_{\text{supply}} = \frac{C^p_{\text{supply}}}{C^J_{\text{supply}}} = \frac{1}{\varepsilon^{v_{\text{demand}}}_p} \tag{6.1}$$

and for the demand

$$\Omega^{J:p}_{\text{demand}} = \frac{C^J_{\text{demand}}}{C^p_{\text{demand}}} = \varepsilon^{v_{\text{supply}}}_p \quad \text{and} \quad \Omega^{p:J}_{\text{demand}} = \frac{C^p_{\text{demand}}}{C^J_{\text{demand}}} = \frac{1}{\varepsilon^{v_{\text{supply}}}_p} \tag{6.2}$$

Values of 1 for $\varepsilon^{v_{\text{demand}}}_p$ and -1 for $\varepsilon^{v_{\text{supply}}}_p$ would indicate a proportional, non-cooperative response of the supply and demand rate to P and are the maximum values the elasticities of a far-from-equilibrium Michaelis-Menten enzyme (Hill coefficient of 1) can attain. An enzyme with these elasticity values can be regarded as unregulated. We therefore choose 1 and -1 as suitable reference values for the co-response coefficients (an obvious advantage being that all four permutations of the co-response coefficients in eqns. 6.1 and 6.2 have a value of either 1 or -1 in this reference state. Better homeostasis would be expected when $\varepsilon^{v_{\text{demand}}}_p$ and $\varepsilon^{v_{\text{supply}}}_p$ have larger values, i.e., when supply and/or demand are more sensitive to changes in P; *J:p* co-response coefficients would become larger, and *p:J* co-response coefficients would become smaller. It is here that the biggest advantage of *p:J* co-response coefficients becomes apparent: their use establishes a scale or index for the degree of homeostatic regulation that ranges between the reference values of 1 and -1, with "perfect" homeostasis (where there is no change in concentration for any finite flux change) obtaining at 0. The equivalent scale based on $J : p$ co-response coefficients would range from 1 to ∞ (or from -1 to $-\infty$). From an operational point of view a *p:J* co-response coefficient also has a intelligible interpretation as the %-change in the steady-state concentration of a metabolite that accompanies 1% change in the flux through the metabolite pool following a perturbation in some parameter. From here on we shall refer to the absolute value of $\Omega^{s_j:J}_i$ as the *homeostatic index* of metabolite S_j with respect to a change in the activity of step i.

6.2 Analysis of homeostasis

Consider now Fig. 6.2-1A, 3A and 4A, which show in panel A how $\Omega^{a:J}_4$, $\Omega^{b:J}_4$, and $\Omega^{p:J}_4$ for the four parameter sets and in panel B how the corresponding

Figure 6.2: Metabolite:flux co-response coefficient profiles of E_4 (A) compared with the corresponding flux-response and concentration-response coefficient profiles of E_4 (B) for parameter sets 1 to 4.

flux and concentration-response coefficients vary with e_4. As mentioned above $\bar{p}$ is homeostatically regulated in the NE and FFE-regions. In the NE-region $\varepsilon_p^{v_{\text{supply}}}$ is extremely large so that the homeostatic index of P tends to zero. Although this seems to be excellent near-perfect homeostasis it must be remembered that it occurs at extremely high near-equilibrium concentrations of P, a condition that may not be physiological. In the FFE-region the homeostatic index of P decreases to a value of 0.25 (which is the inverse of the Hill coefficient of 4 for P binding to E_1). In 1A and 4A $\bar{a}$ and $\bar{b}$ are also homeostatic because they are kept near equilibrium with $\bar{p}$. In 3A $\bar{a}$ and $\bar{b}$ are much more sensitive and less homeostatically regulated because of the lower activities of E_2 and E_3. In the FFE-region of 2B, where the Hill coefficient of E_1 is 1 instead of 4 the homeostatic index of P is more than 1 and $\bar{p}$ is much less homeostatic compared to the other parameter sets.

If one compares panel A with panel B then at first glance it may seem that the concentration-response profiles give the same information as the co-response profiles and that therefore the use of co-response coefficients appears to be an overkill. Closer inspection, however, reveals a number of crucial differences. In the NE and FFE-regions of parameter set 1, 2, and 3 there is very little difference between A and B (the obvious exception being $\Omega_4^{a:J}$ and R_4^a in 2) because here $R_4^J = 1$ and, therefore, $\Omega_4^{a:J} = R_4^a$. However, in the SC-region there is a huge difference: the homeostatic index for A, B, and P is extremely large, approaching $-\infty$ (because R_4^J is zero), while R_4^a and R_4^b tends to zero and R_4^p to -1. This means that in the SC-region the system is structurally very stable with respect to changes in e_4, but not at all homeostatically regulated.

Fig. 6.2-4A and B provide the best examples of the difference between co-response coefficients and concentration-response coefficients, because here R_4^J varies in the FFE-region instead of having a value of 1 as is the case for the other parameter sets. This means that the concentration-response profiles in the FFE-region do not match the co-response profiles as they do for the other parameter sets. Therefore, from 1A and 4A one would conclude that there is virtually no difference in the homeostatic regulation for these two parameter sets, whereas one would not come to this conclusion from 1B and 4B.

Up to now we have only considered the structural stability and homeostatic regulation of the system with respect to a perturbation in e_4, the parameter that has been scanned. However, we can also ask, for the same range of steady states obtained in the e_4 scan-range, how structurally stable or homeostatically

regulated the system is with respect to perturbations in the other three enzymes. Figs. 6.3–6.5 show the co-response coefficient and response coefficient profiles for these three enzymes.

Here, in all three figures, the differences between structural stability and homeostatic regulation are far more pronounced than in Fig. 6.2. In general, for parameter sets 1, 2 and 4 the system is structurally stable with respect to all three metabolites for perturbations in E_2 and E_3. For parameter set 3 the system is less structurally stable with respect to E_2 and E_3, especially around the transition from the FFE to the SC-region (graph 3B in Figs. 6.4 and 6.5). Again this is due to the fact that the lower activities of E_2 and E_3 fail to keep $\bar{a}$ and $\bar{b}$ near-equilibrium with $\bar{p}$. To a large extent, the response coefficient profile for E_1 in Fig. 6.3 is qualitatively a mirror-image around the horizontal of that of E_4 in Fig. 6.2, the most prominent difference being the a and b-response coefficients in the SC-region, which cluster around a value of 1 instead of zero, the exception again being parameter set 3.

In the FFE-region of parameter sets 1, 2 and 3 there is no homeostatic regulation of a, b or p with regard to perturbation in any of the three enzymes because their flux-control coefficients are zero and the co-response coefficients therefore tending to infinity. The best they can do in the SC-region is a homeostatic index of 1. The thermodynamic homeostasis in the NE-regions seen in the co-response coefficient profiles for E_2 and E_3 are due to differences in very small values of the concentration and flux-control coefficients.

For parameter set 4, because the flux-response and concentration-response coefficients of E_1 vary with nearly the same values in the FFE and SC-regions (except around the transition between the two regions—see Fig. 6.3-4B), the co-response coefficients $\Omega_1^{p:J}$, $\Omega_1^{a:J}$, and $\Omega_1^{b:J}$ are 1 or just above to 1. The reason is of course that C_1^J attains non-zero values in the FFE-region, in contrast to the other parameter sets where it is zero. Here the degree of homeostatic regulation of A, B, and P therefore hovers around the homeostatic index baseline of 1. For E_2 with parameter set 4 only B and P (its downstream metabolites) (Fig. 6.4-4B)) and for E_3 with parameter set 4 only P (its downstream metabolite) have the same homeostatic index profile around 1. The upstream metabolites are not homeostatically regulated.

The analysis of homeostasis in this chapter shows that, while homeostasis is closely related to structural stability, an analysis of metabolite concentration changes on their own could give a misleading picture of homeostatic regulation and that, when related to concomitant changes in flux through the metabolite
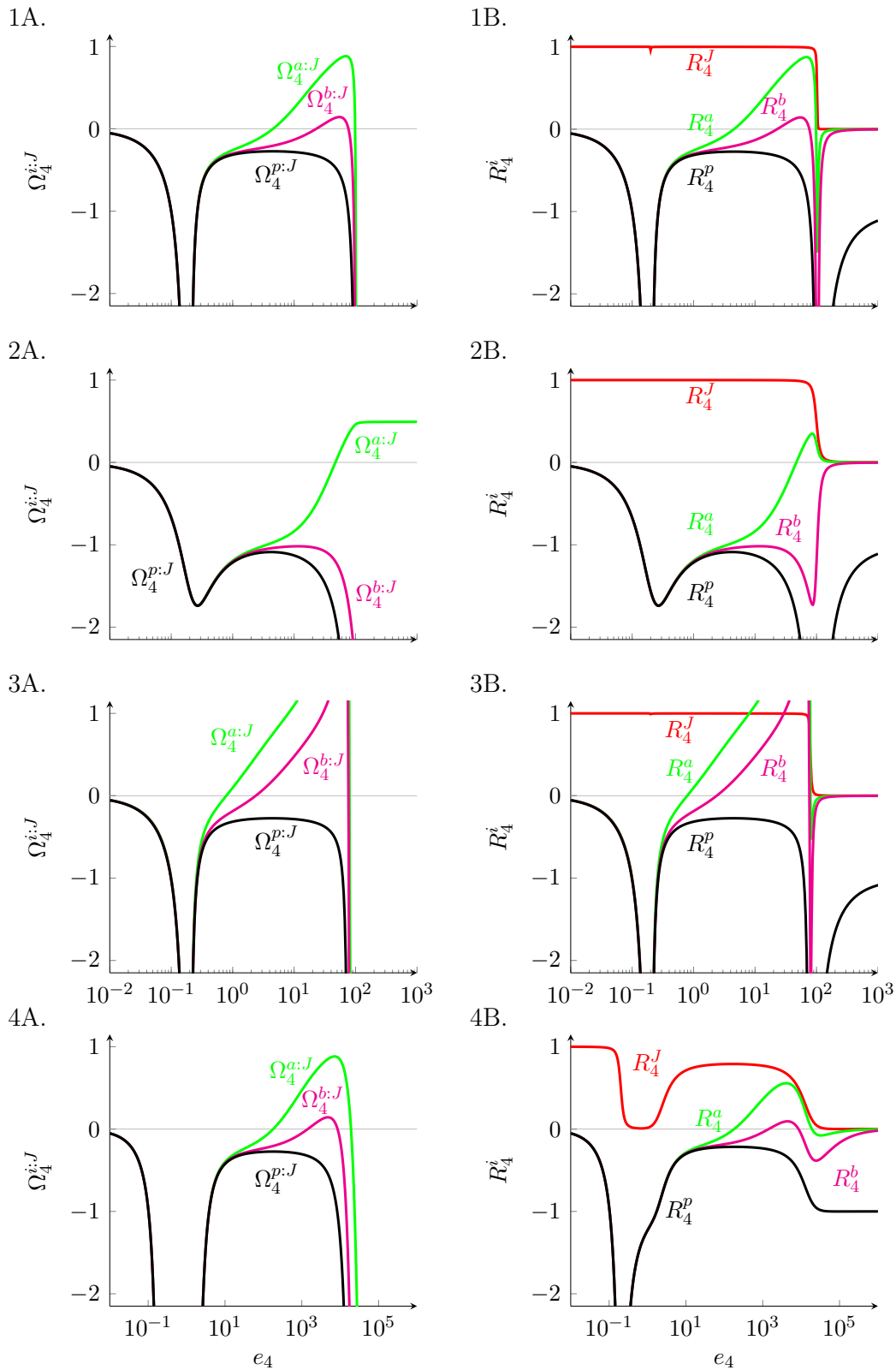
59

pools, a different picture emerges.
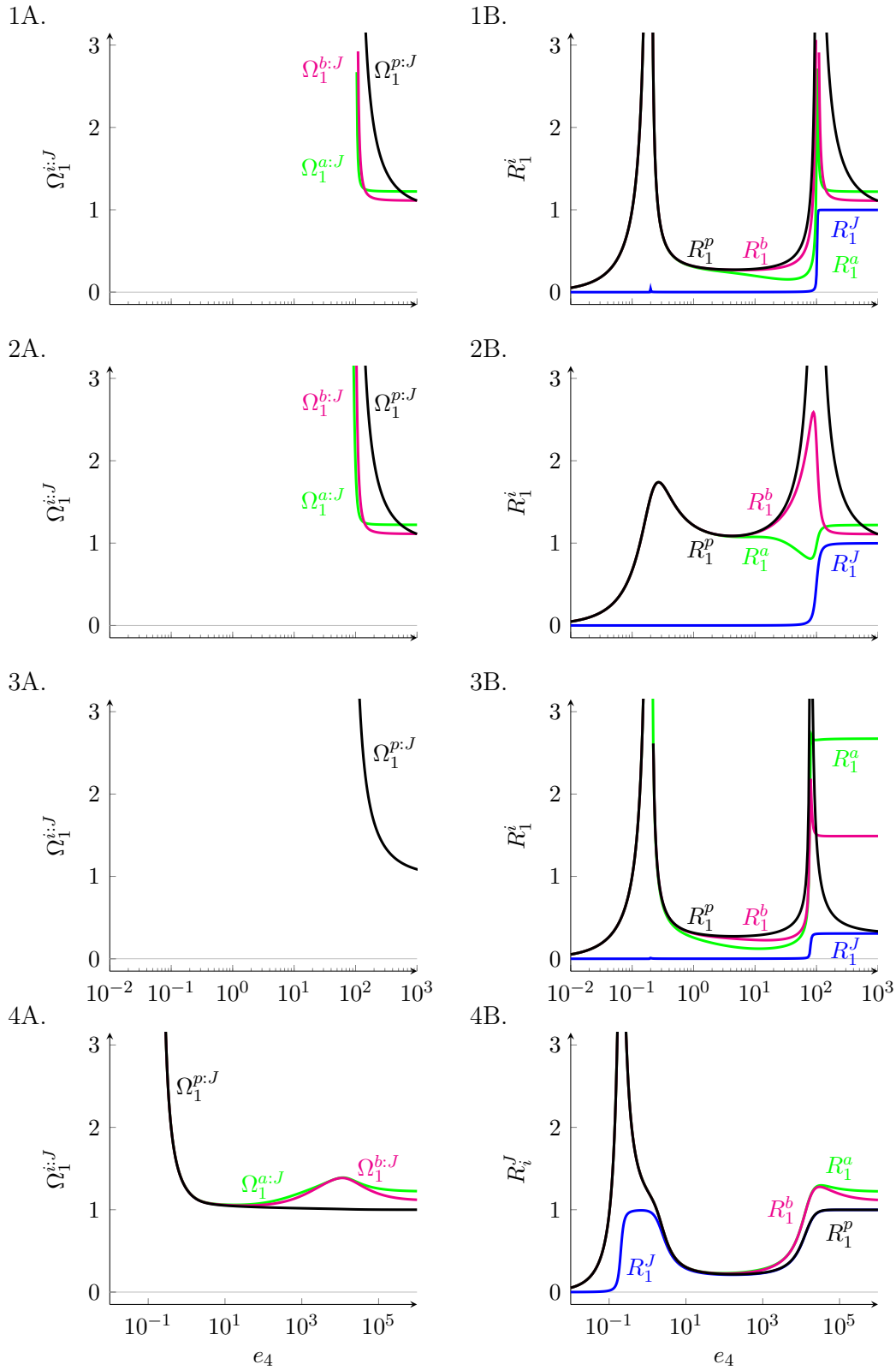
Figure 6.3: Metabolite:flux co-response coefficient profiles of E_1 (A) compared with the corresponding flux-response and concentration-response coefficient profiles of E_1 (B) for parameter sets 1 to 4.
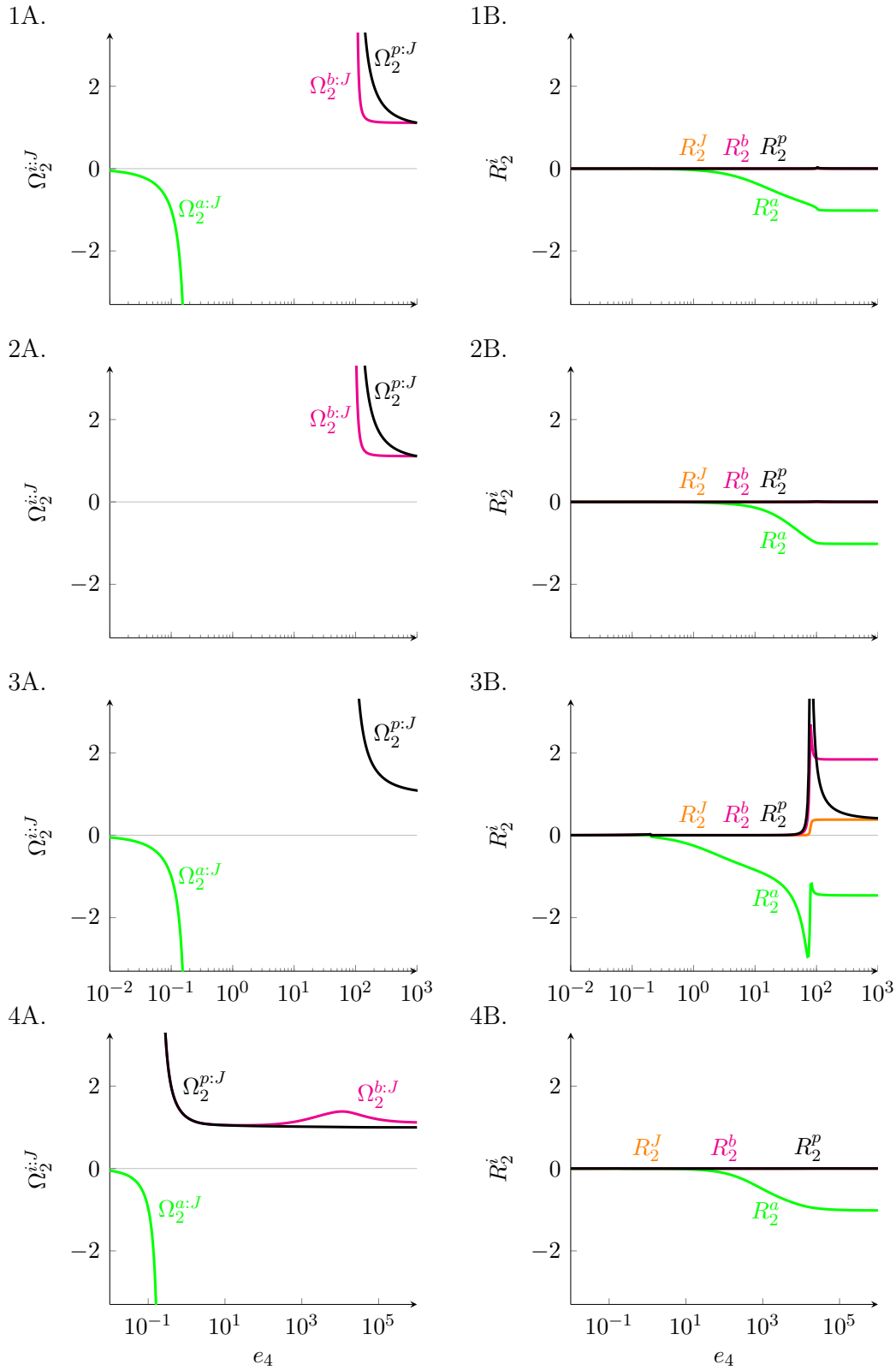
Figure 6.4: Metabolite:flux co-response coefficient profiles of E_2 (A) compared with the corresponding flux-response and concentration-response coefficient profiles of E_2 (B) for parameter sets 1 to 4.
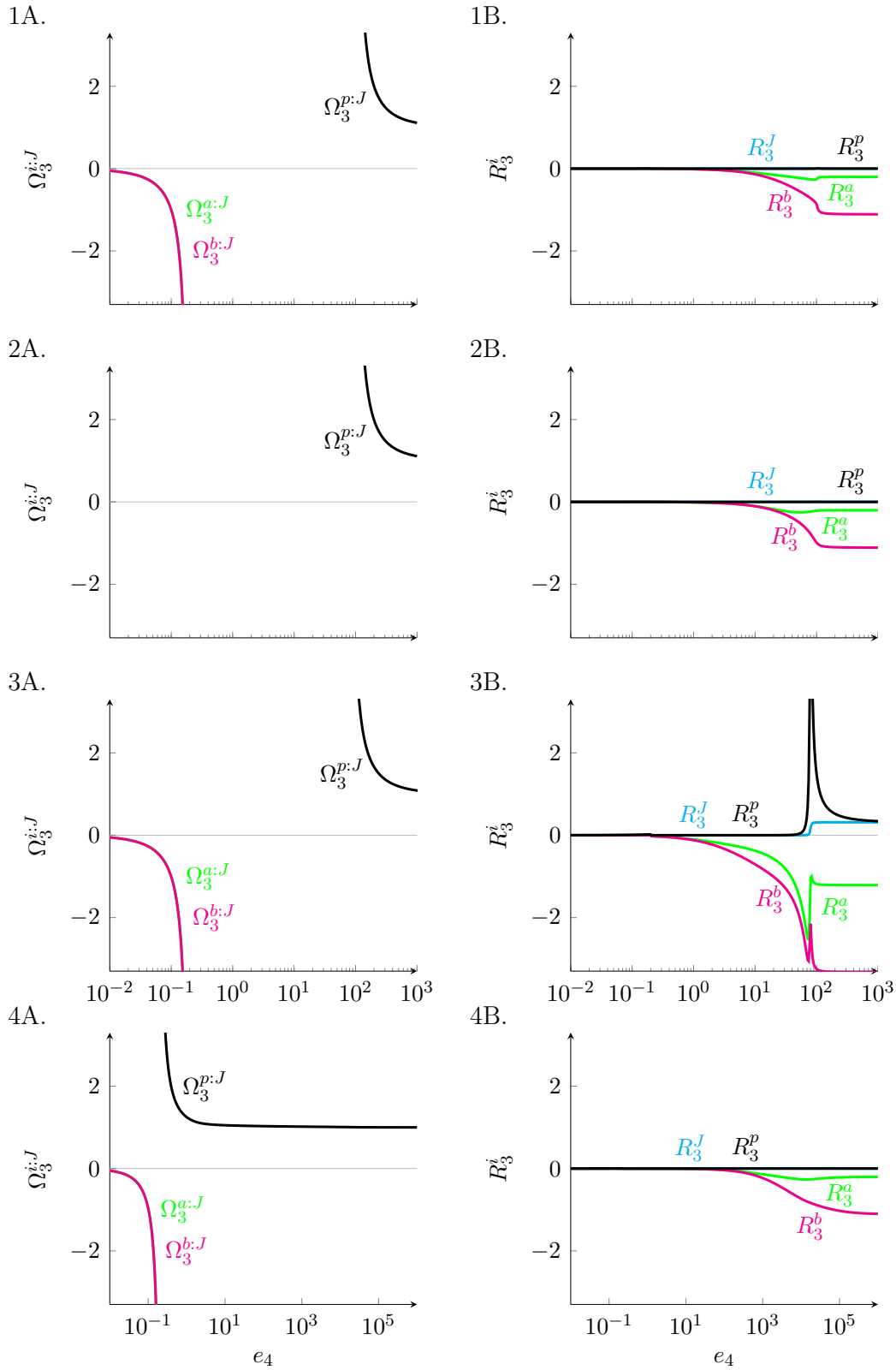
Figure 6.5: Metabolite:flux co-response coefficient profiles of E_3 (A) compared with the corresponding flux-response and concentration-response coefficient profiles of E_3 (B) for parameter sets 1 to 4.

Chapter 7

Dynamic stability and internal-response coefficients

Metabolic systems are continually subject to perturbations in the concentrations of their internal metabolites so that their steady states are continually fluctuating. Dynamic stability of these systems means that the interactions within the system counteract these perturbations and continuously drive the system towards the steady state. The internal-response coefficients that form the terms of the connectivity theorems of metabolic control analysis (Section 2.9), provide one way of quantitatively describing the behaviour of the system as it responds to fluctuations in internal metabolite concentrations. The internal-response coefficients quantify the contributions of internal interaction routes that fan out from the perturbed metabolite through enzymes that are directly affected by the perturbation, as explained by the following thought experiment.

Consider a perturbation $\delta \ln a$ in the concentration of internal metabolite A of the pathway in Fig. 3.1. This change in a directly affects v_1 by (using the definition of the elasticity coefficient)

$$\delta \ln v_1 = \varepsilon_a^{v_1} \cdot \delta \ln a \qquad (7.1)$$

If this were the only effect of $\delta \ln a$ then the steady-state variables would be affected as follows (using the definition of control coefficients):

$$\delta \ln J = C_1^J \cdot \delta \ln v_1 = C_1^J \varepsilon_a^{v_1} \cdot \delta \ln a \qquad (7.2)$$

$$\delta \ln a = C_1^a \cdot \delta \ln v_1 = C_1^a \varepsilon_a^{v_1} \cdot \delta \ln a \qquad (7.3)$$

$$\delta \ln b = C_1^b \cdot \delta \ln v_1 = C_1^b \varepsilon_a^{v_1} \cdot \delta \ln a \qquad (7.4)$$

$$\delta \ln p = C_1^p \cdot \delta \ln v_1 = C_1^p \varepsilon_a^{v_1} \cdot \delta \ln a \qquad (7.5)$$

64

However, $\delta \ln a$ also affects v_2 directly by

$$\delta \ln v_2 = \varepsilon_a^{v_2} \cdot \delta \ln a \tag{7.6}$$

which, if this were the only effect of $\delta \ln a$, would affect the steady state by:

$$
\begin{aligned}
\delta \ln J &= C_2^J \cdot \delta \ln v_2 = C_2^J \varepsilon_a^{v_2} \cdot \delta \ln a & (7.7)\\
\delta \ln a &= C_2^a \cdot \delta \ln v_2 = C_2^a \varepsilon_a^{v_2} \cdot \delta \ln a & (7.8)\\
\delta \ln b &= C_2^b \cdot \delta \ln v_2 = C_2^b \varepsilon_a^{v_2} \cdot \delta \ln a & (7.9)\\
\delta \ln p &= C_2^p \cdot \delta \ln v_2 = C_2^p \varepsilon_a^{v_2} \cdot \delta \ln a & (7.10)
\end{aligned}
$$

However, if the system is asymptotically stable it relaxes back to its original steady state after the perturbation in a, which implies that the effects of $\delta \ln a$ on v_1 and v_2 must cancel:

$$
\begin{aligned}
(C_1^J \varepsilon_a^{v_1} + C_2^J \varepsilon_a^{v_2}) \cdot \delta \ln a &= 0 & (7.11)\\
(C_1^a \varepsilon_a^{v_1} + C_2^a \varepsilon_a^{v_2}) \cdot \delta \ln a &= -\delta \ln a & (7.12)\\
(C_1^b \varepsilon_a^{v_1} + C_2^b \varepsilon_a^{v_2}) \cdot \delta \ln a &= 0 & (7.13)\\
(C_1^p \varepsilon_a^{v_1} + C_2^p \varepsilon_a^{v_2}) \cdot \delta \ln a &= 0 & (7.14)
\end{aligned}
$$

Note that the combined effects of changes in v_1 and v_2 on a itself must be $-\delta \ln a$ if they are to drive a back to its original steady-state value.

The above thought experiment therefore leads directly to the connectivity equations for A, namely:

$$
\begin{aligned}
C_1^J \varepsilon_a^{v_1} + C_2^J \varepsilon_a^{v_2} &= 0 & (7.15)\\
C_1^a \varepsilon_a^{v_1} + C_2^a \varepsilon_a^{v_2} &= -1 & (7.16)\\
C_1^b \varepsilon_a^{v_1} + C_2^b \varepsilon_a^{v_2} &= 0 & (7.17)\\
C_1^p \varepsilon_a^{v_1} + C_2^p \varepsilon_a^{v_2} &= 0 & (7.18)
\end{aligned}
$$

or, in terms of internal-response coefficients:

$$
\begin{aligned}
{}^1R_a^J + {}^2R_a^J &= 0 & (7.19)\\
{}^1R_a^a + {}^2R_a^a &= -1 & (7.20)\\
{}^1R_a^b + {}^2R_a^b &= 0 & (7.21)\\
{}^1R_a^p + {}^2R_a^p &= 0 & (7.22)
\end{aligned}
$$

Kahn and Westerhoff [23] proposed the use of internal-response coefficients of metabolic control analysis to quantify regulation that ensures dynamic stability in state variables when an internal variable metabolite is perturbed.

They used the term "regulatory strengths" for what are here termed internal-response coefficients, in particular for those internal-response coefficients where the state variable under consideration is **not** the same as the concentration that is perturbed; in our example these would be $^1R_a^J$, $^2R_a^J$, $^1R_a^b$, $^2R_{,}^b$ $^1R_a^p$, and $^2R_a^p$. For internal-response coefficients such as $^1R_a^a$, $^2R_a^a$, $^2R_b^b$, $^3R_b^b$, $^1R_p^p$, $^3R_p^p$, and $^4R_p^p$ where the responding variable is the perturbed variable itself they used the term "homeostatic strength", although they preferred to use the *absolute values* of $^1R_a^a$ and $^2R_a^a$.

In general, we prefer the use of the term internal-response coefficient to the terms "regulatory strength" and "homeostatic strength", because, as already discussed in Chapter 4, our concept of homeostasis has nothing to do with dynamic stability. It is not even clear that dynamic stability forms part of what most systems biologists understand under the umbrella term "regulation", although we would argue that it should. But, as we shall soon see, the two types of coefficient behave quite differently and we do need to distinguish them. We shall therefore call "homeostatic strengths" *self-response coefficients* and reserve *internal-response coefficients* for "regulatory strengths".

We first discuss the use of self-response coefficients to analyse the dynamic stability of the model system for the four parameter sets.

7.1 Self-response coefficients

Since the set of self-response coefficients for a metabolite sum to -1 it follows that negative self-response coefficients are stabilising, while positive self-response coefficients are destabilising [23]. The summation to -1 has another pleasing property, and that is if the experimentally determined self-response coefficients do not sum to -1 it means that there is a missing interaction route in need of discovery.

Figs. 7.1–7.3 show how the self-response coefficients of A, B and P vary with e_4. For A and B in the NE-region the interaction that drives the metabolite back to its value before it was perturbed is via the enzyme that lies *upstream* from the metabolite in question, i.e., for which it is a product ($^1R_a^a$ and $^2R_b^b$ for A and B respectively). The reason for this is that the concentration-control coefficient of the downstream enzyme, i.e., for which the metabolite is a substrate ($^2R_a^a$ and $^3R_b^b$ for A and B respectively), is zero in the NE-region (C_2^a in Fig. 3.5 and C_3^b in Fig. 3.6). C_1^a and C_2^b, on the other hand, have non-zero values coupled to extremely large elasticity coefficients ($\varepsilon_a^{v_1}$ and $\varepsilon_b^{v_2}$ in Fig. 3.8
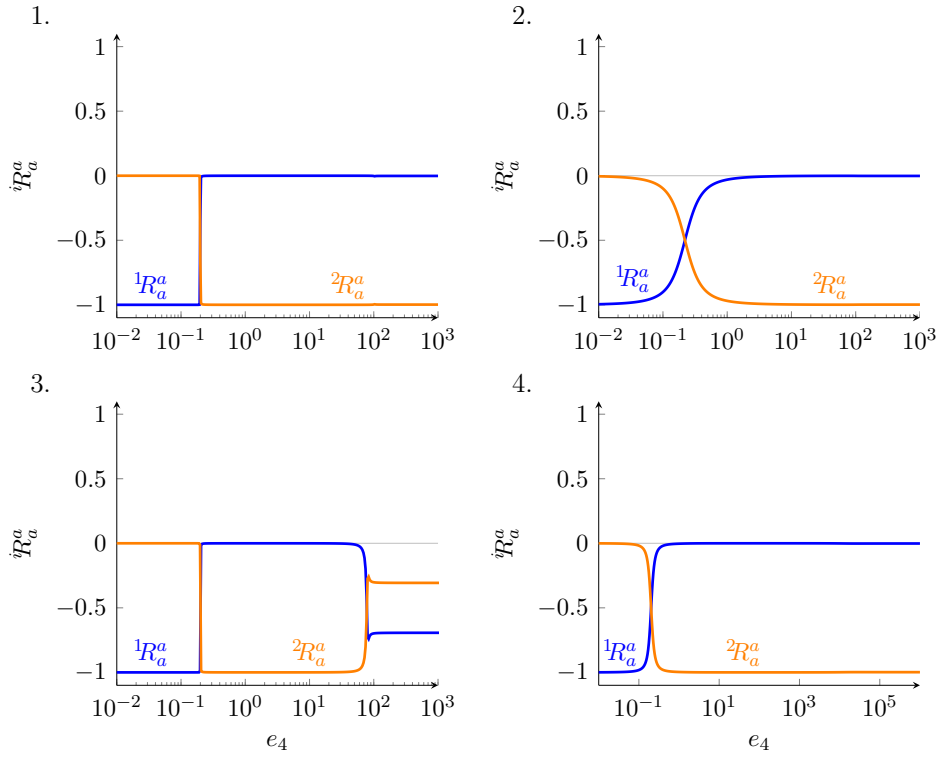
Figure 7.1: Self-response coefficients for A for parameter sets 1 to 4.
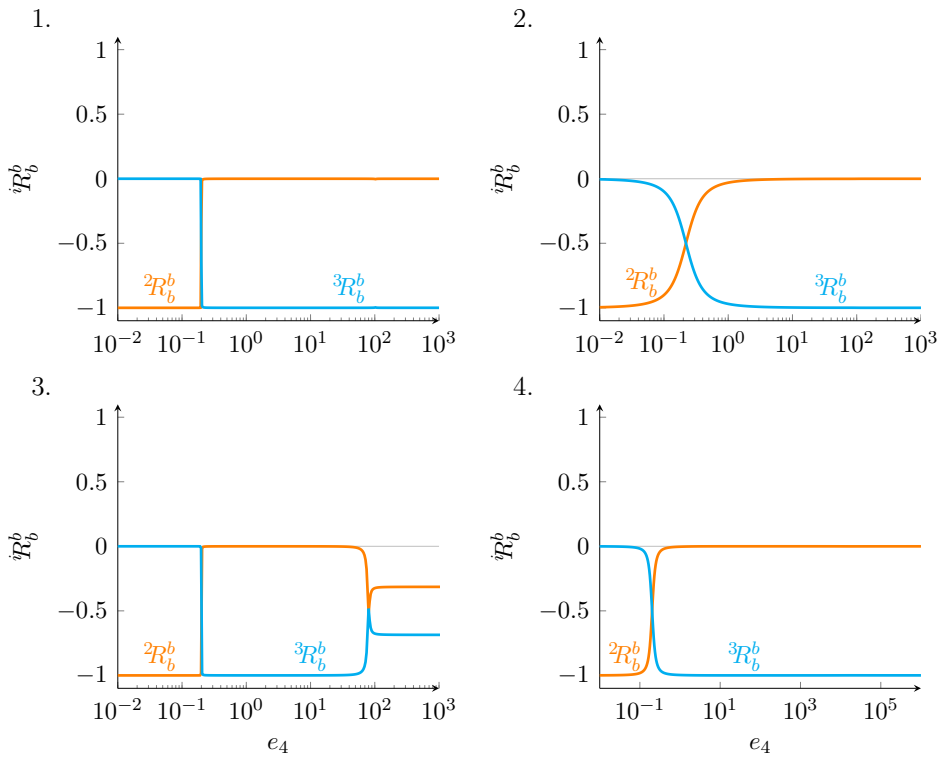
Figure 7.2: Self-response coefficients for B for parameter sets 1 to 4.
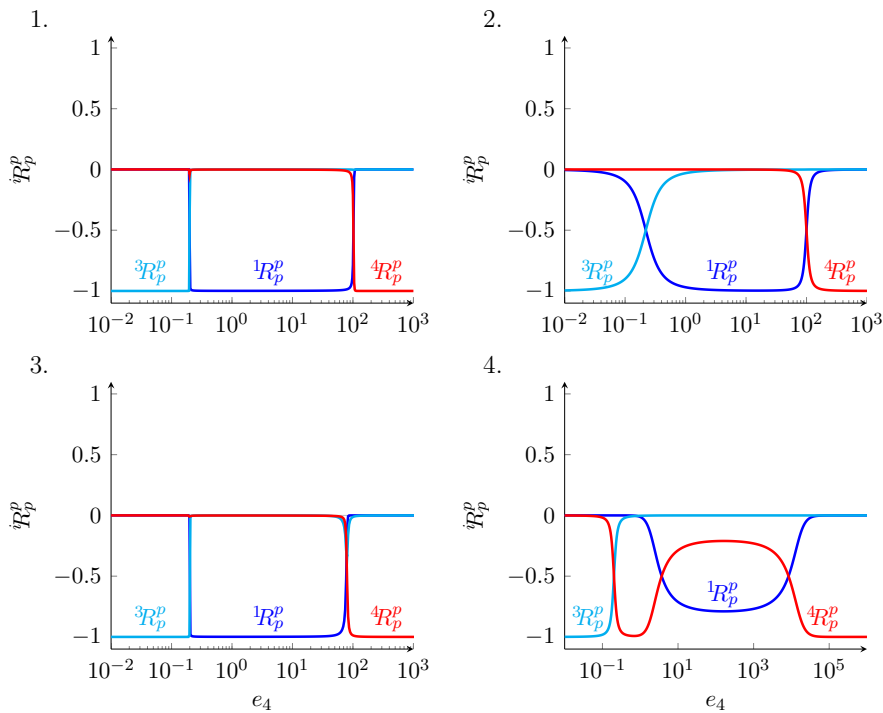
Figure 7.3: Self-response coefficients for P for parameter sets 1 to 4.

in the NE-region. For A and B in the FFE and SC-regions the self-response profiles switches in the sense that now the interaction that drives the metabolite back to its value before it was perturbed is via the enzyme that lies *downstream* from the metabolite in question, i.e., for which it is a substrate. For A this because $\varepsilon_a^{v_1}$, the elasticity component of ${}^1R_a^a$, is zero in this region. For B it is because C_2^b, concentration-control coefficient component of ${}^2R_b^b$, is zero. The more gradual transition from the NE to the FFE-region in parameter set 2 is due to the smaller Hill coefficient of 1 compared to 4 in the other parameter sets.

In the SC-region, parameter set 3 differs from the other sets in that the self-response in A and B is shared between the two coefficients instead of being fully located in one or the other. Here the reason is mainly that, unlike for the other parameter sets, $\varepsilon_a^{v_1}$ is not zero in the SC-region (see Fig. 3.8-3), and therefore does allow an upstream effect of a perturbation in A or B. The degree of sharing of self-response between the two coefficients depends on the values of the elasticity and concentration-control coefficients that make up the

self-response coefficients, which in the SC-region of parameter set 3 is quite complicated.

By now it should be clear that the regulation of dynamic stability revolves around P and not A and B (note that neither the feedback elasticity $\varepsilon_p^{v_1}$ nor the demand elasticity $\varepsilon_p^{v_4}$ have been explicitly implicated in the self-response of A and B). Accordingly, the self-response profile of P differs from that of A and B in important respects. However, as one would expect, they all agree in the NE-region where only upstream communication via the reaction chain takes place ($\varepsilon_p^{v_1}$ and $\varepsilon_p^{v_4}$ are both zero in the NE-region, which eliminates the feedback loop and the downstream effect). For the same reason, i.e., that $\varepsilon_p^{v_4} = 0$ because P saturates E_4, ${}^4R_p^p = 0$ in the FFE-region. Because, as discussed above, $\varepsilon_a^{v_1}$ is also zero in the FFE-region, it is only ${}^1R_p^p$, which has the feedback elasticity $\varepsilon_p^{v_1}$ as component, that is non-zero and therefore fully determines the self-response of P in the FFE-region. In the SC-region both $\varepsilon_a^{v_1} = 0$ and $\varepsilon_p^{v_1} = 0$, which eliminates the upstream and the feedback effect of P and allows only the downstream effect via $\varepsilon_p^{v_4}$.

In the FFE and SC-regions of the self-response profile of P the most important determinants are clearly the feedback and downstream elasticities $\varepsilon_p^{v_1}$ and $\varepsilon_p^{v_4}$. For parameter sets 1, 2, and 3 the situation is clear-cut: when $\varepsilon_P^{v_1} = -1$, $\varepsilon_p^{v_4} = 0$; when $\varepsilon_p^{v_1} = 0$, $\varepsilon_p^{v_4} \to 1$. In parameter set 4, however, $\varepsilon_p^{v_4}$ already attains a value of 1 within the FFE-region so that the downstream effect competes with the feedback effect, leading to sharing of self-response of P between the two routes.

From the above it should be clear that self-response coefficients provide an extremely useful view on the factors that determine what drives metabolite back to the steady-state value that obtained before the metabolite was perturbed, in other words, its dynamic stability.

Self-responses can be regarded as "primary" effects that follow a perturbation in a metabolite. However, a perturbation can also be considered to have "secondary" effects on other steady-state variables such as flux and other internal metabolites. Clearly these effects must cancel if the original steady state is to obtain after the perturbation. The use of internal-response coefficients to study these effects is the subject of the next section.

7.2 Internal-response coefficients

Figs. 7.4–7.9 shows the effects of a perturbation in one metabolite concentration on another metabolite in terms of the internal-response coefficients.

The first obvious observation is that where there are only two interaction routes the internal-response coefficients must have the same absolute values, but differ in sign because they must cancel. This is the situation for the internal-response coefficients of A and of B.

A perturbation in A (Figs. 7.4 and 7.5) affects B and P in the NE-region but not in the other two regions where $\varepsilon_a^{v_1} = 0$ (except for parameter set 3 where $\varepsilon_a^{v_1} \neq 0$—as discussed above—and combine with large concentration-control coefficients to give the spiked transition between the FFE and SC-regions). One would expect both the B and P responses to be qualitatively similar because both metabolites lie downstream from A. Note that any differences in these internal-response profiles can only be due to differences in the concentration-control coefficients, since in all of the internal-response coefficients with respect to a particular metabolite the elasticity coefficients are the same, e.g., both $^1R_a^b$ and $^1R_a^p$ contain $\varepsilon_a^{v_1}$ and both $^2R_a^b$ and $^2R_a^p$ contain $\varepsilon_a^{v_2}$.

A perturbation in B (Figs. 7.6 and 7.7) gives radically different internal-response coefficient profiles for A and P, which is not too surprising because A lies upstream from B while P lies downstream from B. Accordingly, the internal response of P to B looks the same as the responses of B to A and P to A just discussed. As noted above, any differences between the A to B and P to B internal-response profiles must be due to differences in concentration-control coefficients involved. Accordingly, we have to compare C_2^a and C_3^a (in Fig. 3.5) with C_2^p and C_3^p (in Fig. 3.7). Whereas C_2^a and C_3^a are both zero in the NE-region they become non-zero in the FFE-region and couple to extremely large elasticity coefficients, which accounts for the sharp transition observed between the NE and FFE-regions in Fig. 7.6. As the elasticity coefficients decrease in the FFE-region the internal-response coefficients decrease accordingly. Although on the scale of Fig. 7.7 it looks as if C_2^p and C_3^p are zero they have in fact small non-zero values of 10^{-4} which combined with extremely large elasticity coefficients is enough to account for internal-response profile observed.

The internal-response coefficient profiles for P (Figs. 7.8 and 7.9) have three components corresponding to an upstream effect via the chain ($^3R_p^a$, $^3R_p^b$), a downstream effect via the demand for P ($^4R_p^a$, $^4R_p^b$), and an effect via the

Figure 7.4: Internal-response coefficients for B with respect to a change in A for parameter sets 1 to 4.

Figure 7.5: Internal-response coefficients for P with respect to a change in A for parameter sets 1 to 4.

Figure 7.6: Internal-response coefficients for A with respect to a change in B for parameter sets 1 to 4.

Figure 7.7: Internal-response coefficients for P with respect to a change in B for parameter sets 1 to 4.

Figure 7.8: Internal-response coefficients for A with respect to a change in P for parameter sets 1 to 4.
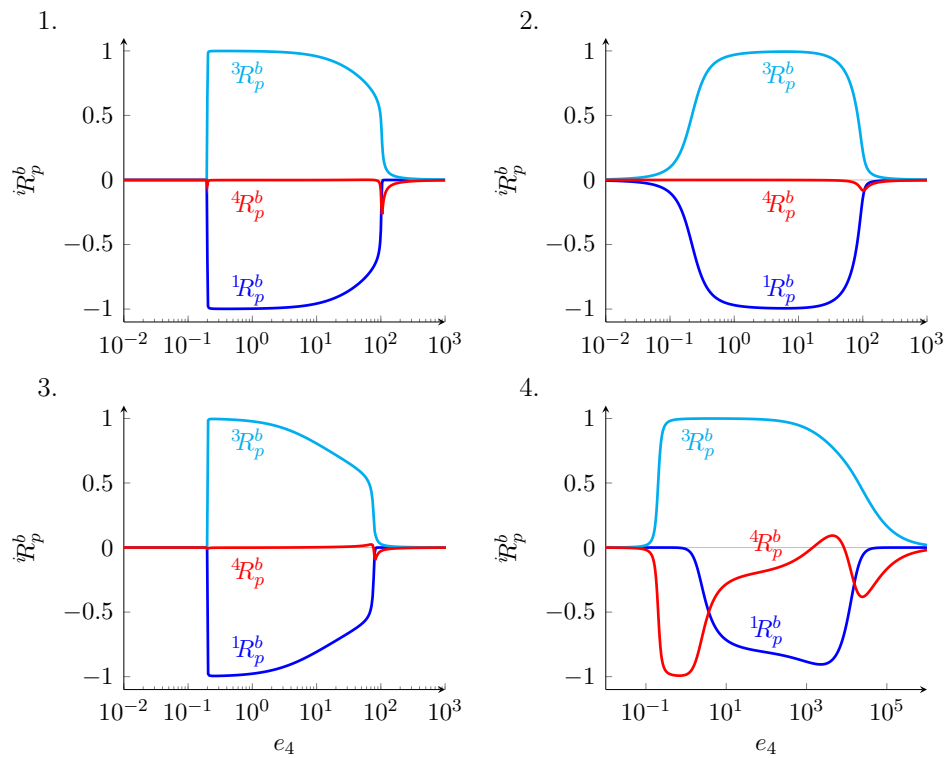
Figure 7.9: Internal-response coefficients for B with respect to a change in P for parameter sets 1 to 4.

feedback loop ($^1R_p^a$, $^1R_p^b$). For parameter sets 1, 2 and 3 the upstream and feedback effects dominate and give profiles that are qualitatively the same as those for B on A in Fig. 7.6, the reasons being the same. In the NE and FFE-regions the effect via E$_4$ is zero because $\varepsilon_p^{v_4}$ is zero. The reason why $^4R_p^a$ and $^4R_p^b$ are also zero in the SC-region while here $\varepsilon_p^{v_4}$ is not zero, is that the concentration-control coefficients C_4^a and C_4^b are both zero in the SC-region.

As expected, parameter set 4 gives different results in the FFE and SC-regions mainly because $\varepsilon_p^{v_4}$ is 1 instead of 0, thereby allowing C_4^a and C_4^b (see Fig. 3.5-4 and Fig. 3.6-4) to determine $^4R_p^a$ and $^4R_p^b$.

Lastly, because there are connectivity relationships for flux-control coefficients with corresponding internal flux-response coefficients, one could also consider the dynamic stability of flux. Figs. 7.10–7.12 show the internal flux-response coefficient profiles for the four parameter sets. The obvious feature of all of these profiles is that the internal-response coefficients are extremely small (note that the y-axis scale if from 10^{-2} to 10^2) and probably impossible to directly determine by experiment. The reason is of course that for E$_1$, E$_2$, and E$_3$ the flux-control coefficient component of the internal-response coefficients are effectively zero in the NE and FFE-regions for parameter sets 1, 2 and 3. Even in parameter set 4, where this is not true in the FFE-region, the internal-response coefficients are still small. The same generalisation holds for the internal-response coefficient profiles of P, except for parameter set 4 where the flux-control is shared between E$_1$ and E$_4$ in the FFE-region and gives larger internal-response coefficient values.

In retrospect, we believe our analysis shows that the self-responses and the internal responses of one metabolite with respect to another provides the most interesting view of dynamic stability, self-responses in particular. Flux responses to perturbations in internal metabolite concentrations probably give less insight.
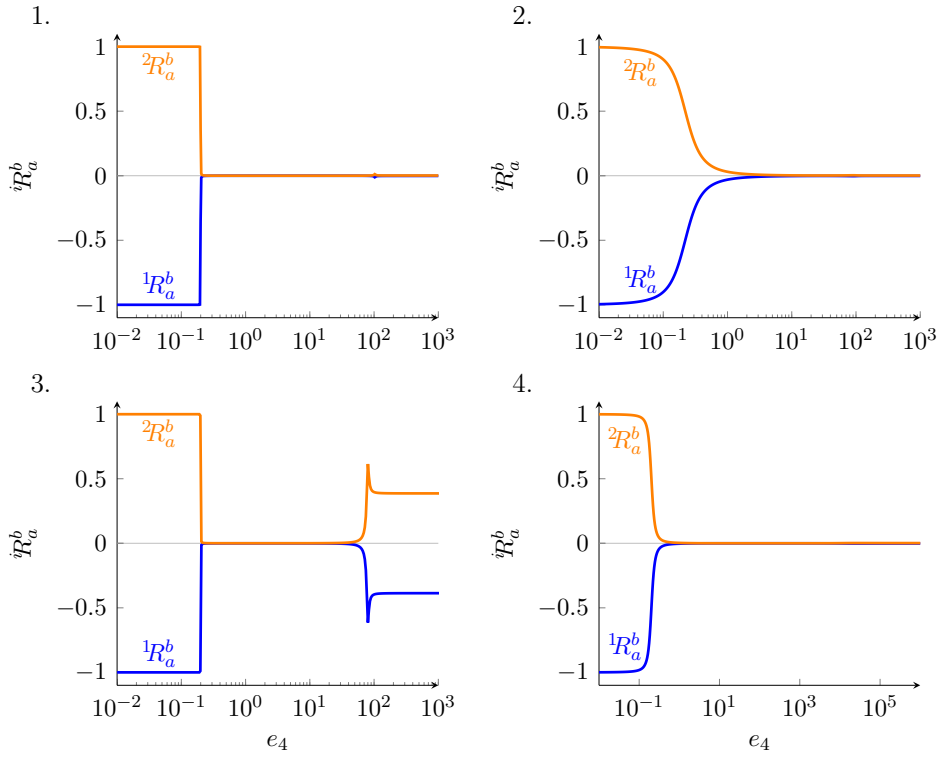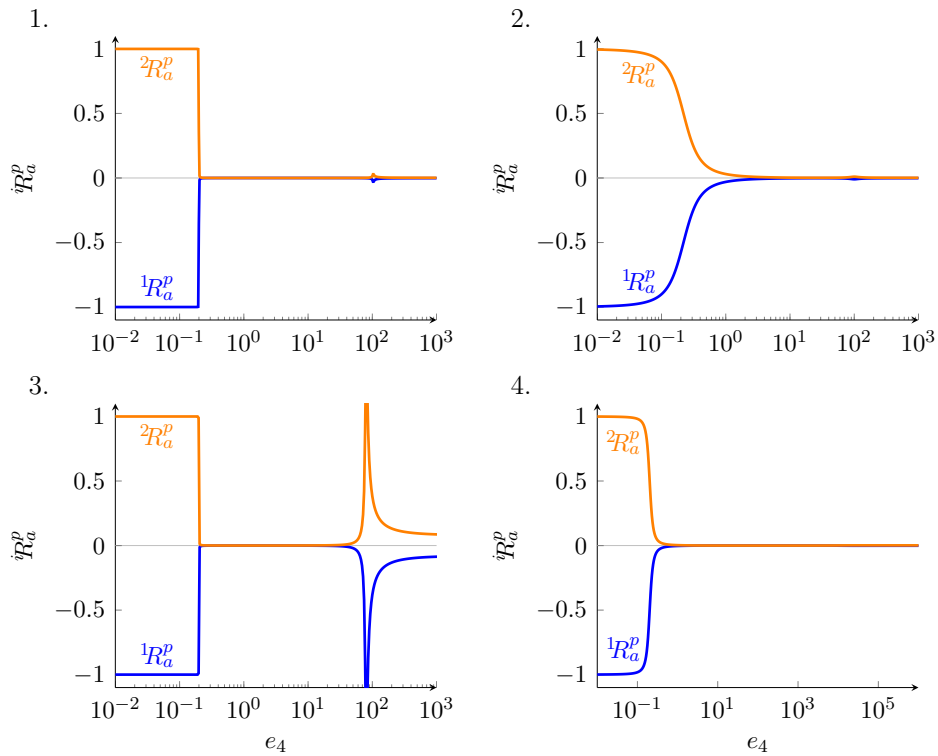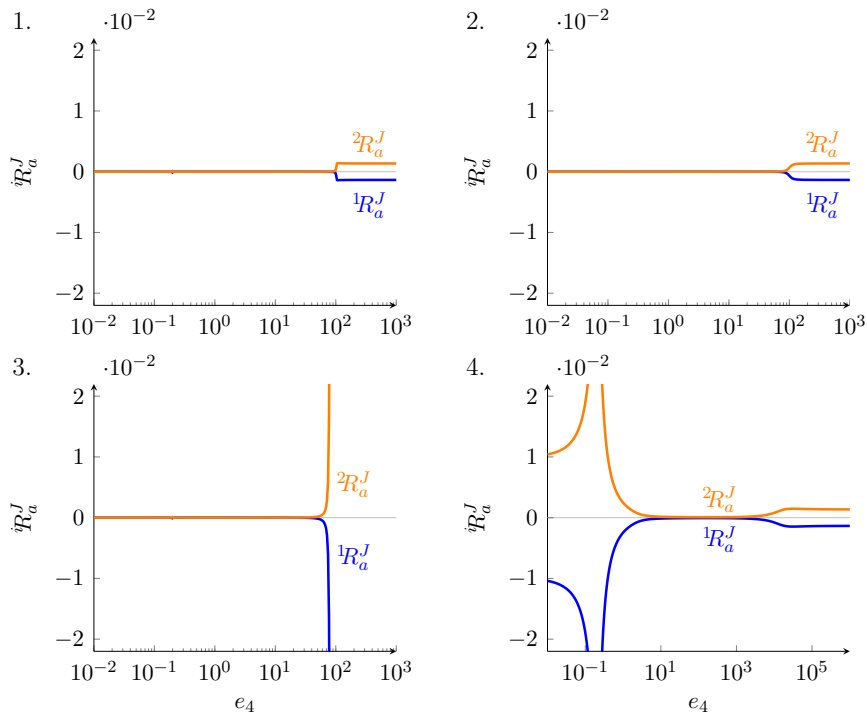
Figure 7.10: Internal-response coefficients for J with respect to a change in A for parameter sets 1 to 4.
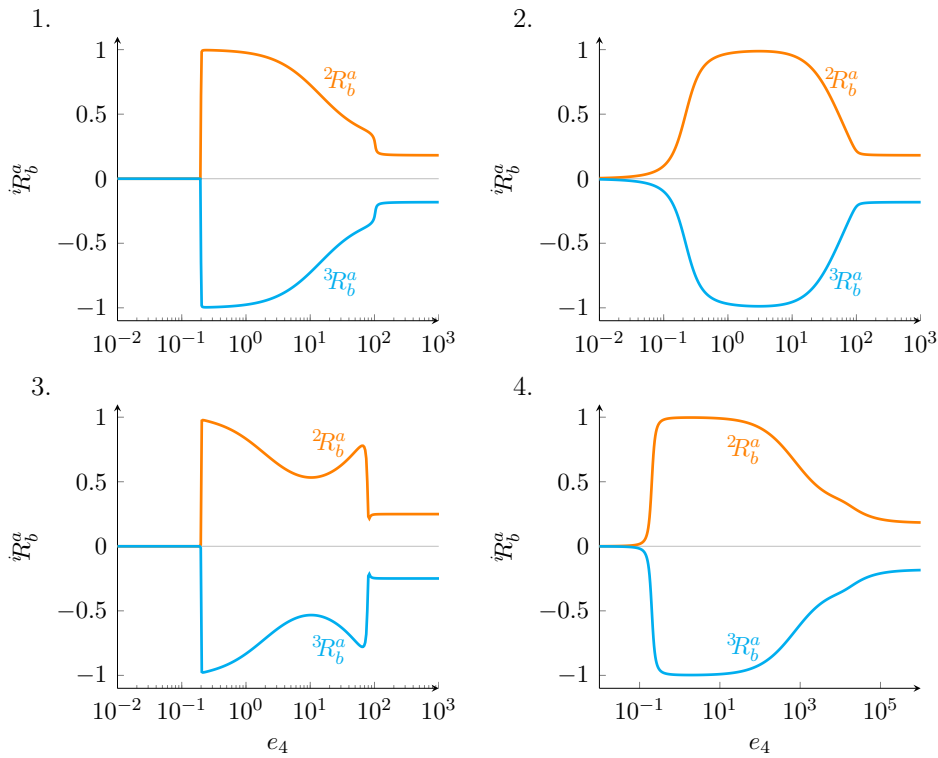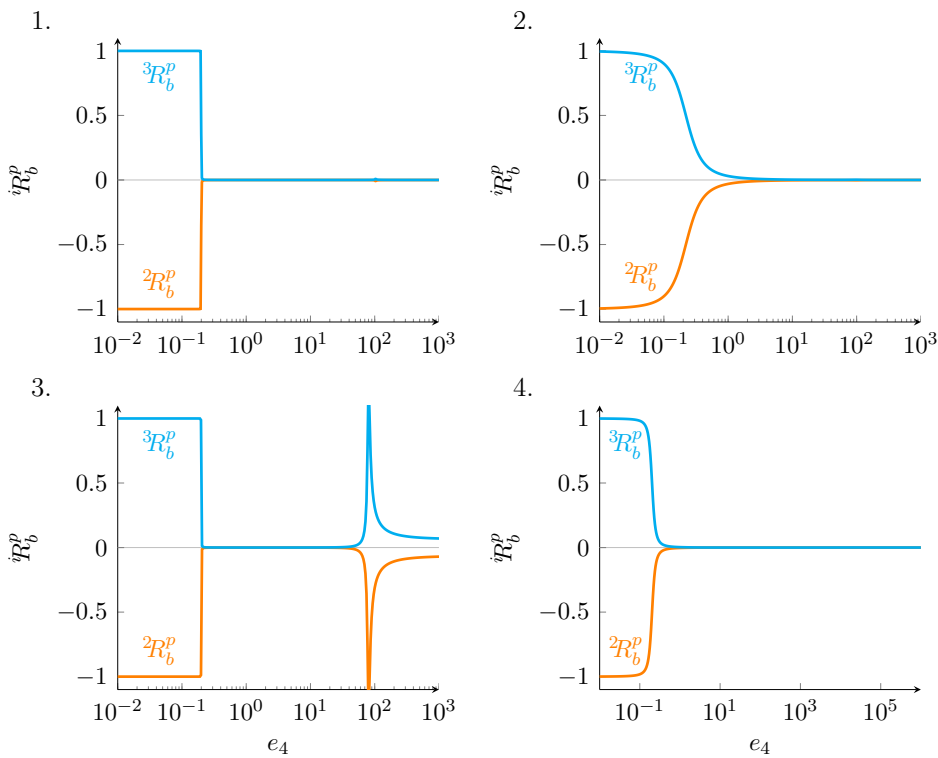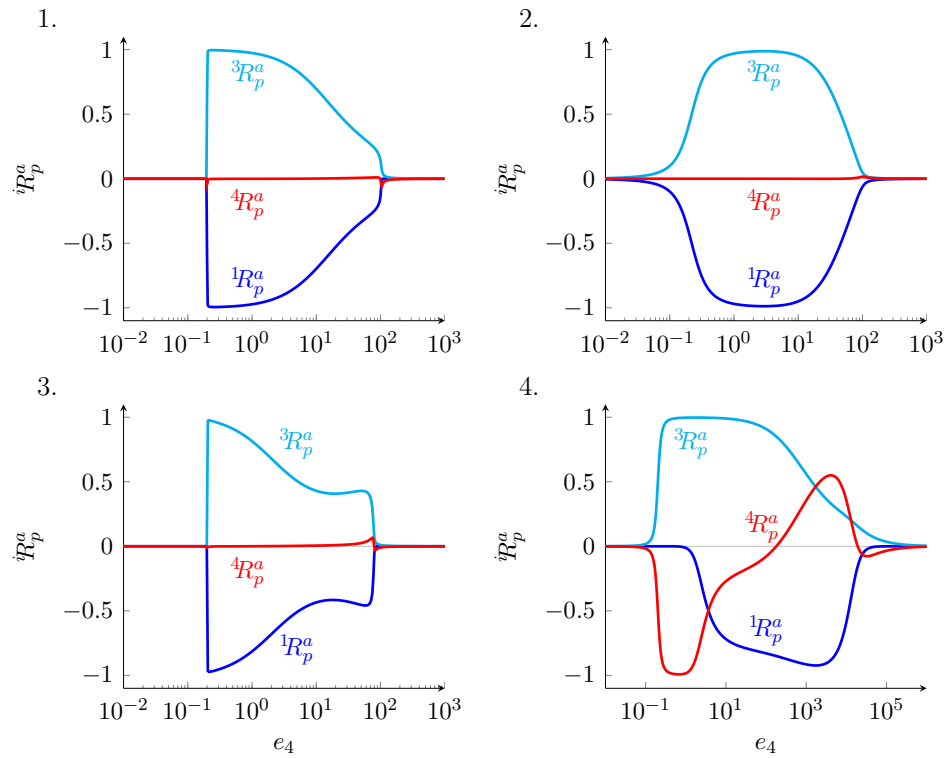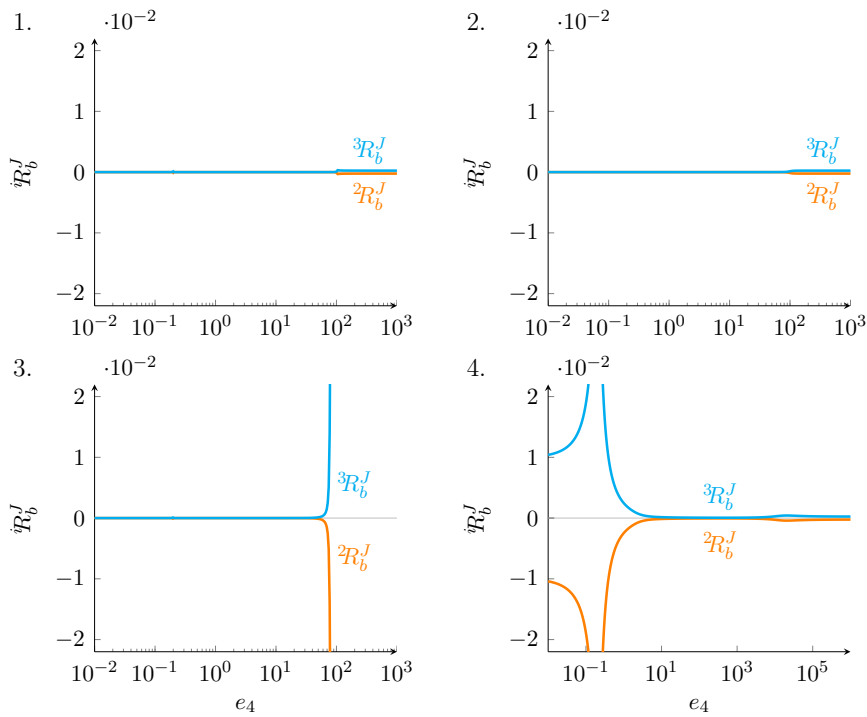

Figure 7.11: Internal-response coefficients for J with respect to a change in B for parameter sets 1 to 4.
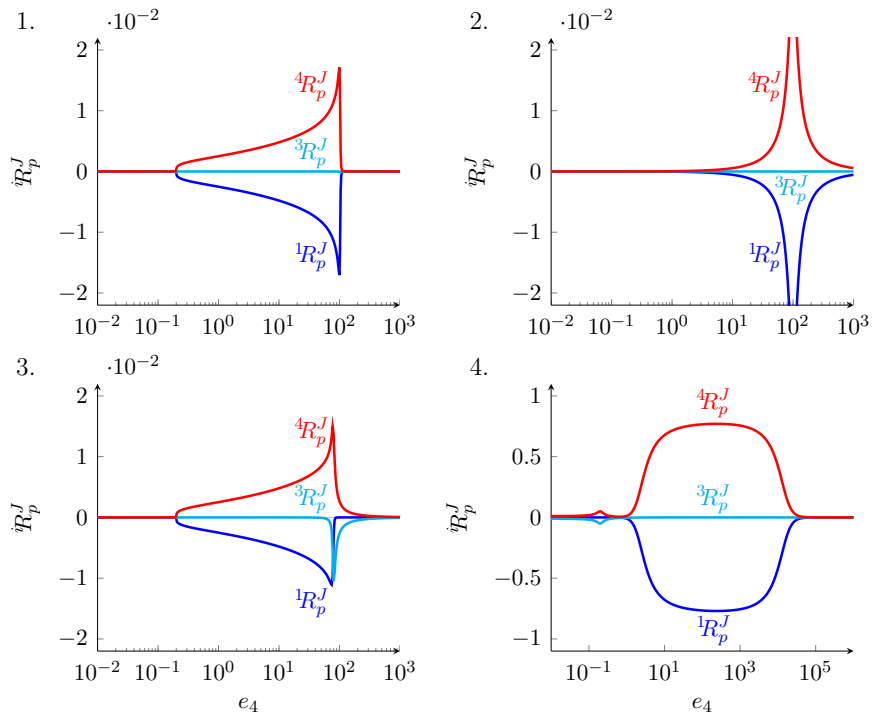
Figure 7.12: Internal-response coefficients for J with respect to change in P for parameter sets 1 to 4.

Chapter 8

Sauro's partitioned regulatory coefficients

Consider a perturbation in the activity of a particular step through a parameter such as its enzyme concentration. Ask the question: For each step in a pathway, what is the contribution to the flux-response in that step through each of the metabolites that directly affects the activity of that enzyme? Sauro [34] suggested a way of quantifying this response in term of what he termed "partitioned regulatory coefficients". Whether this is what most biochemists would understand under the umbrella term "regulation" is questionable. Accordingly, this chapter while reviewing the theory behind Sauro's analysis and suggesting a modified version, does not intend to provide too detailed a treatment.

8.1   Background

The background theory that underlies the relationship between partitioned regulatory coefficients has already been explained in Section 2.10. For a perturbation in, say, v_4 of the reaction scheme in Fig. 3.1, the flux-control coefficient C_4^J can be expressed in four ways, each corresponding to the flux response at a particular reaction:

$$C_4^J = \varepsilon_a^{v_1} C_4^a + \varepsilon_p^{v_1} C_4^p \qquad (8.1)$$

$$C_4^J = \varepsilon_a^{v_2} C_4^a + \varepsilon_b^{v_2} C_4^b \qquad (8.2)$$

$$C_4^J = \varepsilon_b^{v_3} C_4^b + \varepsilon_p^{v_3} C_4^p \qquad (8.3)$$

$$C_4^J = 1 + \varepsilon_p^{v_4} C_4^p \qquad (8.4)$$

These equations can be understood in terms of the simple thought experiment described in Section 2.10.

If both sides in these equations are divided by C_4^J they yield the following:

$$1 \;=\; \varepsilon_a^{v_1}\frac{C_4^a}{C_4^J} + \varepsilon_p^{v_1}\frac{C_4^p}{C_4^J} = \varepsilon_a^{v_1}O_4^{a:J} + \varepsilon_p^{v_1}O_4^{p:J} \tag{8.5}$$

$$1 \;=\; \varepsilon_a^{v_2}\frac{C_4^a}{C_4^J} + \varepsilon_b^{v_2}\frac{C_4^b}{C_4^J} = \varepsilon_a^{v_2}O_4^{a:J} + \varepsilon_b^{v_2}O_4^{b:J} \tag{8.6}$$

$$1 \;=\; \varepsilon_b^{v_3}\frac{C_4^b}{C_4^J} + \varepsilon_p^{v_3}\frac{C_4^p}{C_4^J} = \varepsilon_b^{v_3}O_4^{b:J} + \varepsilon_p^{v_3}O_4^{p:J} \tag{8.7}$$

$$1 \;=\; \frac{1}{C_4^J} + \varepsilon_p^{v_4}\frac{C_4^p}{C_4^J} = \frac{1}{C_4^J} + \varepsilon_p^{v_4}O_4^{p:J} \tag{8.8}$$

Sauro [34] named the right-hand terms *partitioned regulatory coefficients* (although he did not reframe the equations in terms of co-control coefficients, which had not yet been defined at that time). Following Sauro [34], we shall use the symbol $^{s_k}P_{v_i}^{J_j}$ to denote a partitioned regulatory coefficient that describes how a perturbation in rate v_i of reaction i affects the flux J_j through reaction r_j via a change in the concentration s_k of a metabolite that interacts directly with enzyme E_j[1].

Using this symbolism, eqns. 8.5–8.8 become

$$1 \;=\; {}^aP_4^1 + {}^pP_4^1 \tag{8.9}$$

$$1 \;=\; {}^aP_4^2 + {}^bP_4^2 \tag{8.10}$$

$$1 \;=\; {}^bP_4^3 + {}^pP_4^3 \tag{8.11}$$

$$1 \;=\; {}^{v_4}P_4^4 + {}^pP_4^4 \tag{8.12}$$

Note in particular the use of $^{v_4}P_4^4$ to denote $1/C_4^J$, the coefficient that describes the direct effect of the perturbation on the flux through reaction 4 that is not mediated by a metabolite.

On reflection, it is not clear what Sauro gained by scaling with the flux-control coefficient. One obvious problem arises when the scaling flux-control coefficient approaches zero so that the partitioned regulatory coefficients become extremely large. In fact, one loses information by scaling in this way and in our opinion it makes sense to also use the unscaled eqns. 8.1–8.4. We therefore propose to rewrite eqns. 8.1–8.4 using $^{s_k}\pi_{v_i}^{J_j}$ as a symbol for the right hand

---

[1]Sauro used a different configuration of subscripts and superscripts, namely $^{v_i}P_{s_k}^{J_j}$, but we prefer our configuration because it follows the same convention as the other coefficients of MCA, in that the subscript refers to the perturbation, the superscript to the variable affected and the pre-superscript to the route through which the effect is mediated

terms, which we shall just call, for want of a better term, π-*coefficients* (since regulation is a general concept, we prefer not to link the notion of regulation directly to these coefficients, the same reasoning why we preferred "internal-response coefficients" to Kahn and Westerhoff's "regulatory strengths" and "self-response coefficients" to "homeostatic strengths").

$$C_4^J = {}^a\pi_4^1 + {}^p\pi_4^1 \qquad (8.13)$$

$$C_4^J = {}^a\pi_4^2 + {}^b\pi_4^2 \qquad (8.14)$$

$$C_4^J = {}^b\pi_4^3 + {}^p\pi_4^3 \qquad (8.15)$$

$$C_4^J = {}^{v_4}\pi_4^4 + {}^p\pi_4^4 \qquad (8.16)$$

Here ${}^{v_4}\pi_4^4 = 1$ by definition and reflects the fact that the perturbation in the local v_4 has a direct proportional effect on the flux through reaction 4.

Fig. 8.1 compares the two incarnations of Sauro's coefficients for a perturbation in v_4, with panel A depicting the partitioned regulatory coefficients for the four reactions in Fig. 3.1, and panel B the corresponding π-coefficients together with the flux-control coefficient that they sum to. In the NE and FFE-regions where $C_4^J = 1$, the two types of coefficients are of course identical, while in the SC-region where $C_4^J = 0$, the partitioned response coefficients approach $\pm\infty$, while the π-coefficients are zero. The exception is the SC-region in 1A, where the partitioned regulatory coefficients are different (showing that the effect on reaction 1, such as it is, is via A and not via P), while the π-coefficients are both zero. How useful this is, is however debatable, since the actual flux change through reaction 1 is zero. In the rest of this chapter we therefore prefer to use π-coefficients instead of partitioned regulatory coefficients to illustrate Sauro's approach, albeit in a modified form.

8.2 Analysis using π-coefficients

As an example of what one can learn from Sauro's approach, Figs. 8.2–8.5 compare the π-coefficients of all four reactions with respect to a perturbation in v_4 for parameter sets 1 to 4.

Fig. 8.2 shows that in the NE-region the flux response in reaction 1 is solely via A, while in the FFE-region it is via P. This is due to $\varepsilon_p^{v_1}$, which is 0 in both the NE and the SC-regions, forming part of ${}^p\pi_4^1$, and $\varepsilon_a^{v_1}$, which is 0 in the FFE and SC-regions, forming part of ${}^a\pi_4^1$.

For reactions 2 and 3 in Figs. 8.3 and 8.4 the π-coefficients are both very large and of opposite sign in the NE-region and most of the FFE-region;
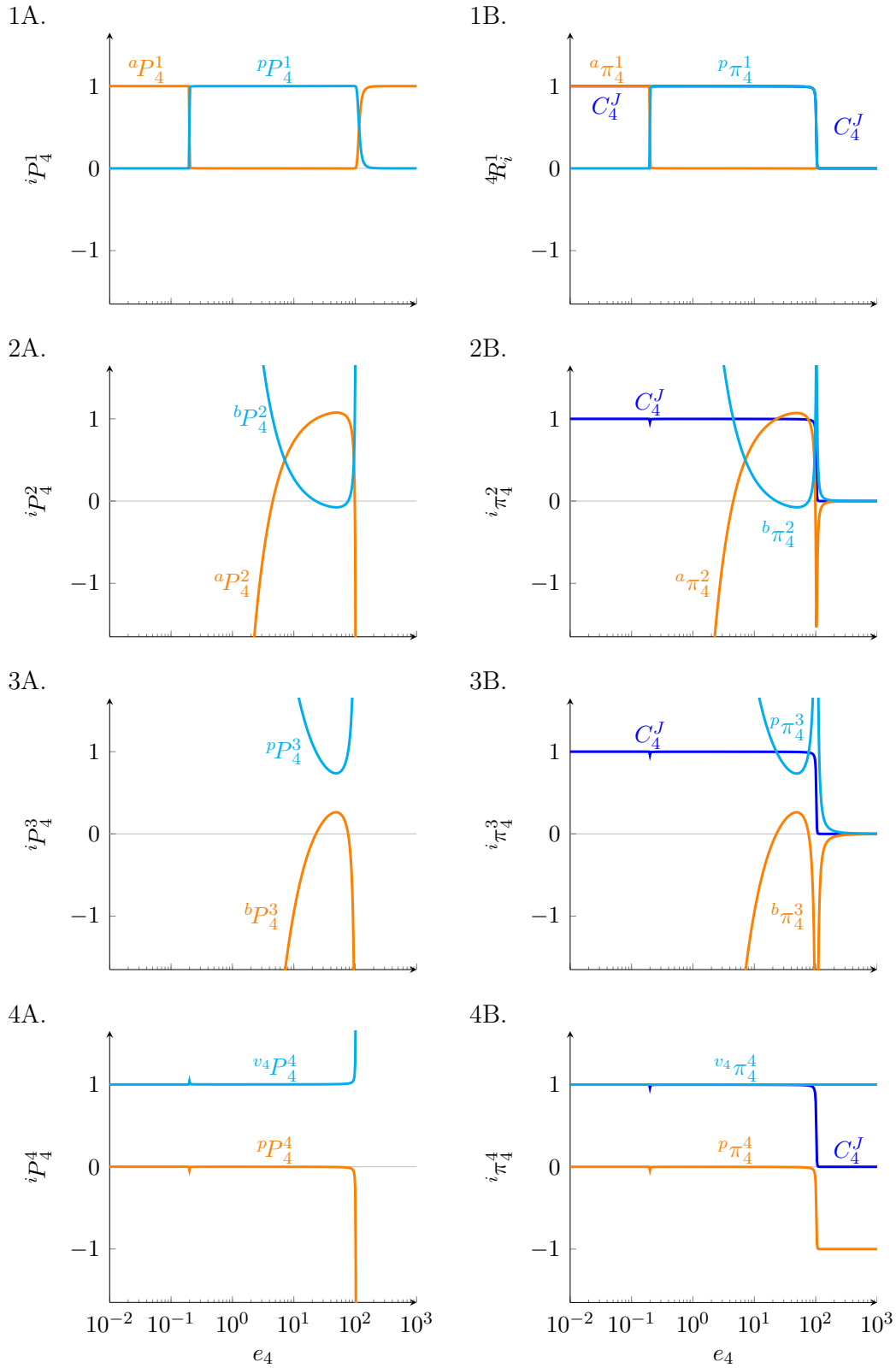
Figure 8.1: Sauro's partitioned regulatory coefficients (A) vs. π-coefficients (B) of E_1–E_4 with respect to a perturbation in v_4 for parameter set 1.

the reason for this is that here these reactions are near-equilibrium due to the high activity of their enzymes and therefore have extremely large elasticity coefficients that dominate the π-coefficients. In that part of the FFE-region closest to the SC-region the π-coefficients deviate from the elasticity profiles in Fig. 3.8; here the π-coefficients are determined by their concentration-control coefficients components (see the profiles of R_4^a and R_4^b in Fig. 3.3-B). In this region most of the response in the flux through reaction 2 is via A. For reaction 3 this is less pronounced.

For reaction 4 in Fig. 8.5, since the ${}^{v_4}\pi_4^4$ term is 1, the π-coefficient ${}^p\pi_4^4$ tracks C_4^J with a fixed difference of 1, so that one cannot learn anything more from these profiles than is already provided by C_4^J.

As stated in the beginning of this chapter, we are of the opinion that the information gained by Sauro's analysis, while interesting in itself, is not what one would usually classify as telling one much about regulation and we have accordingly not attempted a detailed investigation.
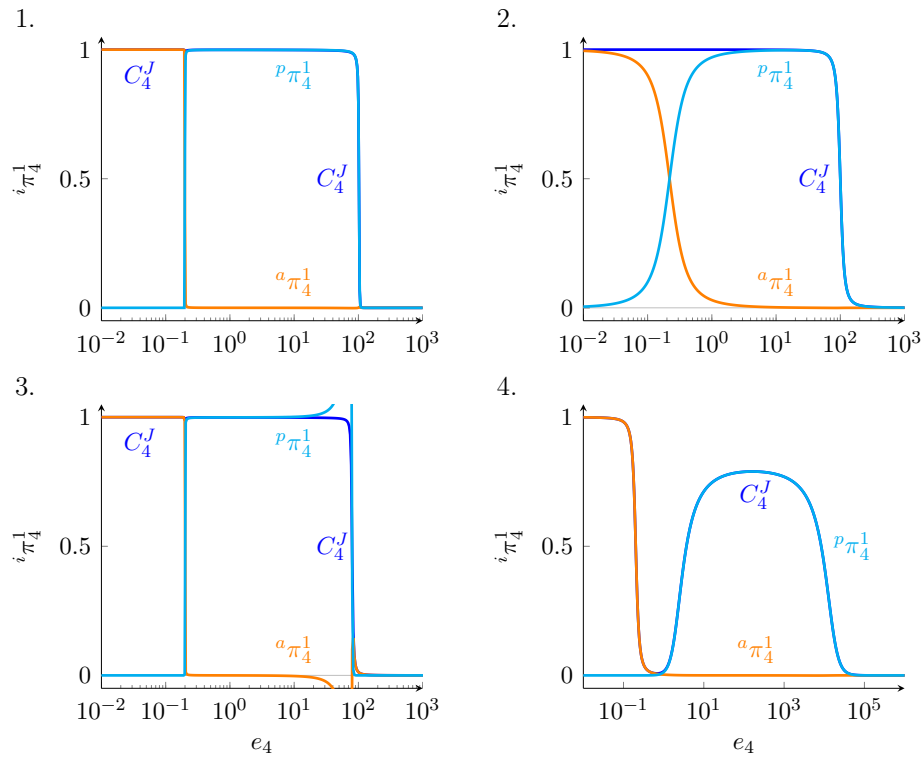
Figure 8.2: π-coefficients of E_1 with respect to a perturbation in v_4 for parameter sets 1 to 4.
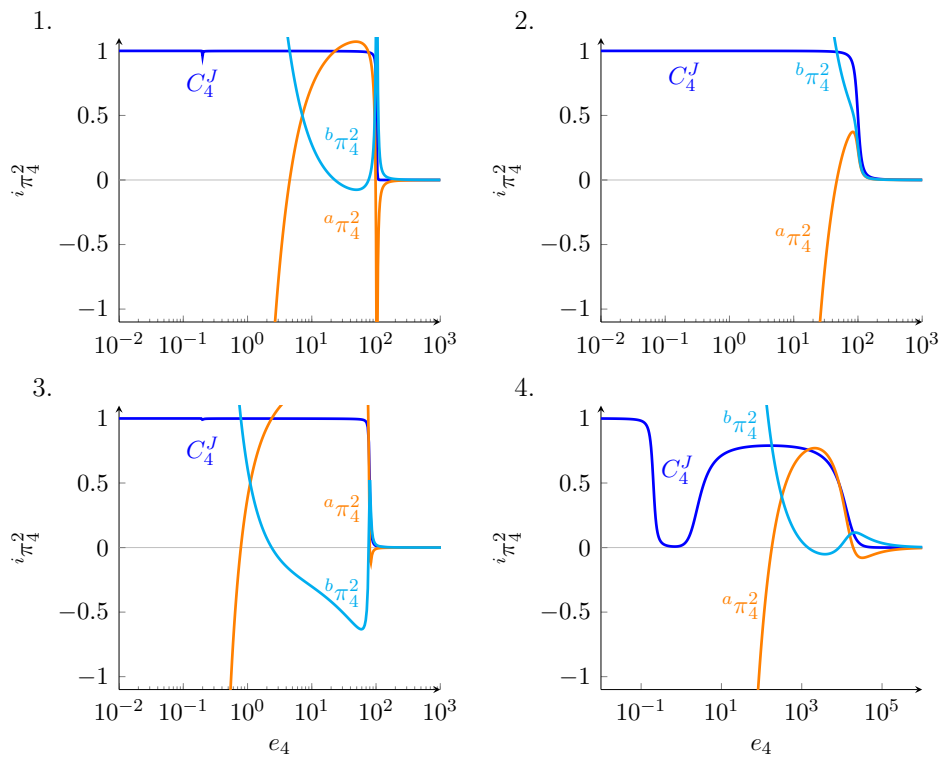
Figure 8.3: π-coefficients of E_2 with respect to a perturbation in v_4 for parameter sets 1 to 4.
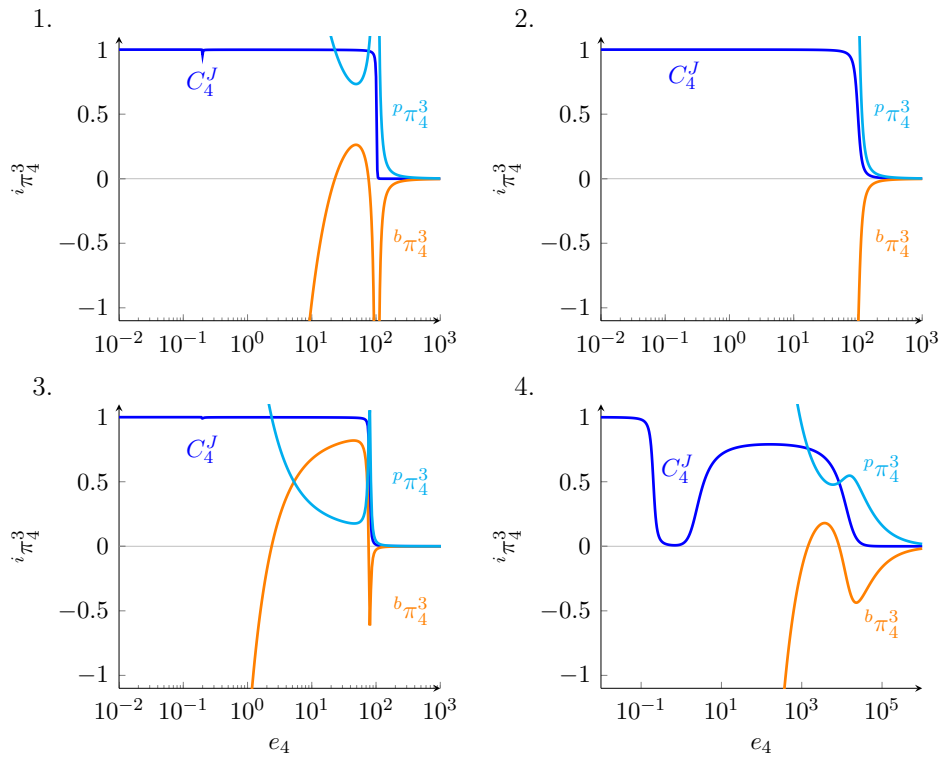
Figure 8.4: π-coefficients of E_3 with respect to a perturbation in v_4 for parameter sets 1 to 4.
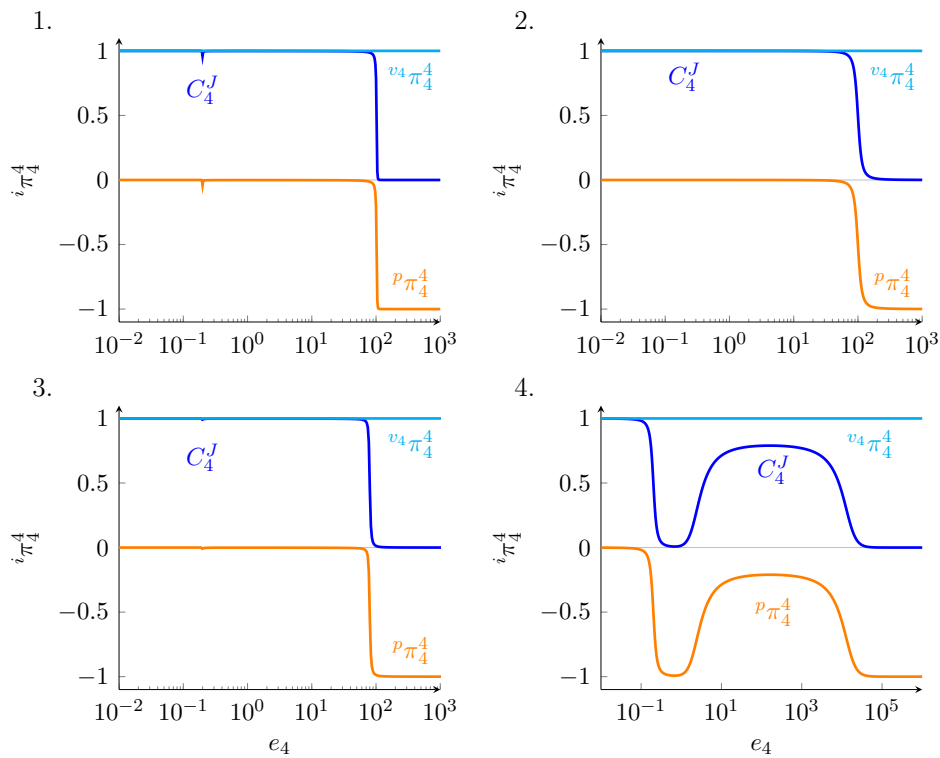
Figure 8.5: π-coefficients of E_4 with respect to a perturbation in v_4 for parameter sets 1 to 4.

Chapter 9

Discussion

Metabolic systems are thermodynamically open systems continually subject to changes in the surrounding environment that cause fluctuations in the state variables and perturbations in the system parameters. It is therefore important that metabolic systems have mechanisms to keep them dynamically and structurally stable in the face of these changes. In addition, metabolic systems should also be able to cope with large changes in the fluxes through the pathways, not letting metabolite concentrations vary wildly. Consider, for example, that human metabolism manages to keep the blood glucose concentration within a narrow range when the flux through the glucose pool increases drastically when going from the fasting to the fed state, an example of metabolic homeostasis.

Metabolic regulation studies often fall into the trap of trying to locate regulation in a few mechanisms such as feedback or feedforward effects, thereby losing sight of the fact to regulation is a systemic property. In the study presented in this dissertation metabolic regulation was approached from such a systemic point of view, using the quantitative framework of Metabolic Control Analysis.

The system chosen to serve as an example had the advantage that its regulatory properties were well understood. The four parameters sets were chosen to illustrate different behavioural aspects of the system. Parameter set 1 defined a system in which the demand is saturated with its substrate P throughout most of the scan range of the demand, and therefore has an elasticity coefficient of zero in this range and has full flux control. Only when demand is so high that the supply becomes limiting does the demand elasticity increase to its limiting value of 1 (typical for an irreversible Michaelis-Menten enzyme). The supply flux itself is controlled by the first enzyme since it was

defined to be virtually insensitive to its immediate product A. This means that in the FFE-region E_1 determines how the steady-state concentration of P changes with demand. In which concentration range and how steeply it changes is determined by how strongly it binds to E_1 and the degree of binding cooperativity. The intermediary supply enzymes E_2 and E_3 were set to be very active and keep the steady-state concentrations of A and B linked in near-equilibrium with P as it varies.

Parameter set 2 demonstrated that when the cooperativity of binding of P to E_1 decreases, the concentration of P varies over a much larger range in the FFE-region. Parameter set 3 showed that when the intermediary supply enzymes E_2 and E_3 are less active they cannot keep A and B in near-equilibrium with P so that their concentrations varies much more with the demand. In parameter set 4 P binds four orders of magnitude less strongly to the demand so that the demand does not have full control over the flux in the FFE-region.

Throughout the study the system was subjected to a wide variation in demand that took it from very low demand, where metabolite concentration tends to near equilibrium with the fixed pathway substrate, to very high demand, where the supply cannot match it. The parameter portraits of steady-state flux and metabolite concentrations (Fig. 3.3) for the four parameter sets clearly delineates three regions as the demand varied from low to high: one near equilibrium, one far from equilibrium, and one where the supply takes over the control of flux completely (the demand having full flux control in the other two regions). In the old parlance the demand is rate-limiting in the NE and FFE regions, while the supply is rate-limiting in the SC-region. From these parameter portraits one could already see that, while qualitatively they give the same profile, quantitatively the metabolite concentrations behave quite differently with the different parameter sets, especially in the FFE region: with parameter set 1 A, B, P remains relatively constant, with parameter set 2 they vary much more, with parameter set 3 P remains relatively constant but A and B do not, with parameter set 4 they give a profile similar to parameter set 1 but the transitions between the regions are much less abrupt.

The study then investigated the use of Metabolic Control Analysis for studying particular aspects of metabolic regulation, namely the regulation of structural stability using concentration-response coefficients, of homeostasis using co-response coefficients, and of dynamic stability using self-response and internal response coefficients. However, just knowing the values of these coefficients was only half of the story. The other half was understanding quanti-

tatively which interactions in the system determine the value of one of these coefficients in a particular steady state. It was shown that control patterns allow the dissection of a control coefficient into chains of local effects that emanate from the perturbation and are therefore valuable in understanding which system properties determine structural stability and to what degree. Similarly, self-response and internal response coefficients give the same type of quantitative insight into dynamic stability, especially self-response coefficients that describe which routes from the perturbed metabolite drive it back to its steady-state value before the perturbation. Metabolite-flux co-response coefficients allow the definition of an index that quantifies to which degree a metabolite is homeostatically regulated. It must be stressed that, although these measures have been proposed before in the literature, they have to our knowledge never been investigated and compared before in the way that this study did.

One of the main insights gained from this study is the importance of elasticity coefficients that tend to zero. In our system these were the elasticity of E_1 to its immediate product A, which ensures that E_1 controls the flux in the supply subsystem in the FFE and SC-regions, and the elasticity of E_4 to its substrate P, which ensures that the demand controls the flux in the NE and FFE-regions. The fact that the feedback elasticity $\varepsilon_p^{v_1}$ is zero in the SC-region also played an important role in determining which other interactions contributed to regulation.

In the regulation of both structural and dynamic stability it was evident that the main factors were interactions up and down the reaction sequence in the NE-region, the feedback loop in the FFE-region, and the demand elasticity in the SC-region.

Although Sauro's [34] approach to metabolic regulation did not originally form part of this investigation, it was felt that at least an explanation and example would be useful and was therefore included. What did come out of this is that the scaled partitioned regulatory coefficients that sum to one may not be the most informative measures, and that the unscaled coefficients, that we called π-coefficients may be more useful.

Although the metabolic system used to demonstrate the concepts developed in this study is rather simple, the analysis is valid for systems of arbitrary complexity. This study has therefore laid the groundwork for future studies of metabolic regulation of more complex core models or of models of real systems such as the ones archived in model databases such as JWS On-

86

line (`http://jjj.biochem.sun.ac.za/`) and BioModels (`http://www.ebi.ac.uk/biomodels-main/`). It also demonstrates the importance of such models to further our understanding of metabolic behaviour, control and regulation. The experimental implementation of the analyses described in this dissertation is probably to a large degree unfeasible at present, but if one has a good model then this is what one could use it for. Too often metabolic models are constructed without ever being interrogated and here one such way of doing it was demonstrated. It is not even necessary to analyse real models. As shown here, much can be learnt from generic models based on proper enzyme kinetics.

Although Sauro's [34] approach to metabolic regulation did not originally form part of this investigation, it was felt that at least an explanation and example would be useful and was therefore included. What did come out of this is that the scaled partitioned regulatory coefficients that sum to one may not be the most informative measures, and that the unscaled coefficients, that we called π-coefficients may be more useful. This study has laid the groundwork for future studies of metabolic regulation of more complex core models or of models of real systems such as the ones archived in model databases such as JWS Online (http://jjj.biochem.sun. ac.za/) and BioModels (http://www.ebi.ac.uk/biomodels-main/). It also demonstrates the importance of such models to further our understanding of metabolic behaviour, control and regulation. The experimental implementation of the analyses described in this dissertation is probably to a large degree unfeasible at present, but if one has a good model then this is what one could use it for. Too often metabolic models are constructed without ever being interrogated and here one such way of doing it was demonstrated. It is not even necessary to analyse real models. As shown here, much can be learnt from generic models based on proper enzyme kinetics.

Chapter 10

Appendices

10.1 **PySCeS** input file for the pathway in Fig. 3.1

```
# A linear pathway consisting of four enzyme-catalysed reactions
# with end-product inhibition of the committing enzyme by the
# pathway product.

# S --E1--> A --E2--> B --E3--> P --E4--> dummy
      |_____|

FIX: S dummy

R1: S = A

    (kcat1*E1/K1s)*(S - A/Keq1)*(S/K1s + A/K1a)**(h-1)/
    ((S/K1s + A/K1a)**h + (1 + (P/K1p)**h)/(1 + alpha*(P/K1p)**h))

R2: A = B

    (kcat2*E2/K2a)*(A - B/Keq2)/(1 + A/K2a + B/K2b)

R3: B = P

    (kcat3*E3/K3b)*(B - P/Keq3)/(1 + B/K3b + P/K3p)

R4: P > dummy

    kcat4*E4*P/(K4p + P)

# Initialise internal metabolite concentrations

A = 0.001
B = 0.001
P = 0.001
```

```
# Initialise external metabolite concentrations

S = 1.0
dummy = 0.0

# Initialise enzyme parameters
# E1
Keq1  = 100.0
kcat1 = 1.0
E1    = 200.0
K1s   = 1.0
K1a   = 1.0e5
h     = 4.0
K1p   = 1.0
alpha = 0.001

# E2
Keq2  = 10.0
kcat2 = 1.0
E2    = 1000.0
K2a   = 1.0
K2b   = 1.0

# E3
Keq3  = 10.0
kcat3 = 1.0
E3    = 1000.0
K3b   = 1.0
K3p   = 1.0

# E4
kcat4 = 1.0
E4    = 50.0
K4p   = 0.01
```

10.2   Python script used to generate all the simulation results

```
# E4-parameter scans

import pysces, scipy

m = pysces.model('lin4fb')

m.doState()
m.doMca()

output_dir = 'data/'

m.scan_in   = 'E4'
```

```
m.scan_out = ['J_R1','A','B','P',
              'ecR1_A','ecR2_A','ecR2_B','ecR3_B',
              'ecR1_P','ecR3_P','ecR4_P',
              'ccJR1_R1','ccJR1_R2','ccJR1_R3','ccJR1_R4',
              'ccA_R1','ccA_R2','ccA_R3','ccA_R4',
              'ccB_R1','ccB_R2','ccB_R3','ccB_R4',
              'ccP_R1','ccP_R2','ccP_R3','ccP_R4']


def create_data_arrays(mod, par_set):
    mod.Scan1(scan_range)

    E4   = mod.scan_res[:,0]


# Steady-state variables
    J_R1 = mod.scan_res[:,1]
    A    = mod.scan_res[:,2]
    B    = mod.scan_res[:,3]
    P    = mod.scan_res[:,4]


# Elasticities
    ec_R1_A = mod.scan_res[:,5]
    ec_R2_A = mod.scan_res[:,6]

    ec_R2_B = mod.scan_res[:,7]
    ec_R3_B = mod.scan_res[:,8]

    ec_R1_P = mod.scan_res[:,9]
    ec_R3_P = mod.scan_res[:,10]
    ec_R4_P = mod.scan_res[:,11]


# Control Coefficients
    cc_J_R1 = mod.scan_res[:,12]
    cc_J_R2 = mod.scan_res[:,13]
    cc_J_R3 = mod.scan_res[:,14]
    cc_J_R4 = mod.scan_res[:,15]

    cc_A_R1 = mod.scan_res[:,16]
    cc_A_R2 = mod.scan_res[:,17]
    cc_A_R3 = mod.scan_res[:,18]
    cc_A_R4 = mod.scan_res[:,19]

    cc_B_R1 = mod.scan_res[:,20]
    cc_B_R2 = mod.scan_res[:,21]
    cc_B_R3 = mod.scan_res[:,22]
    cc_B_R4 = mod.scan_res[:,23]

    cc_P_R1 = mod.scan_res[:,24]
    cc_P_R2 = mod.scan_res[:,25]
    cc_P_R3 = mod.scan_res[:,26]
    cc_P_R4 = mod.scan_res[:,27]

    ss_var_list = ['E4'] + mod.scan_out


# Sauro's scaled partitioned regulatory coefficients for E1
```

```
# through E1
E1_prc_E1_J_via_a  = (ec_R1_A * cc_A_R1) / cc_J_R1
E1_prc_E1_J_via_p  = (ec_R1_P * cc_P_R1) / cc_J_R1
E1_prc_E1_J_via_v1 = 1 / cc_J_R1


# through E2
E1_prc_E2_J_via_a  = (ec_R2_A * cc_A_R1) / cc_J_R1
E1_prc_E2_J_via_b  = (ec_R2_B * cc_B_R1) / cc_J_R1


# through E3
E1_prc_E3_J_via_b  = (ec_R3_B * cc_B_R1) / cc_J_R1
E1_prc_E3_J_via_p  = (ec_R3_P * cc_P_R1) / cc_J_R1


# through E4
E1_prc_E4_J_via_p  = (ec_R4_P * cc_P_R1) / cc_J_R1


E1_prc_list = ['E4',
'E1_J_via_a', 'E1_J_via_p', 'E1_J_via_v1',
'E2_J_via_a', 'E2_J_via_b',
'E3_J_via_b', 'E3_J_via_p',
'E4_J_via_p']


# Sum of partitioned regulatory coefficients: Theory check
sum_E1_prc_E1_J = E1_prc_E1_J_via_a + E1_prc_E1_J_via_p + E1_prc_E1_J_via_v1
sum_E1_prc_E2_J = E1_prc_E2_J_via_a + E1_prc_E2_J_via_b
sum_E1_prc_E3_J = E1_prc_E3_J_via_b + E1_prc_E3_J_via_p
sum_E1_prc_E4_J = E1_prc_E4_J_via_p


sum_E1_prc_list = ['E4',
'J_E1', 'J_E2', 'J_E3', 'J_E4']

# Sauro's Partitioned regulatory coefficients for E2

# through E1
E2_prc_E1_J_via_a  = (ec_R1_A * cc_A_R2) / cc_J_R2
E2_prc_E1_J_via_p  = (ec_R1_P * cc_P_R2) / cc_J_R2


# through E2
E2_prc_E2_J_via_a  = (ec_R2_A * cc_A_R2) / cc_J_R2
E2_prc_E2_J_via_b  = (ec_R2_B * cc_B_R2) / cc_J_R2
E2_prc_E2_J_via_v2 = 1 / cc_J_R2


# through E3
E2_prc_E3_J_via_b  = (ec_R3_B * cc_B_R2) / cc_J_R2
E2_prc_E3_J_via_p  = (ec_R3_P * cc_P_R2) / cc_J_R2


# through E4
E2_prc_E4_J_via_p  = (ec_R4_P * cc_P_R2) / cc_J_R2


E2_prc_list = ['E4',
'E1_J_via_a', 'E1_J_via_p',
'E2_J_via_a', 'E2_J_via_b', 'E2_J_via_v2',
'E3_J_via_b', 'E3_J_via_p',
```

```
    'E4_J_via_p']

    # Sum of partitioned regulatory coefficients: Theory check
    sum_E2_prc_E1_J = E2_prc_E1_J_via_a + E2_prc_E1_J_via_p
    sum_E2_prc_E2_J = E2_prc_E2_J_via_a + E2_prc_E2_J_via_b + E2_prc_E2_J_via_v2
    sum_E2_prc_E3_J = E2_prc_E3_J_via_b + E2_prc_E3_J_via_p
    sum_E2_prc_E4_J = E2_prc_E4_J_via_p

    sum_E2_prc_list = ['E4',
    'J_E1', 'J_E2', 'J_E3', 'J_E4']

# Sauro's Partitioned regulatory coefficients for E3

    # through E1
    E3_prc_E1_J_via_a  = (ec_R1_A * cc_A_R3) / cc_J_R3
    E3_prc_E1_J_via_p  = (ec_R1_P * cc_P_R3) / cc_J_R3

    # through E2
    E3_prc_E2_J_via_a  = (ec_R2_A * cc_A_R3) / cc_J_R3
    E3_prc_E2_J_via_b  = (ec_R2_B * cc_B_R3) / cc_J_R3

    # through E3
    E3_prc_E3_J_via_b  = (ec_R3_B * cc_B_R3) / cc_J_R3
    E3_prc_E3_J_via_p  = (ec_R3_P * cc_P_R3) / cc_J_R3
    E3_prc_E3_J_via_v3 = 1 / cc_J_R3

    # through E4
    E3_prc_E4_J_via_p = (ec_R4_P * cc_P_R3) / cc_J_R3

    E3_prc_list = ['E4',
    'E1_J_via_a', 'E1_J_via_p',
    'E2_J_via_a', 'E2_J_via_b',
    'E3_J_via_b', 'E3_J_via_p', 'E3_J_via_v3',
    'E4_J_via_p']

    # Sum of partitioned regulatory coefficients: Theory check
    sum_E3_prc_E1_J = E3_prc_E1_J_via_a + E3_prc_E1_J_via_p
    sum_E3_prc_E2_J = E3_prc_E2_J_via_a + E3_prc_E2_J_via_b
    sum_E3_prc_E3_J = E3_prc_E3_J_via_b + E3_prc_E3_J_via_p + E3_prc_E3_J_via_v3
    sum_E3_prc_E4_J = E3_prc_E4_J_via_p

    sum_E3_prc_list = ['E4',
    'J_E1', 'J_E2', 'J_E3', 'J_E4']

# Sauro's Partitioned regulatory coefficients for E4

    # through E1
    E4_prc_E1_J_via_a  = (ec_R1_A * cc_A_R4) / cc_J_R4
    E4_prc_E1_J_via_p  = (ec_R1_P * cc_P_R4) / cc_J_R4

    # through E2
    E4_prc_E2_J_via_a  = (ec_R2_A * cc_A_R4) / cc_J_R4
    E4_prc_E2_J_via_b  = (ec_R2_B * cc_B_R4) / cc_J_R4
```

```
    # through E3
    E4_prc_E3_J_via_b  = (ec_R3_B * cc_B_R4) / cc_J_R4
    E4_prc_E3_J_via_p  = (ec_R3_P * cc_P_R4) / cc_J_R4

    # through E4
    E4_prc_E4_J_via_p  = (ec_R4_P * cc_P_R4) / cc_J_R4
    E4_prc_E4_J_via_v4 = 1 / cc_J_R4

    E4_prc_list = ['E4',
    'E1_J_via_a', 'E1_J_via_p',
    'E2_J_via_a', 'E2_J_via_b',
    'E3_J_via_b', 'E3_J_via_p',
    'E4_J_via_p', 'E4_J_via_v4']

    # Sum of partitioned regulatory coefficients: Theory check

    sum_E4_prc_E1_J = E4_prc_E1_J_via_a + E4_prc_E1_J_via_p
    sum_E4_prc_E2_J = E4_prc_E2_J_via_a + E4_prc_E2_J_via_b
    sum_E4_prc_E3_J = E4_prc_E3_J_via_b + E4_prc_E3_J_via_p
    sum_E4_prc_E4_J = E4_prc_E4_J_via_p + E4_prc_E4_J_via_v4

    sum_E4_prc_list = ['E4',
    'J_E1', 'J_E2', 'J_E3', 'J_E4']

# Unscaled partitioned regulatory coefficients for E1 (from EC = I)

    # through E1
    E1_pc_E1_J_via_a  = (ec_R1_A * cc_A_R1)
    E1_pc_E1_J_via_p  = (ec_R1_P * cc_P_R1)
    E1_pc_E1_J_via_v1 = cc_J_R1 / cc_J_R1

    # through E2
    E1_pc_E2_J_via_a  = (ec_R2_A * cc_A_R1)
    E1_pc_E2_J_via_b  = (ec_R2_B * cc_B_R1)

    # through E3
    E1_pc_E3_J_via_b  = (ec_R3_B * cc_B_R1)
    E1_pc_E3_J_via_p  = (ec_R3_P * cc_P_R1)

    # through E4
    E1_pc_E4_J_via_p  = (ec_R4_P * cc_P_R1)

    E1_pc_list = ['E4',
    'E1_J_via_a', 'E1_J_via_p', 'E1_J_via_v1',
    'E2_J_via_a', 'E2_J_via_b',
    'E3_J_via_b', 'E3_J_via_p',
    'E4_J_via_p']

    # Sum of partitioned regulatory coefficients: Theory check
    sum_E1_pc_E1_J = E1_pc_E1_J_via_a + E1_pc_E1_J_via_p + E1_pc_E1_J_via_v1
    sum_E1_pc_E2_J = E1_pc_E2_J_via_a + E1_pc_E2_J_via_b
    sum_E1_pc_E3_J = E1_pc_E3_J_via_b + E1_pc_E3_J_via_p
    sum_E1_pc_E4_J = E1_pc_E4_J_via_p
```

```
    sum_E1_pc_list = ['E4',
    'J_E1', 'J_E2', 'J_E3', 'J_E4']


# Unscaled partitioned regulatory coefficients for E2 (from EC = I)

    # through E1
    E2_pc_E1_J_via_a  = (ec_R1_A * cc_A_R2)
    E2_pc_E1_J_via_p  = (ec_R1_P * cc_P_R2)

    # through E2
    E2_pc_E2_J_via_a  = (ec_R2_A * cc_A_R2)
    E2_pc_E2_J_via_b  = (ec_R2_B * cc_B_R2)
    E2_pc_E2_J_via_v2 = cc_J_R2 / cc_J_R2

    # through E3
    E2_pc_E3_J_via_b  = (ec_R3_B * cc_B_R2)
    E2_pc_E3_J_via_p  = (ec_R3_P * cc_P_R2)

    # through E4
    E2_pc_E4_J_via_p  = (ec_R4_P * cc_P_R2)

    E2_pc_list = ['E4',
    'E1_J_via_a', 'E1_J_via_p',
    'E2_J_via_a', 'E2_J_via_b', 'E2_J_via_v2',
    'E3_J_via_b', 'E3_J_via_p',
    'E4_J_via_p']

    # Sum of partitioned regulatory coefficients: Theory check
    sum_E2_pc_E1_J = E2_pc_E1_J_via_a + E2_pc_E1_J_via_p
    sum_E2_pc_E2_J = E2_pc_E2_J_via_a + E2_pc_E2_J_via_b + E2_pc_E2_J_via_v2
    sum_E2_pc_E3_J = E2_pc_E3_J_via_b + E2_pc_E3_J_via_p
    sum_E2_pc_E4_J = E2_pc_E4_J_via_p

    sum_E2_pc_list = ['E4',
    'J_E1', 'J_E2', 'J_E3', 'J_E4']

# Unscaled partitioned regulatory coefficients for E3 (from EC = I)

    # through E1
    E3_pc_E1_J_via_a  = (ec_R1_A * cc_A_R3)
    E3_pc_E1_J_via_p  = (ec_R1_P * cc_P_R3)

    # through E2
    E3_pc_E2_J_via_a  = (ec_R2_A * cc_A_R3)
    E3_pc_E2_J_via_b  = (ec_R2_B * cc_B_R3)

    # through E3
    E3_pc_E3_J_via_b  = (ec_R3_B * cc_B_R3)
    E3_pc_E3_J_via_p  = (ec_R3_P * cc_P_R3)
    E3_pc_E3_J_via_v3 = cc_J_R3 / cc_J_R3

    # through E4
    E3_pc_E4_J_via_p  = (ec_R4_P * cc_P_R3)
```

94

```
    E3_pc_list = ['E4',
    'E1_J_via_a', 'E1_J_via_p',
    'E2_J_via_a', 'E2_J_via_b',
    'E3_J_via_b', 'E3_J_via_p', 'E3_J_via_v3',
    'E4_J_via_p']

    # Sum of partitioned regulatory coefficients: Theory check
    sum_E3_pc_E1_J = E3_pc_E1_J_via_a + E3_pc_E1_J_via_p
    sum_E3_pc_E2_J = E3_pc_E2_J_via_a + E3_pc_E2_J_via_b
    sum_E3_pc_E3_J = E3_pc_E3_J_via_b + E3_pc_E3_J_via_p + E3_pc_E3_J_via_v3
    sum_E3_pc_E4_J = E3_pc_E4_J_via_p

    sum_E3_pc_list = ['E4',
    'J_E1', 'J_E2', 'J_E3', 'J_E4']

# Unscaled partitioned regulatory coefficients for E4 (from EC = I)

    # through E1
    E4_pc_E1_J_via_a  = (ec_R1_A * cc_A_R4)
    E4_pc_E1_J_via_p  = (ec_R1_P * cc_P_R4)

    # through E2
    E4_pc_E2_J_via_a  = (ec_R2_A * cc_A_R4)
    E4_pc_E2_J_via_b  = (ec_R2_B * cc_B_R4)

    # through E3
    E4_pc_E3_J_via_b  = (ec_R3_B * cc_B_R4)
    E4_pc_E3_J_via_p  = (ec_R3_P * cc_P_R4)

    # through E4
    E4_pc_E4_J_via_p  = (ec_R4_P * cc_P_R4)
    E4_pc_E4_J_via_v4 = cc_J_R4 / cc_J_R4

    E4_pc_list = ['E4',
    'E1_J_via_a', 'E1_J_via_p',
    'E2_J_via_a', 'E2_J_via_b',
    'E3_J_via_b', 'E3_J_via_p',
    'E4_J_via_p', 'E4_J_via_v4']

    # Sum of partitioned regulatory coefficients: Theory check
    sum_E4_pc_E1_J = E4_pc_E1_J_via_a + E4_pc_E1_J_via_p
    sum_E4_pc_E2_J = E4_pc_E2_J_via_a + E4_pc_E2_J_via_b
    sum_E4_pc_E3_J = E4_pc_E3_J_via_b + E4_pc_E3_J_via_p
    sum_E4_pc_E4_J = E4_pc_E4_J_via_p + E4_pc_E4_J_via_v4

    sum_E4_pc_list = ['E4',
    'J_E1', 'J_E2', 'J_E3', 'J_E4']

# Internal response coefficients

    irc_J_a_R1 = ec_R1_A * cc_J_R1
    irc_J_a_R2 = ec_R2_A * cc_J_R2
    irc_a_a_R1 = ec_R1_A * cc_A_R1
    irc_a_a_R2 = ec_R2_A * cc_A_R2
```

```
    irc_b_a_R1 = ec_R1_A * cc_B_R1
    irc_b_a_R2 = ec_R2_A * cc_B_R2
    irc_p_a_R1 = ec_R1_A * cc_P_R1
    irc_p_a_R2 = ec_R2_A * cc_P_R2

    irc_J_b_R2 = ec_R2_B * cc_J_R2
    irc_J_b_R3 = ec_R3_B * cc_J_R3
    irc_a_b_R2 = ec_R2_B * cc_A_R2
    irc_a_b_R3 = ec_R3_B * cc_A_R3
    irc_b_b_R2 = ec_R2_B * cc_B_R2
    irc_b_b_R3 = ec_R3_B * cc_B_R3
    irc_p_b_R2 = ec_R2_B * cc_P_R2
    irc_p_b_R3 = ec_R3_B * cc_P_R3

    irc_J_p_R1 = ec_R1_P * cc_J_R1
    irc_J_p_R3 = ec_R3_P * cc_J_R3
    irc_J_p_R4 = ec_R4_P * cc_J_R4
    irc_a_p_R1 = ec_R1_P * cc_A_R1
    irc_a_p_R3 = ec_R3_P * cc_A_R3
    irc_a_p_R4 = ec_R4_P * cc_A_R4
    irc_b_p_R1 = ec_R1_P * cc_B_R1
    irc_b_p_R3 = ec_R3_P * cc_B_R3
    irc_b_p_R4 = ec_R4_P * cc_B_R4
    irc_p_p_R1 = ec_R1_P * cc_P_R1
    irc_p_p_R3 = ec_R3_P * cc_P_R3
    irc_p_p_R4 = ec_R4_P * cc_P_R4

    irc_list = ['E4',
    'J_a_R1','J_a_R2','a_a_R1','a_a_R2','b_a_R1','b_a_R2','p_a_R1','p_a_R2',
    'J_b_R2','J_b_R3','a_b_R2','a_b_R3','b_b_R2','b_b_R3',
    'p_b_R2','p_b_R3',
    'J_p_R1','J_p_R3','J_p_R4',
    'a_p_R1','a_p_R3','a_p_R4',
    'b_p_R1','b_p_R3','b_p_R4',
    'p_p_R1','p_p_R3','p_p_R4']

# Connectivities: Sum of internal response coefficients: Theory check

    sum_irc_J_a = irc_J_a_R1 + irc_J_a_R2
    sum_irc_a_a = irc_a_a_R1 + irc_a_a_R2
    sum_irc_b_a = irc_b_a_R1 + irc_b_a_R2
    sum_irc_p_a = irc_p_a_R1 + irc_p_a_R2

    sum_irc_J_b = irc_J_b_R2 + irc_J_b_R3
    sum_irc_a_b = irc_a_b_R2 + irc_a_b_R3
    sum_irc_b_b = irc_b_b_R2 + irc_b_b_R3
    sum_irc_p_b = irc_p_b_R2 + irc_p_b_R3

    sum_irc_J_p = irc_J_p_R1 + irc_J_p_R3 + irc_J_p_R4
    sum_irc_a_p = irc_a_p_R1 + irc_a_p_R3 + irc_a_p_R4
    sum_irc_b_p = irc_b_p_R1 + irc_b_p_R3 + irc_b_p_R4
    sum_irc_p_p = irc_p_p_R1 + irc_p_p_R3 + irc_p_p_R4

    sum_irc_list = ['E4',
```

```
         'J_a', 'a_a', 'b_a', 'p_a',
         'J_b', 'a_b', 'b_b', 'p_b',
         'J_p', 'a_p', 'b_p', 'p_p']

# Regulatory potential

    rp_J_p_pos = irc_J_p_R4
    rp_J_p_neg = irc_J_p_R1 + irc_J_p_R3

    rp_list = ['E4', 'rp_J_p_pos', 'rp_J_p_neg']

# Co-control coefficients

    coc_a_J_R1 = cc_A_R1 / cc_J_R1
    coc_a_J_R2 = cc_A_R2 / cc_J_R2
    coc_a_J_R3 = cc_A_R3 / cc_J_R3
    coc_a_J_R4 = cc_A_R4 / cc_J_R4
    coc_J_a_R1 = cc_J_R1 / cc_A_R1
    coc_J_a_R2 = cc_J_R2 / cc_A_R2
    coc_J_a_R3 = cc_J_R3 / cc_A_R3
    coc_J_a_R4 = cc_J_R4 / cc_A_R4
    coc_abs_J_a_R1 = scipy.absolute(cc_J_R1 / cc_A_R1)
    coc_abs_J_a_R2 = scipy.absolute(cc_J_R2 / cc_A_R2)
    coc_abs_J_a_R3 = scipy.absolute(cc_J_R3 / cc_A_R3)
    coc_abs_J_a_R4 = scipy.absolute(cc_J_R4 / cc_A_R4)

    coc_b_J_R1 = cc_B_R1 / cc_J_R1
    coc_b_J_R2 = cc_B_R2 / cc_J_R2
    coc_b_J_R3 = cc_B_R3 / cc_J_R3
    coc_b_J_R4 = cc_B_R4 / cc_J_R4
    coc_J_b_R1 = cc_J_R1 / cc_B_R1
    coc_J_b_R2 = cc_J_R2 / cc_B_R2
    coc_J_b_R3 = cc_J_R3 / cc_B_R3
    coc_J_b_R4 = cc_J_R4 / cc_B_R4
    coc_abs_J_b_R1 = scipy.absolute(cc_J_R1 / cc_B_R1)
    coc_abs_J_b_R2 = scipy.absolute(cc_J_R2 / cc_B_R2)
    coc_abs_J_b_R3 = scipy.absolute(cc_J_R3 / cc_B_R3)
    coc_abs_J_b_R4 = scipy.absolute(cc_J_R4 / cc_B_R4)

    coc_p_J_R1 = cc_P_R1 / cc_J_R1
    coc_p_J_R2 = cc_P_R2 / cc_J_R2
    coc_p_J_R3 = cc_P_R3 / cc_J_R3
    coc_p_J_R4 = cc_P_R4 / cc_J_R4
    coc_J_p_R1 = cc_J_R1 / cc_P_R1
    coc_J_p_R2 = cc_J_R2 / cc_P_R2
    coc_J_p_R3 = cc_J_R3 / cc_P_R3
    coc_J_p_R4 = cc_J_R4 / cc_P_R4
    coc_abs_J_p_R1 = scipy.absolute(cc_J_R1 / cc_P_R1)
    coc_abs_J_p_R2 = scipy.absolute(cc_J_R2 / cc_P_R2)
    coc_abs_J_p_R3 = scipy.absolute(cc_J_R3 / cc_P_R3)
    coc_abs_J_p_R4 = scipy.absolute(cc_J_R4 / cc_P_R4)

    coc_list = ['E4',
    'a_J_R1','a_J_R2','a_J_R3','a_J_R4',
```

97

```
        'abs_J_a_R1','abs_J_a_R2','abs_J_a_R3','abs_J_a_R4',
        'b_J_R1','b_J_R2','b_J_R3','b_J_R4',
        'abs_J_b_R1','abs_J_b_R2','abs_J_b_R3','abs_J_b_R4',
        'p_J_R1','p_J_R2','p_J_R3','p_J_R4',
        'abs_J_p_R1','abs_J_p_R2','abs_J_p_R3','abs_J_p_R4',
        'J_a_R1','J_a_R2','J_a_R3','J_a_R4',
        'J_b_R1','J_b_R2','J_b_R3','J_b_R4',
        'J_p_R1','J_p_R2','J_p_R3','J_p_R4']

# Control patterns

    # Flux-control patterns
    ConPat_J_R1  =  ec_R2_A * ec_R3_B * ec_R4_P
    ConPat_J_R2  = -ec_R1_A * ec_R3_B * ec_R4_P
    ConPat_J_R3  =  ec_R1_A * ec_R2_B * ec_R4_P
    ConPat_J_R4a = -ec_R1_A * ec_R2_B * ec_R3_P
    ConPat_J_R4b = -ec_R2_A * ec_R3_B * ec_R1_P

    # a-control patterns
    ConPat_a_R1a =  ec_R3_B * ec_R4_P
    ConPat_a_R1b = -ec_R2_B * ec_R4_P
    ConPat_a_R1c =  ec_R2_B * ec_R3_P
    ConPat_a_R2a =  ec_R3_B * ec_R1_P
    ConPat_a_R2b = -ec_R3_B * ec_R4_P
    ConPat_a_R3a =  ec_R2_B * ec_R4_P
    ConPat_a_R3b = -ec_R2_B * ec_R1_P
    ConPat_a_R4a = -ec_R2_B * ec_R3_P
    ConPat_a_R4b = -ec_R3_B * ec_R1_P
    ConPat_a_R4c =  ec_R2_B * ec_R1_P

    # b-control patterns
    ConPat_b_R1a =  ec_R2_A * ec_R4_P
    ConPat_b_R1b = -ec_R2_A * ec_R3_P
    ConPat_b_R2a =  ec_R1_A * ec_R3_P
    ConPat_b_R2b = -ec_R1_A * ec_R4_P
    ConPat_b_R3a = -ec_R2_A * ec_R4_P
    ConPat_b_R3b =  ec_R1_A * ec_R4_P
    ConPat_b_R3c =  ec_R2_A * ec_R1_P
    ConPat_b_R4a =  ec_R2_A * ec_R3_P
    ConPat_b_R4b = -ec_R1_A * ec_R3_P
    ConPat_b_R4c = -ec_R2_A * ec_R1_P

    # p-control patterns
    ConPat_p_R1  =  ec_R2_A * ec_R3_B
    ConPat_p_R2  = -ec_R1_A * ec_R3_B
    ConPat_p_R3  =  ec_R1_A * ec_R2_B
    ConPat_p_R4a = -ec_R2_A * ec_R3_B
    ConPat_p_R4b =  ec_R1_A * ec_R3_B
    ConPat_p_R4c = -ec_R1_A * ec_R2_B

    denominator = ConPat_J_R1 + ConPat_J_R2 + ConPat_J_R3
                + ConPat_J_R4a + ConPat_J_R4b

    conpat_list = ['E4',
```

```
'J_R1','J_R2','J_R3','J_R4a','J_R4b',
'a_R1a','a_R1b','a_R1c','a_R2a','a_R2b','a_R3a','a_R3b',
'a_R4a','a_R4b','a_R4c',
'b_R1a','b_R1b','b_R2a','b_R2b','b_R3a','b_R3b','b_R3c',
'b_R4a','b_R4b','b_R4c',
'p_R1','p_R2','p_R3','p_R4a','p_R4b','p_R4c',
'Denom']

# Scaled control patterns
ScConPat_J_R1  = ConPat_J_R1  / denominator
ScConPat_J_R2  = ConPat_J_R2  / denominator
ScConPat_J_R3  = ConPat_J_R3  / denominator
ScConPat_J_R4a = ConPat_J_R4a / denominator
ScConPat_J_R4b = ConPat_J_R4b / denominator

ScConPat_a_R1a = ConPat_a_R1a / denominator
ScConPat_a_R1b = ConPat_a_R1b / denominator
ScConPat_a_R1c = ConPat_a_R1c / denominator
ScConPat_a_R2a = ConPat_a_R2a / denominator
ScConPat_a_R2b = ConPat_a_R2b / denominator
ScConPat_a_R3a = ConPat_a_R3a / denominator
ScConPat_a_R3b = ConPat_a_R3b / denominator
ScConPat_a_R4a = ConPat_a_R4a / denominator
ScConPat_a_R4b = ConPat_a_R4b / denominator
ScConPat_a_R4c = ConPat_a_R4c / denominator

ScConPat_b_R1a = ConPat_b_R1a / denominator
ScConPat_b_R1b = ConPat_b_R1b / denominator
ScConPat_b_R2a = ConPat_b_R2a / denominator
ScConPat_b_R2b = ConPat_b_R2b / denominator
ScConPat_b_R3a = ConPat_b_R3a / denominator
ScConPat_b_R3b = ConPat_b_R3b / denominator
ScConPat_b_R3c = ConPat_b_R3c / denominator
ScConPat_b_R4a = ConPat_b_R4a / denominator
ScConPat_b_R4b = ConPat_b_R4b / denominator
ScConPat_b_R4c = ConPat_b_R4c / denominator

ScConPat_p_R1  = ConPat_p_R1  / denominator
ScConPat_p_R2  = ConPat_p_R2  / denominator
ScConPat_p_R3  = ConPat_p_R3  / denominator
ScConPat_p_R4a = ConPat_p_R4a / denominator
ScConPat_p_R4b = ConPat_p_R4b / denominator
ScConPat_p_R4c = ConPat_p_R4c / denominator

sc_conpat_list = ['E4',
'J_R1','J_R2','J_R3','J_R4a','J_R4b',
'a_R1a','a_R1b','a_R1c','a_R2a','a_R2b','a_R3a','a_R3b',
'a_R4a','a_R4b','a_R4c',
'b_R1a','b_R1b','b_R2a','b_R2b','b_R3a','b_R3b','b_R3c',
'b_R4a','b_R4b','b_R4c',
'p_R1','p_R2','p_R3','p_R4a','p_R4b','p_R4c']

# Data arrays
```

```
E1_prc_data = scipy.hstack((E4.reshape(steps,1),
  E1_prc_E1_J_via_a.reshape(steps,1), E1_prc_E1_J_via_p.reshape(steps,1),
  E1_prc_E1_J_via_v1.reshape(steps,1),
  E1_prc_E2_J_via_a.reshape(steps,1), E1_prc_E2_J_via_b.reshape(steps,1),
  E1_prc_E3_J_via_b.reshape(steps,1), E1_prc_E3_J_via_p.reshape(steps,1),
  E1_prc_E4_J_via_p.reshape(steps,1)))

sum_E1_prc_data = scipy.hstack((E4.reshape(steps,1),
  sum_E1_prc_E1_J.reshape(steps,1),
  sum_E1_prc_E2_J.reshape(steps,1),
  sum_E1_prc_E3_J.reshape(steps,1),
  sum_E1_prc_E4_J.reshape(steps,1)))

E2_prc_data = scipy.hstack((E4.reshape(steps,1),
  E2_prc_E1_J_via_a.reshape(steps,1), E2_prc_E1_J_via_p.reshape(steps,1),
  E2_prc_E2_J_via_a.reshape(steps,1), E2_prc_E2_J_via_b.reshape(steps,1),
  E2_prc_E2_J_via_v2.reshape(steps,1),
  E2_prc_E3_J_via_b.reshape(steps,1), E2_prc_E3_J_via_p.reshape(steps,1),
  E2_prc_E4_J_via_p.reshape(steps,1)))

sum_E2_prc_data = scipy.hstack((E4.reshape(steps,1),
  sum_E2_prc_E1_J.reshape(steps,1),
  sum_E2_prc_E2_J.reshape(steps,1),
  sum_E2_prc_E3_J.reshape(steps,1),
  sum_E2_prc_E4_J.reshape(steps,1)))

E3_prc_data = scipy.hstack((E4.reshape(steps,1),
  E3_prc_E1_J_via_a.reshape(steps,1), E3_prc_E1_J_via_p.reshape(steps,1),
  E3_prc_E2_J_via_a.reshape(steps,1), E3_prc_E2_J_via_b.reshape(steps,1),
  E3_prc_E3_J_via_b.reshape(steps,1), E3_prc_E3_J_via_p.reshape(steps,1),
  E3_prc_E3_J_via_v3.reshape(steps,1),
  E3_prc_E4_J_via_p.reshape(steps,1)))

sum_E3_prc_data = scipy.hstack((E4.reshape(steps,1),
  sum_E3_prc_E1_J.reshape(steps,1),
  sum_E3_prc_E2_J.reshape(steps,1),
  sum_E3_prc_E3_J.reshape(steps,1),
  sum_E3_prc_E4_J.reshape(steps,1)))

E4_prc_data = scipy.hstack((E4.reshape(steps,1),
  E4_prc_E1_J_via_a.reshape(steps,1), E4_prc_E1_J_via_p.reshape(steps,1),
  E4_prc_E2_J_via_a.reshape(steps,1), E4_prc_E2_J_via_b.reshape(steps,1),
  E4_prc_E3_J_via_b.reshape(steps,1), E4_prc_E3_J_via_p.reshape(steps,1),
  E4_prc_E4_J_via_p.reshape(steps,1), E4_prc_E4_J_via_v4.reshape(steps,1)))

sum_E4_prc_data = scipy.hstack((E4.reshape(steps,1),
  sum_E4_prc_E1_J.reshape(steps,1),
  sum_E4_prc_E2_J.reshape(steps,1),
  sum_E4_prc_E3_J.reshape(steps,1),
  sum_E4_prc_E4_J.reshape(steps,1)))

E1_pc_data = scipy.hstack((E4.reshape(steps,1),
  E1_pc_E1_J_via_a.reshape(steps,1), E1_pc_E1_J_via_p.reshape(steps,1),
  E1_pc_E1_J_via_v1.reshape(steps,1),
```

100

```
          E1_pc_E2_J_via_a.reshape(steps,1), E1_pc_E2_J_via_b.reshape(steps,1),
          E1_pc_E3_J_via_b.reshape(steps,1), E1_pc_E3_J_via_p.reshape(steps,1),
          E1_pc_E4_J_via_p.reshape(steps,1)))

    sum_E1_pc_data = scipy.hstack((E4.reshape(steps,1),
      sum_E1_pc_E1_J.reshape(steps,1),
      sum_E1_pc_E2_J.reshape(steps,1),
      sum_E1_pc_E3_J.reshape(steps,1),
      sum_E1_pc_E4_J.reshape(steps,1)))

    E2_pc_data = scipy.hstack((E4.reshape(steps,1),
      E2_pc_E1_J_via_a.reshape(steps,1), E2_pc_E1_J_via_p.reshape(steps,1),
      E2_pc_E2_J_via_a.reshape(steps,1), E2_pc_E2_J_via_b.reshape(steps,1),
      E2_pc_E2_J_via_v2.reshape(steps,1),
      E2_pc_E3_J_via_b.reshape(steps,1), E2_pc_E3_J_via_p.reshape(steps,1),
      E2_pc_E4_J_via_p.reshape(steps,1)))

    sum_E2_pc_data = scipy.hstack((E4.reshape(steps,1),
      sum_E2_pc_E1_J.reshape(steps,1),
      sum_E2_pc_E2_J.reshape(steps,1),
      sum_E2_pc_E3_J.reshape(steps,1),
      sum_E2_pc_E4_J.reshape(steps,1)))

    E3_pc_data = scipy.hstack((E4.reshape(steps,1),
      E3_pc_E1_J_via_a.reshape(steps,1), E3_pc_E1_J_via_p.reshape(steps,1),
      E3_pc_E2_J_via_a.reshape(steps,1), E3_pc_E2_J_via_b.reshape(steps,1),
      E3_pc_E3_J_via_b.reshape(steps,1), E3_pc_E3_J_via_p.reshape(steps,1),
      E3_pc_E3_J_via_v3.reshape(steps,1),
      E3_pc_E4_J_via_p.reshape(steps,1)))

    sum_E3_pc_data = scipy.hstack((E4.reshape(steps,1),
      sum_E3_pc_E1_J.reshape(steps,1),
      sum_E3_pc_E2_J.reshape(steps,1),
      sum_E3_pc_E3_J.reshape(steps,1),
      sum_E3_pc_E4_J.reshape(steps,1)))

    E4_pc_data = scipy.hstack((E4.reshape(steps,1),
      E4_pc_E1_J_via_a.reshape(steps,1), E4_pc_E1_J_via_p.reshape(steps,1),
      E4_pc_E2_J_via_a.reshape(steps,1), E4_pc_E2_J_via_b.reshape(steps,1),
      E4_pc_E3_J_via_b.reshape(steps,1), E4_pc_E3_J_via_p.reshape(steps,1),
      E4_pc_E4_J_via_p.reshape(steps,1), E4_pc_E4_J_via_v4.reshape(steps,1)))

    sum_E4_pc_data = scipy.hstack((E4.reshape(steps,1),
      sum_E4_pc_E1_J.reshape(steps,1),
      sum_E4_pc_E2_J.reshape(steps,1),
      sum_E4_pc_E3_J.reshape(steps,1),
      sum_E4_pc_E4_J.reshape(steps,1)))

    irc_data = scipy.hstack((E4.reshape(steps,1),
      irc_J_a_R1.reshape(steps,1), irc_J_a_R2.reshape(steps,1),
      irc_a_a_R1.reshape(steps,1), irc_a_a_R2.reshape(steps,1),
      irc_b_a_R1.reshape(steps,1), irc_b_a_R2.reshape(steps,1),
      irc_p_a_R1.reshape(steps,1), irc_p_a_R2.reshape(steps,1),
      irc_J_b_R2.reshape(steps,1), irc_J_b_R3.reshape(steps,1),
```

```
            irc_a_b_R2.reshape(steps,1), irc_a_b_R3.reshape(steps,1),
            irc_b_b_R2.reshape(steps,1), irc_b_b_R3.reshape(steps,1),
            irc_p_b_R2.reshape(steps,1), irc_p_b_R3.reshape(steps,1),
            irc_J_p_R1.reshape(steps,1), irc_J_p_R3.reshape(steps,1),
            irc_J_p_R4.reshape(steps,1),
            irc_a_p_R1.reshape(steps,1), irc_a_p_R3.reshape(steps,1),
            irc_a_p_R4.reshape(steps,1),
            irc_b_p_R1.reshape(steps,1), irc_b_p_R3.reshape(steps,1),
            irc_b_p_R4.reshape(steps,1),
            irc_p_p_R1.reshape(steps,1), irc_p_p_R3.reshape(steps,1),
            irc_p_p_R4.reshape(steps,1)))

    sum_irc_data = scipy.hstack((E4.reshape(steps,1),
      sum_irc_J_a.reshape(steps,1), sum_irc_a_a.reshape(steps,1),
      sum_irc_b_a.reshape(steps,1), sum_irc_p_a.reshape(steps,1),
      sum_irc_J_b.reshape(steps,1), sum_irc_a_b.reshape(steps,1),
      sum_irc_b_b.reshape(steps,1), sum_irc_p_b.reshape(steps,1),
      sum_irc_J_p.reshape(steps,1), sum_irc_a_p.reshape(steps,1),
      sum_irc_b_p.reshape(steps,1), sum_irc_p_p.reshape(steps,1)))

    rp_data = scipy.hstack((E4.reshape(steps,1),
      rp_J_p_pos.reshape(steps,1),
      rp_J_p_neg.reshape(steps,1)))

    coc_data = scipy.hstack((E4.reshape(steps,1),
      coc_a_J_R1.reshape(steps,1),     coc_a_J_R2.reshape(steps,1),
      coc_a_J_R3.reshape(steps,1),     coc_a_J_R4.reshape(steps,1),
      coc_abs_J_a_R1.reshape(steps,1), coc_abs_J_a_R2.reshape(steps,1),
      coc_abs_J_a_R3.reshape(steps,1), coc_abs_J_a_R4.reshape(steps,1),
      coc_b_J_R1.reshape(steps,1),     coc_b_J_R2.reshape(steps,1),
      coc_b_J_R3.reshape(steps,1),     coc_b_J_R4.reshape(steps,1),
      coc_abs_J_b_R1.reshape(steps,1), coc_abs_J_b_R2.reshape(steps,1),
      coc_abs_J_b_R3.reshape(steps,1), coc_abs_J_b_R4.reshape(steps,1),
      coc_p_J_R1.reshape(steps,1),     coc_p_J_R2.reshape(steps,1),
      coc_p_J_R3.reshape(steps,1),     coc_p_J_R4.reshape(steps,1),
      coc_abs_J_p_R1.reshape(steps,1), coc_abs_J_p_R2.reshape(steps,1),
      coc_abs_J_p_R3.reshape(steps,1), coc_abs_J_p_R4.reshape(steps,1),
      coc_J_a_R1.reshape(steps,1),     coc_J_a_R2.reshape(steps,1),
      coc_J_a_R3.reshape(steps,1),     coc_J_a_R4.reshape(steps,1),
      coc_J_b_R1.reshape(steps,1),     coc_J_b_R2.reshape(steps,1),
      coc_J_b_R3.reshape(steps,1),     coc_J_b_R4.reshape(steps,1),
      coc_J_p_R1.reshape(steps,1),     coc_J_p_R2.reshape(steps,1),
      coc_J_p_R3.reshape(steps,1),     coc_J_p_R4.reshape(steps,1)))

    conpat_data = scipy.hstack((E4.reshape(steps,1),
      ConPat_J_R1.reshape(steps,1),  ConPat_J_R2.reshape(steps,1),
      ConPat_J_R3.reshape(steps,1),  ConPat_J_R4a.reshape(steps,1),
      ConPat_J_R4b.reshape(steps,1), ConPat_a_R1a.reshape(steps,1),
      ConPat_a_R1b.reshape(steps,1), ConPat_a_R1c.reshape(steps,1),
      ConPat_a_R2a.reshape(steps,1), ConPat_a_R2b.reshape(steps,1),
      ConPat_a_R3a.reshape(steps,1), ConPat_a_R3b.reshape(steps,1),
      ConPat_a_R4a.reshape(steps,1), ConPat_a_R4b.reshape(steps,1),
      ConPat_a_R4c.reshape(steps,1), ConPat_b_R1a.reshape(steps,1),
      ConPat_b_R1b.reshape(steps,1), ConPat_b_R2a.reshape(steps,1),
```

```python
    ConPat_b_R2b.reshape(steps,1), ConPat_b_R3a.reshape(steps,1),
    ConPat_b_R3b.reshape(steps,1), ConPat_b_R3c.reshape(steps,1),
    ConPat_b_R4a.reshape(steps,1), ConPat_b_R4b.reshape(steps,1),
    ConPat_b_R4c.reshape(steps,1), ConPat_p_R1.reshape(steps,1),
    ConPat_p_R2.reshape(steps,1),  ConPat_p_R3.reshape(steps,1),
    ConPat_p_R4a.reshape(steps,1), ConPat_p_R4b.reshape(steps,1),
    ConPat_p_R4c.reshape(steps,1), denominator.reshape(steps,1)))

sc_conpat_data = scipy.hstack((E4.reshape(steps,1),
    ScConPat_J_R1.reshape(steps,1),  ScConPat_J_R2.reshape(steps,1),
    ScConPat_J_R3.reshape(steps,1),  ScConPat_J_R4a.reshape(steps,1),
    ScConPat_J_R4b.reshape(steps,1), ScConPat_a_R1a.reshape(steps,1),
    ScConPat_a_R1b.reshape(steps,1), ScConPat_a_R1c.reshape(steps,1),
    ScConPat_a_R2a.reshape(steps,1), ScConPat_a_R2b.reshape(steps,1),
    ScConPat_a_R3a.reshape(steps,1), ScConPat_a_R3b.reshape(steps,1),
    ScConPat_a_R4a.reshape(steps,1), ScConPat_a_R4b.reshape(steps,1),
    ScConPat_a_R4c.reshape(steps,1), ScConPat_b_R1a.reshape(steps,1),
    ScConPat_b_R1b.reshape(steps,1), ScConPat_b_R2a.reshape(steps,1),
    ScConPat_b_R2b.reshape(steps,1), ScConPat_b_R3a.reshape(steps,1),
    ScConPat_b_R3b.reshape(steps,1), ScConPat_b_R3c.reshape(steps,1),
    ScConPat_b_R4a.reshape(steps,1), ScConPat_b_R4b.reshape(steps,1),
    ScConPat_b_R4c.reshape(steps,1), ScConPat_p_R1.reshape(steps,1),
    ScConPat_p_R2.reshape(steps,1),  ScConPat_p_R3.reshape(steps,1),
    ScConPat_p_R4a.reshape(steps,1), ScConPat_p_R4b.reshape(steps,1),
    ScConPat_p_R4c.reshape(steps,1)))

res_file = open(output_dir + par_set + '_ss' + '.dat', 'w')
mod.Write_array(mod.scan_res, res_file, Col = ss_var_list, close_file=1)

res_file = open(output_dir + par_set + '_E1_prc' + '.dat', 'w')
mod.Write_array(E1_prc_data, res_file, Col = E1_prc_list, close_file=1)

res_file = open(output_dir + par_set + '_sum_E1_prc' + '.dat', 'w')
mod.Write_array(sum_E1_prc_data, res_file, Col = sum_E1_prc_list,
close_file=1)

res_file = open(output_dir + par_set + '_E2_prc' + '.dat', 'w')
mod.Write_array(E2_prc_data, res_file, Col = E2_prc_list, close_file=1)

res_file = open(output_dir + par_set + '_sum_E2_prc' + '.dat', 'w')
mod.Write_array(sum_E2_prc_data, res_file, Col = sum_E2_prc_list,
close_file=1)

res_file = open(output_dir + par_set + '_E3_prc' + '.dat', 'w')
mod.Write_array(E3_prc_data, res_file, Col = E3_prc_list, close_file=1)

res_file = open(output_dir + par_set + '_sum_E3_prc' + '.dat', 'w')
mod.Write_array(sum_E3_prc_data, res_file, Col = sum_E3_prc_list,
close_file=1)

res_file = open(output_dir + par_set + '_E4_prc' + '.dat', 'w')
mod.Write_array(E4_prc_data, res_file, Col = E4_prc_list, close_file=1)

res_file = open(output_dir + par_set + '_sum_E4_prc' + '.dat', 'w')
```

103

```
    mod.Write_array(sum_E4_prc_data, res_file, Col = sum_E4_prc_list,
    close_file=1)

    res_file = open(output_dir + par_set + '_E1_pc' + '.dat', 'w')
    mod.Write_array(E1_pc_data, res_file, Col = E1_pc_list, close_file=1)

    res_file = open(output_dir + par_set + '_sum_E1_pc' + '.dat', 'w')
    mod.Write_array(sum_E1_pc_data, res_file, Col = sum_E1_pc_list,
    close_file=1)

    res_file = open(output_dir + par_set + '_E2_pc' + '.dat', 'w')
    mod.Write_array(E2_pc_data, res_file, Col = E2_pc_list, close_file=1)

    res_file = open(output_dir + par_set + '_sum_E2_pc' + '.dat', 'w')
    mod.Write_array(sum_E2_pc_data, res_file, Col = sum_E2_pc_list,
    close_file=1)

    res_file = open(output_dir + par_set + '_E3_pc' + '.dat', 'w')
    mod.Write_array(E3_pc_data, res_file, Col = E3_pc_list, close_file=1)

    res_file = open(output_dir + par_set + '_sum_E3_pc' + '.dat', 'w')
    mod.Write_array(sum_E3_pc_data, res_file, Col = sum_E3_pc_list,
    close_file=1)

    res_file = open(output_dir + par_set + '_E4_pc' + '.dat', 'w')
    mod.Write_array(E4_pc_data, res_file, Col = E4_pc_list, close_file=1)

    res_file = open(output_dir + par_set + '_sum_E4_pc' + '.dat', 'w')
    mod.Write_array(sum_E4_pc_data, res_file, Col = sum_E4_pc_list,
    close_file=1)

    res_file = open(output_dir + par_set + '_irc' + '.dat', 'w')
    mod.Write_array(irc_data, res_file, Col = irc_list, close_file=1)

    res_file = open(output_dir + par_set + '_sum_irc' + '.dat', 'w')
    mod.Write_array(sum_irc_data, res_file, Col = sum_irc_list,
    close_file=1)

    res_file = open(output_dir + par_set + '_rp' + '.dat', 'w')
    mod.Write_array(rp_data, res_file, Col = rp_list, close_file=1)

    res_file = open(output_dir + par_set + '_coc' + '.dat', 'w')
    mod.Write_array(coc_data, res_file, Col = coc_list, close_file=1)

    res_file = open(output_dir + par_set + '_conpat' + '.dat', 'w')
    mod.Write_array(conpat_data, res_file, Col = conpat_list, close_file=1)

    res_file = open(output_dir + par_set + '_sc_conpat' + '.dat', 'w')
    mod.Write_array(sc_conpat_data, res_file, Col = sc_conpat_list,
    close_file=1)

    return

steps      = 501
```

104

```
scan_min   = 0.01
scan_max   = 1.0e6
scan_range = scipy.logspace(scipy.log10(scan_min),scipy.log10(scan_max), steps)


#-------------------------------------------------------------
# Parameter set 1: Strong p-homeostasis, tight P-binding by E4,
#                   E2 and E3 near equilibrium
#-------------------------------------------------------------

m.K4p = 0.01
m.h   = 4.0
m.E2  = 1000.0
m.E3  = 1000.0

parameter_set = 'lin4fb_E4_K4p=0.01_h=4'
data = create_data_arrays(m, parameter_set)


#-------------------------------------------------------------
# Parameter set 2: Weak p-homeostasis, tight P-binding by E4,
#                   E2 and E3 near equilibrium
#-------------------------------------------------------------

m.K4p = 0.01
m.h   = 1.0
m.E2  = 1000.0
m.E3  = 1000.0

parameter_set = 'lin4fb_E4_K4p=0.01_h=1'
data = create_data_arrays(m, parameter_set)


#-------------------------------------------------------------
# Parameter set 3: Strong p-homeostasis, tight P-binding by E4,
#                   E2 and E3 further away from equilibrium
#-------------------------------------------------------------

m.K4p = 0.01
m.h   = 4.0
m.E2  = 100.0
m.E3  = 100.0

parameter_set = 'lin4fb_E4_K4p=0.01_h=4_E2E3=100'
data = create_data_arrays(m, parameter_set)


#-------------------------------------------------------------
# Parameter set 4: Strong p-homeostasis, weak P-binding by E4,
#                   E2 and E3 near equilibrium
#-------------------------------------------------------------

m.K4p = 100.0
m.h   = 4.0
m.E2  = 1000.0
m.E3  = 1000.0

scan_max   = 1.0e6
```

105

```
scan_range = scipy.logspace(scipy.log10(scan_min),scipy.log10(scan_max), steps)


parameter_set = 'lin4fb_E4_K4p=100_h=4'
data = create_data_arrays(m, parameter_set)
```

Bibliography

[1] Chen, Y.-D. and Westerhoff, H. V. [1986] "How do inhibitors and modifiers of individual enzymes affect steady-state fluxes and concentrations in metabolic systems?" *Math. Modelling* **7**, 1173–1180.

[2] Cornish-Bowden, A. and Hofmeyr, J.-H. S. [1991] "MetaModel: a program for modelling and control analysis of metabolic pathways on the IBM PC and compatibles" *Comput. Appl. Biosci.* **7**, 89–93.

[3] Fell, D. A. and Sauro, H. M. [1985] "Metabolic control and its analysis: additional relationships between elasticities and control coefficients" *Eur. J. Biochem.* **148**, 555–561.

[4] Hanekom, A. J. [2006] *Generic kinetic equations for modelling multisubstrate reactions in computational systems biology* M.Sc. (Biochemistry) Univ. of Stellenbosch.

[5] Heinrich, R. and Rapoport, T. A. [1974] "A linear steady-state treatment of enzymatic chains: Critique of the crossover theorem and general procedure to identify interaction sites with an effector" *Eur. J. Biochem.* **42**, 97–105.

[6] Heinrich, R. and Rapoport, T. A. [1974] "A linear steady-state treatment of enzymatic chains: General properties, control and effector strength" *Eur. J. Biochem.* **42**, 89–95.

[7] Heinrich, R. and Schuster, S. [1996] *The regulation of cellular systems* Chapman & Hall, New York.

[8] Hofmeyr, J.-H. S. [1989] "Control-pattern analysis of metabolic pathways. flux and concentration control in linear pathways" *Eur. J. Biochem.* **186**, 343–354.

[9]   Hofmeyr, J.-H. S. [1995] "Metabolic regulation: a control analytic perspective" *J. Bioenerg. Biomembr.* **27**, 479–490.

[10]   Hofmeyr, J.-H. S. [2001] "Metabolic control analysis in a nutshell" in *Proc. of the 2nd International Conference on Systems Biology* (Yi, T.-M., Hucka, M., Morohashi, M. and Kitano, H., eds.) pp. 291–300 Omnipress, Wisconsin.

[11]   Hofmeyr, J.-H. S. and Cornish-Bowden, A. [1991] "Quantitative assessment of regulation in metabolic systems" *Eur. J. Biochem.* **200**, 223–236.

[12]   Hofmeyr, J.-H. S. and Cornish-Bowden, A. [1996] "Co-response analysis: a new experimental strategy for metabolic control analysis" *J. Theor. Biol.* **182**, 371–380.

[13]   Hofmeyr, J.-H. S. and Cornish-Bowden, A. [1997] "The reversible Hill equation: how to incorporate cooperative enzymes into metabolic models" *Comput. Appl. Biosci.* **13**, 377–385.

[14]   Hofmeyr, J.-H. S. and Cornish-Bowden, A. [2000] "Regulating the cellular economy of supply and demand" *FEBS Lett.* **476**, 47–51.

[15]   Hofmeyr, J.-H. S., Cornish-Bowden, A. and Rohwer, J. M. [1993] "Taking enzyme kinetics out of control; putting control into regulation" *Eur. J. Biochem.* **212**, 833–837.

[16]   Hofmeyr, J.-H. S., Kacser, H. and van der Merwe, K. J. [1986] "Metabolic control analysis of moiety-conserved cycles" *Eur. J. Biochem.* **155**, 631–641.

[17]   Hofmeyr, J.-H. S. and Rohwer, J. M. [2011] "Supply-demand analysis: A framework for exploring the regulatory design of metabolism" *Methods Enzymol.* **500**, 533–554.

[18]   Hofmeyr, J.-H. S. and van der Merwe, K. J. [1986] "METAMOD: software for steady-state modelling and control analysis of metabolic pathways on the BBC microcomputer" *Comput. Appl. Biosci.* **2**, 243–249.

[19]   Hofmeyr, J.-H. S. and Westerhoff, H. V. [2001] "Building the cellular puzzle: control in multi-level reaction networks" *J. Theor. Biol.* **208**, 261–285.

[20] Hoops, S., Sahle, S., Gauges, R., Lee, C., Pahle, J., Simus, N., Singhal, M., Xu, L., Mendes, P. and Kummer, U. [2006] "Copasi–a complex pathway simulator" *Bioinformatics* **22**, 3067–3074.

[21] Kacser, H. and Burns, J. A. [1973] "The control of flux" *Sym. Soc. Exp. Biol.* **32**, 65–104.

[22] Kacser, H., Burns, J. A. and Fell, D. A. [1995] "The control of flux: 21 years on" *Biochem. Soc. Trans.* **23**, 341–366.

[23] Kahn, D. and Westerhoff, H. V. [1993] "The regulatory strength: how to be precise about regulation and homeostasis" *Acta Biotheor.* **41**, 85–96.

[24] Kholodenko, B. N. [1988] "How do external parameters control fluxes and concentrations of metabolites? An additional relationship in the theory of metabolic control" *FEBS Lett.* **232**, 383–386.

[25] Mendes, P. [1993] "GEPASI: a software package for modelling the dynamics, steady states and control of biochemical and other systems" *Comput. Appl. Biosci.* **9**, 563–571.

[26] Novick, A. and Szilard, L. [1954] "Experiments with the chemostat on the rates of amino acid synthesis in bacteria" in *Dynamics of Growth Processes* (Boell, E., ed.) pp. 21–32 Princeton University Press, Princeton, NJ.

[27] Olivier, B. G. and Rohwer, J. M.and Hofmeyr, J.-H. S. [2005] "Modelling cellular systems with PySCeS" *Bioinformatics* **21**, 560–56.

[28] Reder, C. [1988] "Metabolic control theory: a structural approach" *J. Theor. Biol.* **135**, 175–201.

[29] Rohwer, J. M., Akhurst, T. J. and Hofmeyr, J.-H. S. [2008] "Symbolic control analysis of cellular systems" in *Proceedings of 3rd International ES-CEC Symposium on Experimental Standard Conditions on Enzyme Characterizations, September 23rd–26th, 2007, Rüdesheim/Rhein, Germany* (Kettner, C. and Hicks, M. G., eds.) pp. 137–148.

[30] Rohwer, J. M., Hanekom, A. J., Crous, C., Snoep, J. L. and Hofmeyr, J.-H. S. [2006] "Evaluation of a simplified generic bi-substrate rate equation for computational systems biology" *IEE Proc.-Syst. Biol.* **153**, 338–341.

[31] Rohwer, J. M., Hanekom, A. J. and Hofmeyr, J.-H. S. [2007] "A universal rate equation for systems biology" in *Proceedings of 2nd International ES-CEC Symposium on Experimental Standard Conditions on Enzyme Characterizations, March 19th – 23rd, 2006, Ruedesheim/Rhein, Germany* (Kettner, C. and Hicks, M. G., eds.).

[32] Rohwer, J. M. and Hofmeyr, J.-H. S. [2008] "Identifying and characterising regulatory metabolites with generalised supply-demand analysis" *J. Theor. Biol.* **252**, 546–554.

[33] Rosen, R. [1971] "Some realizations of (M,R)-systems and their interpretation" *Bull. Math. Biophys.* **33**, 303–319.

[34] Sauro, H. M. [1990] "Regulatory responses and control analysis: assessment of the relative importance of internal effectors" in *Control of Metabolic Processes* (Cornish-Bowden, A. and Cardenas, M. L., eds.) vol. 190 of *Nato ASI Seris* pp. 225–230 Plenum Press.

[35] Sauro, H. M. [2000] "Jarnac: a system for interactive metabolic analysis" in *Animating the Cellular Map* (Hofmeyr, J.-H. S., Rohwer, J. M. and Snoep, J. L., eds.) pp. 221–228 Stellenbosch University Press, Stellenbosch.

[36] Sauro, H. M. and Fell, D. A. [1991] "Scamp: a metabolic simulator and control analysis program" *Math. Comput. Modelling* **15**, 15–28.

[37] Savageau, M. A. [1969] "Biochemical systems analysis. I. Some mathematical properties of the rate law for the component enzymatic reactions" *J. Theor. Biol.* **25**, 365–369.

[38] Savageau, M. A. [1969] "Biochemical systems analysis. II. The steady-state solutions for an n-pool system using a power-law approximation" *J. Theor. Biol.* **25**, 370–379.

[39] Savageau, M. A. [1970] "Biochemical systems analysis. III. Dynamic solutions using a power-law approximation" *J. Theor. Biol.* **26**, 215–226.

[40] Strogatz, S. H. [2000] *Nonlinear Dynamics and Chaos: With Applications to Physics, Biology, Chemistry, and Engineering* Westview Press, Cambridge, Massachusetts.

[41] Umbarger, H. E. [1958] "Evidence for a negative-feedback mechanism in the biosynthesis of isoleucine" *Science* **123**, 848.

[42] Yates, R. A. and Pardee, A. B. [1956] "Control of pyrimidine biosynthesis in *Escherichia coli* by a feed-back mechanism" *J. Biol. Chem.* **221**, 757–770.